western australian marine science institution

Numerical modelling of dredge plumes

Chaojiao Sun[1,2], Paul Branson[1,2]

[1] *CSIRO Ocean and Atmosphere, Perth, Western Australia, Australia*

[2] *Western Australian Marine Science Institution (WAMSI), Perth, Western Australia, Australia*

WAMSI Dredging Science Node

Theme 3 Report

Project 3.4

January 2018

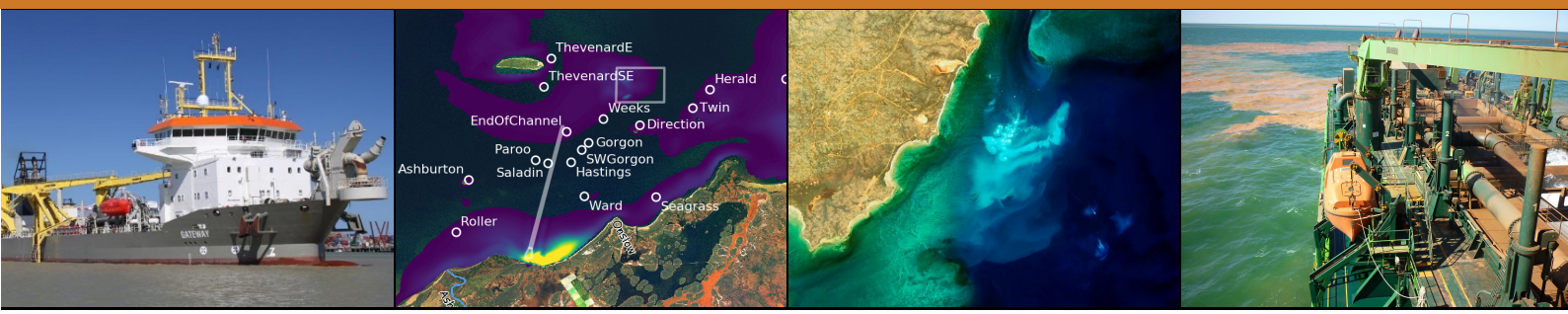

WESTERN AUSTRALIAN MARINE SCIENCE INSTITUTION

CSIRO

WAMSI Dredging Science Node

The WAMSI Dredging Science Node is a strategic research initiative that evolved in response to uncertainties in the environmental impact assessment and management of large-scale dredging operations and coastal infrastructure developments. Its goal is to enhance capacity within government and the private sector to predict and manage the environmental impacts of dredging in Western Australia, delivered through a combination of reviews, field studies, laboratory experimentation, relationship testing and development of standardised protocols and guidance for impact prediction, monitoring and management.

Ownership of Intellectual property rights

Copyright

Funding Sources

The $20million Dredging Science Node is delivering one of the largest single issue environmental research programs in Australia. This applied research is funded by **Woodside Energy, Chevron Australia, BHP Billiton and the WAMSI Partners** and designed to provide a significant and meaningful improvement in the certainty around the effects, and management, of dredging operations in Western Australia. Although focussed on port and coastal development in Western Australia, the outputs will also be broadly applicable across Australia and globally.

This remarkable **collaboration between industry, government and research** extends beyond the classical funder-provider model. End-users of science in regulator and conservation agencies, and consultant and industry groups are actively involved in the governance of the node, to ensure ongoing focus on applicable science and converting the outputs into fit-for-purpose and usable products. The governance structure includes clear delineation between end-user focussed scoping and the arms-length research activity to ensure it is independent, unbiased and defensible.

And critically, the trusted across-sector collaboration developed through the WAMSI model has allowed the sharing of hundreds of millions of dollars' worth of environmental monitoring data, much of it collected by environmental consultants on behalf of industry. By providing access to this usually **confidential data,** the **Industry Partners** are substantially enhancing WAMSI researchers' ability to determine the real-world impacts of dredging projects, and how they can best be managed. Rio Tinto's voluntary data contribution is particularly noteworthy, as it is not one of the funding contributors to the Node.

Funding and critical data

Critical data

Legal Notice

Year of publication: 2018

Metadata: http://catalogue.aodn.org.au/geonetwork/srv/eng/metadata.show?uuid=00562caf-3ddf-59e3-e053-08114f8cd206

Citation: Sun C Branson PM (2018) Numerical modelling of dredge plumes. Report of Theme 3 - Project 3.4 prepared for the Dredging Science Node, Western Australian Marine Science Institution, Perth, Western Australia. 81pp.

Author Contributions: Chaojiao Sun and Paul Branson conducted the analyses? and wrote the report.

Corresponding author and Institution: C Sun (CSIRO). Email address: Chaojiao.Sun@csiro.au

Competing Interests: The commercial investors and data providers had no role in the data analysis, data interpretation, the decision to publish or in the preparation of the manuscript. The authors have declared that no competing interests exists.

Acknowledgements: Graham Symonds, Kenji Shimizu, Nick Mortimer and Stephanie Contardo contributed to the early stages of the work presented here. Graham Symonds was the theme leader of Theme 2/3 from July 2013 to June 2015. We thank Nugzar Margvelashvili and Jo Myers for peer reviewing this report. We acknowledge the use of Fugro's Airborne LiDAR Bathymetry datasets of the North West Shelf of Australia, which were Acquired & Owned by ©Fugro.

Collection permits/ethics approval: No collection occurred in the production of this report.

Front cover images (L-R)

Image 1: Trailing Suction Hopper Dredge *Gateway* in operation during the Fremantle Port Inner Harbour and Channel Deepening Project. (Source: OEPA)

Image 2: Model simulated near surface Total suspended solids (TSS) on 27 August 2013 during intense nearshore dredging and net north easterly drift. (Source: CSIRO)

Image 3: Dredge Plume at Barrow Island. Image produced with data from the Japan Aerospace Exploration Agency (JAXA) Advanced Land Observing Satellite (ALOS) taken on 29 August 2010.

Image 4: Trailing Suction Hopper Dredge *Brabo* in operation during the Wheatstone Dredging Project off Onslow. (Source: Paul Zahra, OEPA) – is this photo legitimate? i.e. normally they take all cameras off you

Contents

Executive Summary

Port and coastal developments often involve large-scale dredge activities and are subject to environmental impact assessment (EIA) as part of their approval. Fundamental to EIA is the evaluation of environmental impacts and judgements about the degree to which management strategies are likely to be effective at mitigating environmental impact risk. Numerical modelling using sediment transport models (coupled to hydrodynamics and wave models) can be used to predict the ecological pressure caused by dredging activities (through increases in suspended solids, sediment smothering and light reduction). The responses of the biological assemblages to these pressure fields are then predicted by biological response models. The likely extent, severity and persistence of environmental impacts associated with dredging is then predicted.

Modelling is increasingly being used to quantify the transport and fate of sediments released during dredging operations. Model outputs are used to predict the spatial extent and intensity of the 'pressure' field generated by dredging related activities, including how it develops and changes over time. Model results are frequently used to predict the consequences of the modelled pressure field on the health of benthic communities and their habitats, such as coral reefs and seagrass meadows, which may be particularly sensitive.

Whilst fundamental to the prediction of environmental impact, dredge plume modelling at the EIA stage is challenging due to limited information available such as model input data and detailed information relating to the dredging campaign. There are significant benefits to improving the modelling process, giving proponent's greater clarity around key data requirements and standards for model calibration and validation, and providing environmental regulators greater confidence when making decisions using modelled outputs.

The goal of the Numerical Modelling Project (Dredge Science Node Project 3.4) is to improve the prediction of the transport and fate of dredge-generated sediments by developing an improved understanding of key physical processes that control the extent, intensity and duration of sediment plumes. The project sought to improve the modelling of the dynamics and fate of total suspended solids (TSS) in the passive dredge plumes by developing a hindcast model of a large-scale capital dredging campaign in the Pilbara, with the goal of improving the estimation of source terms for the passive far-field model, identifying and improving the estimates of important model parameters, and calculating measures of ecologically relevant pressure fields. The modelling approach was consistent with what is typically applied in EIA. The study assessed how effectively the model could reproduce the observed far-field TSS dynamics of a major capital dredging project in Western Australia and the ambient sediment dynamics of the system.

A frequent question encountered during the modelling of passive dredging plumes is if a 3D model is needed, or if the circulation and plume dispersion can be considered quasi-two dimensional such that 2D modelling is sufficient. This study identified that even in very shallow water strong vertical gradients in TSS and sub-surface plumes were observed in both field data and model results. In order to make use of both remotely sensed (near surface) and *in situ* (near bed) TSS in the model calibration it was necessary to utilise a 3D model due to the vertical gradients in TSS. This is particularly important for the sediment resuspension process which establishes a near-bed peak in TSS. Furthermore, a secondary circulation that was established due to wind stress was better resolved in the 3D model compared to the 2D model, and this is consistent with recent analytical argument whichsuggests the fundamental assumptions of quasi-two dimensionality break down in shallow seas (Cushman-Roisin & Deleersnijder, 2017).

In this study, effort was focused on identifying the most important model processes and parameters, in particular, the bed schematization and cohesive sediment transport model parameters. Analysis of a broad range of data was used to define the sediment transport model parameters and processes. Hydrodynamic and wave models were set up using the best available bathymetry and metocean forcing for the region. The models were calibrated and validated against available wave and current data and bed shear stress climatology analysed. A sediment transport model was set up using source terms derived from the analysis of dredging logs, and sediment characteristics were based on analysis of baseline and monitoring data. Model sensitivity to different parameters was analysed and model parameters which are important, difficult to establish, or interdependent

were identified. A hindcast of dredge plume evolution was produced. Once calibrated, the model was applied to assess the relative contributions of both the ambient and dredging fine sediment fractions, and methods of translating plume model output into ecologically relevant pressure fields were demonstrated using several statistical measures. Note that due to the lack of detailed habitat data, some of these ecological pressure field calculations are purely hypothetical and for demonstration purpose only, using thresholds derived from a different environment.

A detailed sensitivity analysis of the sediment transport model parameters highlighted the complexity in modelling cohesive sediment transport due to numerous sensitive and interdependent parameters. The final model parameter set and configuration was identified through an extensive set of model simulations that compared qualitatively and quantitatively against observations of TSS, including near-surface TSS derived from remote sensing data from Moderate resolution Imaging Spectroradiometer (MODIS) which was specifically developed for this dredging campaign by Theme 3 Project 3.2, and near-bed TSS derived from the *in situ* monitoring instruments (Project 3.2 final report is available at https://www.wamsi.org.au/dredging-science-node/dsn-reports).

The sediment transport model uses a single fine sediment fraction for the dredged material and a single fine sediment fraction for the ambient sediment. This approach made it feasible to carry out extensive model simulations, enhancing the effectiveness of the investigation of model parameter sensitivity. The use of a single sediment fraction reproduced the initial plume settling and resuspension processes well but was not able to maintain a low background TSS concentration of ~2 mg/L that was observed across the shelf.

The study established that use of a two-layer (fluff and buffer layer) schematisation of the seabed was crucial for adequately reproducing the resuspension of recently deposited dredging fines on the inner shelf region of the study site (between water depths of 7 m and 15 m). We found that resuspension of ambient fine sediments is more sensitive to the parameterisation of the buffer layer while resuspension of dredging fine sediments is more sensitive to the parameterisation of the fluff layer. There exists a complex interaction between the various fluff layer parameters which significantly influences the spatial distribution of dredging fines at the sea bed. Further research is needed to identify the fluff layer model parameter ranges and effective seabed schematisation.

Reproducing the spatial distribution of ambient TSS is challenging due to the large range of bed shear stress present in the study domain and limited information on the spatial availability of fine sediment in the bed. Nevertheless, the model was able to successfully reproduce the TSS dynamics across the majority of the system influenced by passive dredging plumes.

Detailed analysis of dredging logs established the location and timing for over 22,000 separate dredging plumes across eight different operational modes utilised during the dredging campaign. An established empirical source term model was utilised to estimate the fine sediment flux introduced into the water column for each of the plumes. The spatially and temporally varying source terms were validated to ensure mass closure of the fine sediment budget available in the excavation, consistent with the assumed parameterisation of source terms in the empirical model. The crucial calibration parameters to ensure mass closure were the duration of the dredging and placement phases of the dredging cycle. Based on comparison with the measured data, in particular at sites close to the dredging, the empirical model was found to be a reasonable approach to the estimation of source terms.

One challenge in assessing the environmental impact of dredging is in translation of modelled far-field dredging plumes into pressure parameters that are measurable in the field and able to account for the combined effect of both ambient and dredging pressure. For demonstration purpose, the output from the calibrated model was used to estimate pressure fields relevant for coral health and mortality established by DSN Theme 4 (Theme 4 reports are available at https://www.wamsi.org.au/dredging-science-node/dsn-reports). Theme 4 research found strong relationships between coral mortality and several water quality indicators during dredging management near Barrow Island. It is important to note that this case study does not consider the benthic habitats present across the study site and, in that sense, the estimated pressure fields are not indicators of the

pressure fields realised during the dredging campaign. This study highlights the difficulty in applying thresholds developed for different regions and where there is significant variability in the ambient TSS climatology.

The modelling of ambient sediments provides the opportunity to utilise the model to inform the application of thresholds to systems with significant spatial variability in TSS climatology. This depends on the model adequately reproducing the ambient probability distribution of TSS across the system which are impacted by a dredging campaign. Research from Theme 4 identified the importance of assessing both chronic and acute pressure due to dredging, which requires assessment of TSS variance across different temporal scales. This case study considers the 80th and 95th percentiles of the modelled ambient TSS and near-bed light to assess the frequency and duration of potential ecological pressure. The use of model-derived spatially variable percentiles of TSS and light presents a modelling challenge, however, there are significant benefits as model output can be (1) directly compared against measurements, (2) used to select representative baseline and control monitoring sites, and (3) used as an operational tool to identify where the impacts of dredging are likely predictable with water quality metrics, in particular in naturally turbid environments.

Considerations for predicting and managing the impacts of dredging

Improved reporting of model parameters and assumptions

An extensive review of previous EIA modelling studies highlighted significant inconsistency in the reporting of model parameters and assumptions. It is **recommended that key model parameters and formulations be a basic reporting requirement for all EIA dredge plume modelling studies**. It is also **recommended that a brief justification for the selected model formulation or value is provided to develop knowledge of reasonable parameter values and to identify those that have undergone significant sensitivity analysis and calibration**. Often model default values have been subjected to extensive testing and may be appropriate in many contexts.

Establishment of a data reference library for EIA dredge plume modelling

When setting up and validating dredge plume models, modelling practitioners would have a good starting point if they are able to access past datasets gathered in similar circumstances and knowledge of a reasonable range of parameter values that have been documented from earlier studies. It is **recommended that a data library for EIA dredge plume modelling be established and all EIA studies are required to submit modelling data as part of the approval process, including input data, calibration and subsequent validation data, along with key parameter values.** The data library will provide benefits to both the practitioners and regulators by informing valid ranges of model parameters, sample model input and validation data for hindcast studies, and data to assess basic assumptions for source term estimation. The data reference library will provide a key knowledge base for future studies and increased consistency among EIA assessments.

Estimation and reporting of source terms

The estimation of source terms based on empirical models is appropriate at the EIA stage. However empirical models rely on several parameters to distribute the available fines throughout the dredging process and may not account for fines due to ancillary operations/propeller wash. Whilst some of these parameters can be estimated from more detailed models, many parameters remain empirical and need to be estimated using professional judgement and experience. For these reasons it is **strongly recommended that the source term parameters utilised during EIA are reported, validated with a plume characterisation exercise and recorded in the EIA dredge plume modelling data library for future use.**

Number of sediment fractions and settling velocities

Five sediment fractions are likely to be sufficient in many systems to model the combined effects of dredging and ambient fine sediment loads. **It is recommended that the following sediment fractions be utilised for far-field dredging plume models where fine sediment is the primary source of suspended solids: one sand fraction in the buffer layer, with four sediment fractions for fine material: two fractions for natural sediments, two for dredged material.** Due to difficulty in accounting for flocculation and uncertainty around suspended sediment

particle densities, the appropriate parameter to use to describe each fine fraction is the settling velocity, not particle size, although the class of particles are useful references.

For modelling fine sediment fractions in the passive plume, the order of magnitude for settling velocity is typically between 0.01 to 2 mm/s. A lower settling velocity is needed to reproduce the background TSS concentration and a higher settling velocity to reproduce the magnitude of resuspension events (nominally in the range 0.1 to 1 mm/s). Higher settling velocities (> 2 mm/s) are typically only valid very close to dredging sources, where large particles and strong flocculation are present due to the high sediment concentration. In this region the influence of density in the dynamic plume is greater and are not resolved in a far-field model.

It is recognised that the use of additional sediment fractions increases the complexity and uncertainty in the model and model parameters. To establish the mass distribution of the source terms across the sediment fractions is a challenging problem. **It is recommended that the number of sediment fractions be kept to a minimum so that greater effort could be focussed on establishing appropriate model parameters.**

3D modelling.

It is increasingly apparent that three-dimensional modelling is necessary to correctly resolve wind-driven circulation in shallow water. In addition, at locations where the primary driver of resuspension is wave stirring, strong vertical gradients in TSS can be present, and these were observed both in the model and in the data collected from field experiments. **It is recommended that three-dimensional numerical modelling be undertaken unless the two-dimensionality of the flow and passive plume can be demonstrated.** Three-dimensional modelling will become increasingly important with the growing use of remote sensing techniques for model validation and operational monitoring.

Ecological pressure field prediction and modelling of ambient sediment dynamics

The modelling of ambient sediment dynamics in the dredging plume model significantly improves the utility of model predictions and comparison against baseline data. Through modelling both the ambient and dredging suspended solids, model results can be directly compared to monitoring data. When the ambient sediment dynamics are validated and model error well characterised, shifts in the cumulative probability distribution of modelled TSS at each point can be examined, which could be a more robust approach to characterisation of the pressure field rather than single thresholds at the sites. Furthermore, in order to assess the combined impact of both ambient and dredging TSS it is essential to resolve the ambient TSS. **It is strongly recommended that the modelling of ambient suspended solids dynamics be undertaken as part of the EIA process.** The modelling of the ambient suspended solids dynamics also assists in establishing the reasonable range of several critical model parameters associated with resuspension and the sea-bed schematisation. In addition, it assists in establishing the relative contribution of dredging to TSS.

It should be noted that it is problematic to apply the thresholds derived from other regions or locations due to the significant variability in TSS dynamics that may be present between the sites. In addition, significant spatial variability in TSS can be present within a site due to variations in depth, exposure (to winds and waves) and sediment availability.

Initialising ambient sediments at the seabed.

The accuracy of the ambient TSS model is strongly influenced by the availability of fine sediment at the seabed. A reasonable approach to estimate the sediment distribution at the bed is to undertake a so-called ‘warm up’ simulation for a sufficient duration so that the modelled availability of fines at the seabed reaches some dynamic equilibrium with the modelled bed shear stress forcing. Depending on the system this can take a significant period of model time (up to several model years) which requires that natural sediment fluxes into the model domain be adequately resolved. **It is recommended that baseline data collection be expanded to include additional spatial sampling in surficial sediment particle size distributions**. This data collection would assist in establishing the initial conditions for sediment cover and could be informed by the numerical modelling to span the range in bed shear stress climatology and natural sediment supply.

Calibration/validation of the model.

It is recommended that model calibration and validation is performed on relevant variables, such as residual currents and TSS and near-bed light, in addition to assessment of tidal water levels, tidal currents and waves. It is often more important (from an ecological perspective) to reproduce the cumulative probability distribution of a parameter rather than capture individual events. As such a quantile-quantile plot can be more informative than a typical scatter plot, where small errors in the phase of an event (i.e. dredging plume release or resuspension) can significantly affect a scatter plot or model skill calculation.

Bed shear stress in vegetated canopies

The presence of seabed canopies can significantly alter the shear stress imparted on the bed within the canopy. Work undertaken as part of the DSN Theme 3 research program in Project 3.3 has developed a new model to predict the reduction in bed shear stress caused by the presence of the canopy which significantly alters the in-canopy sediment fluxes compared to bare sediment beds (Project 3.3 final report is available at https://www.wamsi.org.au/dredging-science-node/dsn-reports). However, measurements of the spatial distribution of canopy density was insufficient to appropriately schematise these processes in the far field model. In addition, Project 3.3 have been developed for carbonate sands in rigid coral reef environments and require further development and field scale testing for the fine cohesive sediments that comprise passive dredging plumes. The effects of macroscopic roughness on sediment transport has been examined in detail in Project 3.3; the implementation and validation of the models developed in that project into coastal-scale numerical models is a logical extension of this work. In the interim it may be possible to utilise the passive plume model results as a boundary condition in simple 1D modelling of sedimentation and erosion for specific canopies that are predicted to be impacted, and where additional field work can be undertaken to estimate the required canopy properties.

Residual knowledge gaps

Fluff layer model parameters

The use of a fluff layer model was essential in the Wheatstone Project case study to reproduce the resuspension of freshly deposited, more easily eroded dredging fines on the inner shelf, due to the large range in shear stress forcing across the shelf. It is difficult to systematically establish the model parameters required by a fluff layer model due to the complex interaction of numerous parameters. The choice and combination of model parameters have a significant impact on the mass distribution at the seabed and resuspension processes. **Further research is required to identify reasonable model parameter combinations and seabed schematisations for the broad range of coastal systems present across Western Australia.**

Sediment transport model parameter estimation

Interdependence of model parameters, particularly in the cohesive sediment transport models, makes model sensitivity analysis, parameter estimation and calibration challenging. **Further research into model parameter estimation techniques for sediment transport models is required.** Such approaches require improvements in the scalability and computational efficiency of hydrodynamic and sediment transport models to make effective use of the growth in computational capacity and parallelisation.

Best-case and worst-case scenarios

The establishment of ‘best case’ and ‘worst case’ scenarios remains a challenge for EIA. Whilst assessment of the metocean conditions of the site remains a critical step in appropriately defining likely current and wave forcing scenarios, **further research is required to investigate the application of input reduction techniques commonly applied in morphological models to passive dredging plume models**. Whilst best- and worst-case scenarios must be developed within the context of the specific details of the dredging site and program, the likelihood of significant resuspension events should be assessed against the cumulative deposition likely associated with the full dredging program. This should be assessed for conditions with a high and low probability of exceedance.

Dynamic Plume

Where high-protection-value ecological systems are present in close proximity (< ~2 km) to the dredging activities, it is necessary to consider the impacts of the dynamic plume. Whilst not addressed in detail in this study, **further research is required to advance dynamic plume modelling in order to better predict the extent and thickness of dynamic plumes at the seabed in a computationally efficient manner that can be applied during an EIA study**. It is noted that significant advancement in the modelling of the dynamic plume associated with hopper overflow has been achieved in de Wit (2014), and the parametric model developed in that work is appropriate for informing the estimation of overflow source terms.

Wind forcing that resolves sea/land breeze

The accuracy of wind forcing is critical for estimating the residual currents and locally generated seas. The development of high-resolution meteorological models which are capable of resolving sea breeze or assimilating local met station wind data will be beneficial for providing appropriate mesoscale and local forcing.

1 Introduction

Dredge plume modelling is often used in Environmental Impact Assessment (EIA) of large-scale port and coastal developments to quantify and model the transport and fate of sediments released during dredging operations. The modelling is used to describe the spatial extent and intensity of the 'pressure' field generated by dredging related activities, including how it develops and changes over time. The model results are frequently used in biological response models to predict the consequences of the estimated pressure field on the health of benthic communities and their habitats which may be particularly sensitive, such as coral reefs and seagrass meadows.

Whilst fundamental to the predictions of environmental impact, dredge plume modelling at the EIA stage is challenging due to limited available information such as model input data and detailed information of the dredging campaign is often not known. There are significant benefits to be gained by improving the modelling process so that proponents have more clarity around appropriate data requirements and standards for model calibration and validation, and environmental regulators have greater confidence when making decisions based on modelling outputs.

As part of the Western Australian Marine Science Institution (WAMSI) Dredging Science Node (DSN) Theme 2/3, the Numerical Modelling Project 3.4 sought to provide insight and guidance to improve dredge plume dispersal and fate modelling. Under the agreement with WAMSI, Chevron Australia Pty Ltd (here after referred to as Chevron) provided unprecedented access to its baseline, dredging and monitoring data from the Wheatstone Project.

Prior to the start of the research program our understanding of the accuracy of dredge plume transport and fate modelling undertaken to support the EIA was poor. There is a lack of consistency among EIA modelling studies, such as lack of a consistent approach for model calibration and validation, evaluation of model skills, number of sediment fractions needed. There are knowledge gaps in the sediment plume modelling, such as a lack of understanding on sources of model uncertainty, source terms, model parameters and their appropriate range of values, settling velocities, modelling of ambient sediment, and approach to determine plume propagation.

At the commencement of the research project, literature review was conducted to benchmark current understanding (Sun et al 2016). A two-part large field program was undertaken in 2013 and 2014 during the Wheatstone Project to collect environmental data for optical, hydrodynamic and sediment transport model calibration and validation during the inshore and offshore dredging campaigns.

Effort focused on modelling the dynamics and fate of total suspended solids (TSS) in the passive dredging plume, with the goal of identifying the most important processes and model parameters, in particular, the bed schematization and cohesive sediment transport model parameters. The modelling approach is consistent with what is typically applied in EIA and assessed how effectively the observed TSS dynamics could be reproduced by the model. Detailed data analysis was completed to obtain the estimates for model parameters from the available data and additional targeted field and laboratory data collection exercises.

Importantly, the research program was undertaken to ensure the model output variables, and their representations and analyses, were compatible with the critical effects thresholds (e.g. 14-day running mean of daily light integral and turbidity, 60-day running mean of deposition, percentage exceedance of deposition, light and turbidity, maximum number of consecutive days of stress exceedance) that were being generated by the biological themes of the WAMSI DSN.

In this report, we will first describe the study site and the data provided, and environmental conditions of the study site using information from the available datasets and knowledge acquired through literature review. We then describe the models used for this study and their set up. Next, we present the results from hydrodynamics and wave models. We then present the analysis of the datasets which informed the setup of the sediment transport model. Next, the results from the sediment transport modelling was presented. In Discussion and Conclusions, we summarize the major findings and discuss alternative explanations, caveats and limitations, and

elaborate on practical advances and relevance of findings and implications for management. Finally, we suggest future research based on our study and conclude with key findings.

2 Data and Methods

2.1 Study site

The Wheatstone Project, located 12 km west of Onslow (in the Pilbara region of Western Australia), involved the dredging of sediment and rock to establish an access channel, berth pocket and trenching for a gas trunkline to supply the Liquid Nitrogen Gas (LNG) plant at Ashburton North. This study specifically addressed the dredging associated with the access channel, turning basin and berth pocket (28 million cubic meters) with the study site (Figure 1) extending from North West Cape to Barrow Island. The dredging associated with the trunkline was not included in this study.

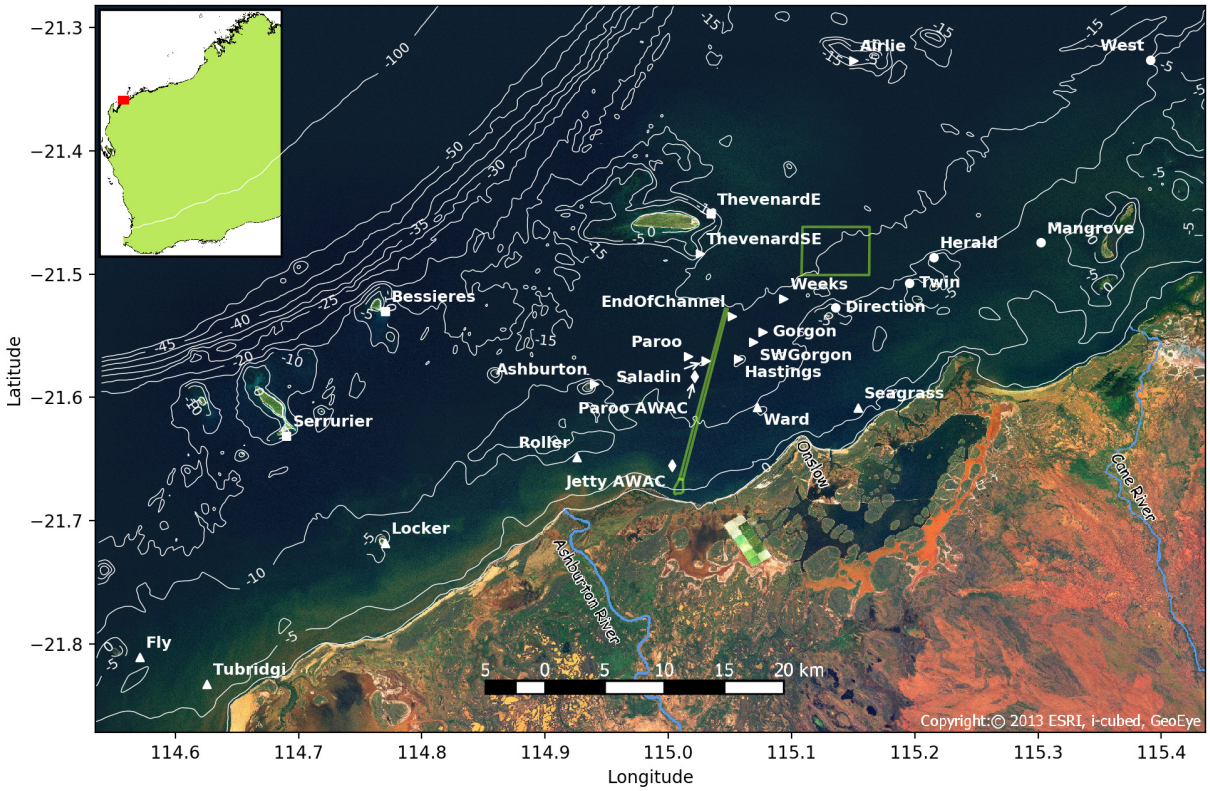

Figure 1. Study site and locations of fixed monitoring stations. (◆) are wave/current measurement instruments and the various groups of water quality monitoring stations: (▲) Nearshore, (▶) Inner Shelf, (●) Eastern islands and (■) Offshore. Green lines demark the access channel and Spoil Ground C locations of the Wheatstone Project. White lines are labelled contours of seabed level (m MSL).

2.2 Data

Data from a range of sources were compiled and analysed for use in the study. As part of the agreement with the WAMSI DSN, Chevron made available a significant range of datasets including electronic and daily dredging logs, current meters, Conductivity Temperature Depth (CTD) measurements, turbidity (NTU) sensors, photosynthetically active radiation (PAR) sensors, sediment traps and multi-beam bathymetric survey data. The data generally covered the baseline period (May 2011 through to March 2013) and the dredging period (April 2013 through to January 2015).

A summary of the fixed monitoring station instrumentation is provided in Table 1 with a map of their locations. The fixed monitoring stations were deployed for a baseline data collection period from May 2011 to March 2013. Dredging commenced in April 2013 and continued until January 2015. The Wetlabs ECO NTU sensors were located approximately 1.1 m above the seabed. CTD, NTU and PAR data was logged at a half hourly interval and

provided with quality control flags. It was evident that intermittent spikes in the NTU data had not been captured in the supplied quality flags. A running median filter with a window size of 5 samples was applied to the NTU data to remove spikes and the data averaged to an hourly interval for comparison against the model.

A detailed analysis of the water quality data collected during the baseline and dredging period of the Wheatstone Project was undertaken by Wahab et al. (2017). This included a cluster analysis of the measured turbidity data in order to group sites with similar variability in turbidity. Conceptually, the cluster analysis segmented the sites into four group (Nearshore, Inner Shelf, Eastern Islands and Offshore). These groups were adopted for the purposes of this study:

- Nearshore sites: generally in water depth < 8 m Mean Sea Level (MSL) and adjacent to the mainland;
- Inner Shelf sites: depths between 8 m to 25 m MSL;
- Eastern Island sites: located east of the dredging adjacent to islands; and
- Offshore sites: adjacent to islands located near the 50 m MSL depth contour (shelf break).

In addition to the fixed monitoring stations, ten mobile water quality monitoring stations were managed by the Wheatstone Project dredging contractor and deployed at a range of locations depending on where dredging was occurring at different time (see Table 2 and Figure 2).

Sediment traps were recovered at a one to two-month time interval, in conjunction with mooring servicing activities. The material accumulated in each trap was dried and weighed to calculate sediment trap accumulation rate. The particle size distribution of trapped material was determined via laser diffraction (Mastersizer3000) for size fractions < 500 µm; and wet sieving for size fractions > 500 µm.

A 14-year-long derived TSS dataset for the Pilbara region using Moderate resolution Imaging Spectroradiometer (MODIS) satellite was developed by Project 3.2 and the reader is referred to Dorji et al. (2016) for detailed discussions. This covered the February 2000 to December 2016 period. The years 2013 and 2014 were utilised for comparison against the upper layers of the numerical model and complemented the near bed *in situ* measurements of TSS to constrain parameter estimates of fine sediment settling velocity and resuspension. The MODIS TSS data was analysed within 10 polygons to extract a time series of TSS within each polygon based on the average TSS for valid pixels within the respective polygon (Figure 3). The same valid pixel mask was applied to the modelled near surface TSS for comparison against the MODIS TSS. Whilst the MODIS TSS product provided reasonable estimates of near surface TSS, from time to time the cloud masking algorithm applied generated a spurious fringing effect that introduced noise into the dataset with an example provided in Figure 4. It is noted that for remote sensing of TSS within a dredge plume, the 'depth of penetration' of the sensor, or more correctly, the depths from which the sensor can detect light, depends on the water turbidity but is usually of the order of a few metres or less. Therefore, only the near surface TSS from the model output is compared with MODIS TSS in this study.

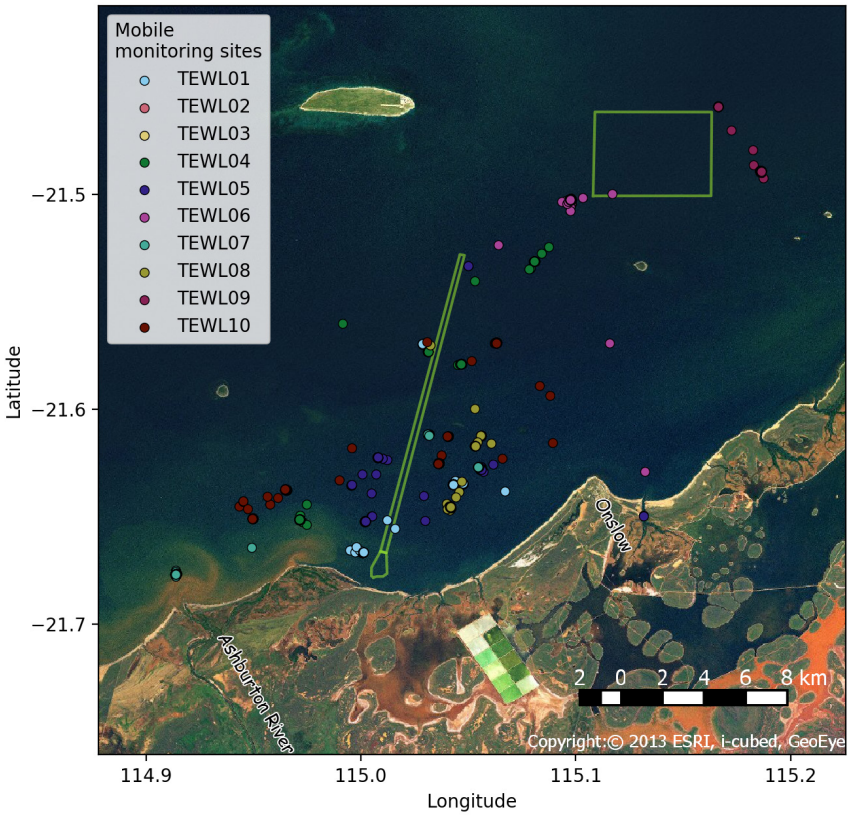

Figure 2. Locations of mobile water quality monitoring stations at various times throughout the dredging campaign. Green lines demark the access channel, Spoil Ground C and trunkline locations of the Wheatstone Project.

Table 1. Details of fixed monitoring stations. Groups are defined based on the cluster analysis of Wahab et al. (2017).

Site Name	Group	Instrument/Equipment	Sensor Depth (m)	Latitude	Longitude	Start Date	End Date
Jetty AWAC	-	Nortek AWAC	7.8	-21.6552	115.0036	1/11/2011	17/06/2014
Paroo AWAC	-	Nortek AWAC	9.9	-21.5833	115.0213	20/11/2011	13/11/2013
Airlie	Inner shelf	Wetlabs ECO NTU, PAR, CTD, Sediment Traps	6.3	-21.3270	115.1502	19/05/2011	27/02/2015
Ashburton	Inner shelf	Wetlabs ECO NTU, PAR, CTD, Sediment Traps	9.5	-21.5891	114.9401	20/05/2011	27/02/2015
Bessieres	Offshore	Wetlabs ECO NTU, PAR, CTD, Sediment Traps	7.5	-21.5300	114.7704	21/05/2011	27/02/2015
Direction	Offshore	Wetlabs ECO NTU, PAR, CTD, Sediment Traps	7.3	-21.5270	115.1354	21/05/2011	27/02/2015
EndOfChannel	Inner shelf	Wetlabs ECO NTU, PAR, CTD, Sediment Traps	12.1	-21.5343	115.0518	18/05/2011	27/02/2015
Fly	Nearshore	Wetlabs ECO NTU, PAR, Pressure	10.6	-21.8105	114.5711	7/11/2012	27/02/2015
Gorgon	Inner shelf	Wetlabs ECO NTU, PAR, CTD, Sediment Traps	10.8	-21.5470	115.0769	18/05/2011	27/02/2015
Hastings	Inner shelf	Wetlabs ECO NTU, PAR, CTD, Sediment Traps	4.7	-21.5690	115.0569	17/05/2011	27/02/2015
Herald	Eastern islands	Wetlabs ECO NTU, PAR, CTD, Sediment Traps	7.2	-21.4865	115.2153	18/05/2011	27/02/2015
Locker	Nearshore	Wetlabs ECO NTU, PAR, CTD, Sediment Traps	5.9	-21.7180	114.7705	21/05/2011	27/02/2015
Mangrove	Eastern islands	Wetlabs ECO NTU, PAR, Pressure	8.4	-21.4745	115.3022	4/11/2012	27/02/2015
Paroo	Inner shelf	Wetlabs ECO NTU, PAR, CTD, Sediment Traps	7.3	-21.5667	115.0164	20/05/2011	27/02/2015
Roller	Nearshore	Wetlabs ECO NTU, PAR, CTD, Sediment Traps	9.2	-21.6485	114.9259	20/05/2011	27/02/2015
SWGorgon	Inner shelf	Wetlabs ECO NTU, PAR, CTD, Sediment Traps	9.8	-21.5550	115.0690	20/05/2011	27/02/2015
Saladin	Inner shelf	Wetlabs ECO NTU, PAR, CTD, Sediment Traps	6.7	-21.5702	115.0306	17/05/2011	27/02/2015
Seagrass	Nearshore	Wetlabs ECO NTU, PAR, CTD, Sediment Traps	5.8	-21.6086	115.1538	11/04/2013	27/02/2015
Serrurier	Offshore	Wetlabs ECO NTU, PAR, CTD, Sediment Traps	6.5	-21.6312	114.6903	21/05/2011	27/02/2015
ThevenardE	Offshore	Wetlabs ECO NTU, PAR, CTD, Sediment Traps	7.2	-21.4512	115.0343	20/05/2011	27/02/2015
ThevenardSE	Inner shelf	Wetlabs ECO NTU, PAR, CTD, Sediment Traps	8.8	-21.4834	115.0259	20/05/2011	27/02/2015
Tubridgi	Nearshore	Wetlabs ECO NTU, PAR, Pressure	6.7	-21.8326	114.6257	7/11/2012	27/02/2015
Twin	Eastern islands	Wetlabs ECO NTU, PAR, CTD, Sediment Traps	6.8	-21.5075	115.1958	18/05/2011	27/02/2015
Ward	Nearshore	Wetlabs ECO NTU, PAR, CTD, Sediment Traps	5.6	-21.6077	115.0720	17/05/2011	27/02/2015
Weeks	Inner shelf	Wetlabs ECO NTU, PAR, CTD, Sediment Traps	11.9	-21.5199	115.0937	18/05/2011	27/02/2015
West	Eastern island	Wetlabs ECO NTU, PAR, CTD, Sediment Traps	9.8	-21.3263	115.3912	18/05/2011	27/02/2015

Table 2. Details of mobile 'Sentinel' monitoring stations deployed during the dredging campaign.

Site Name	Instrument/Equipment	Start Date	End Date
TEWL01	Wetlabs ECO NTU	11/04/2013	12/01/2015
TEWL02	Wetlabs ECO NTU	24/01/2014	12/01/2015
TEWL03	Wetlabs ECO NTU	10/04/2014	30/12/2014
TEWL04	Wetlabs ECO NTU	11/04/2013	12/01/2015
TEWL05	Wetlabs ECO NTU	11/04/2013	26/06/2014
TEWL06	Wetlabs ECO NTU	11/04/2013	24/01/2014
TEWL07	Wetlabs ECO NTU	11/04/2013	12/01/2015
TEWL08	Wetlabs ECO NTU	11/04/2013	12/01/2015
TEWL09	Wetlabs ECO NTU	01/05/2013	12/01/2015
TEWL10	Wetlabs ECO NTU	11/04/2013	12/01/2015

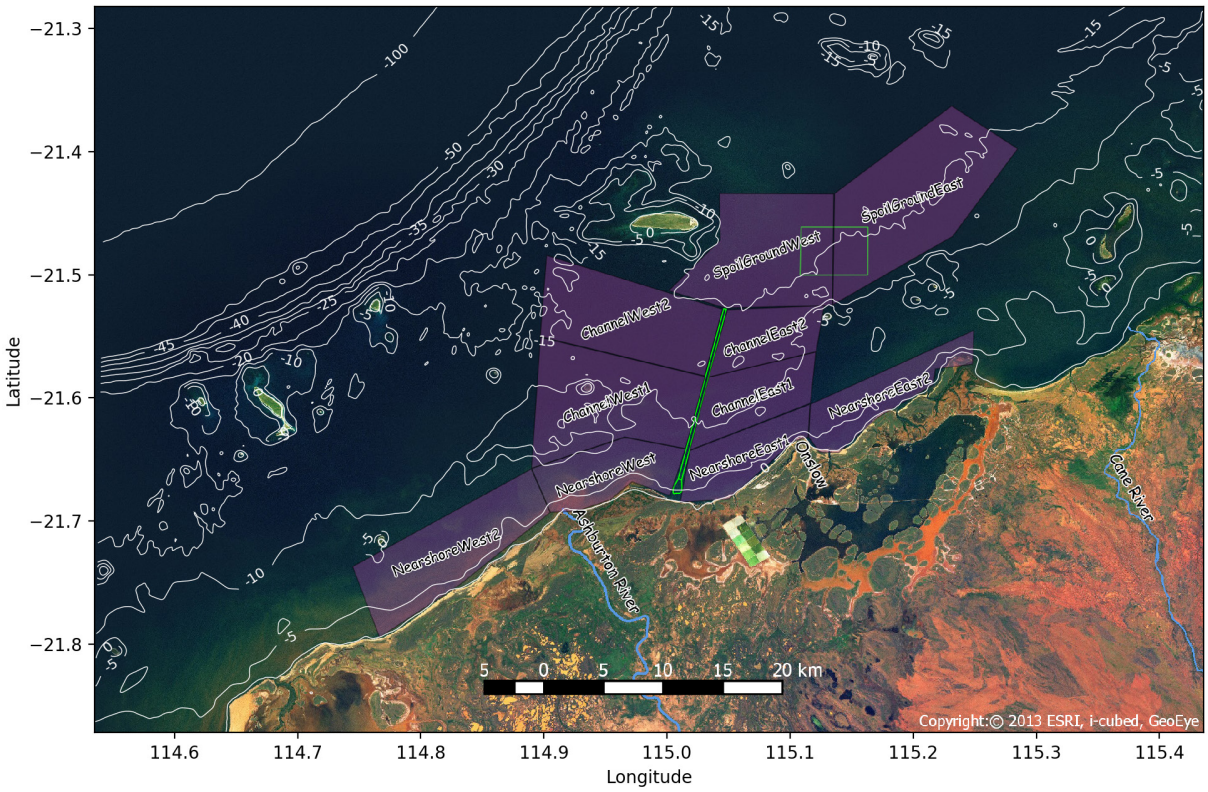

Figure 3. Polygons defined for time series comparison between MODIS TSS and modelled TSS. The valid pixel mask from each MODIS TSS image was applied to the modelled near surface TSS with each polygon.

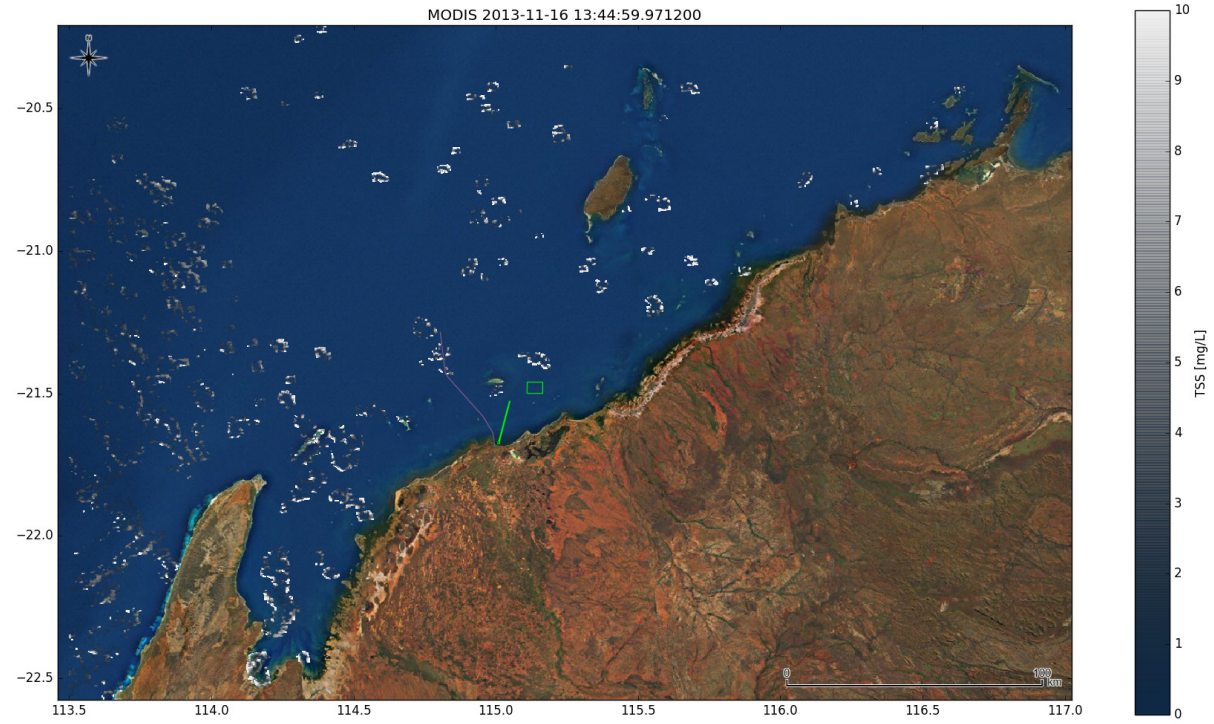

Figure 4. Example MODIS TSS image with noise introduced due to the cloud masking algorithm applied in the generation of the dataset. This impacts the model comparison from time to time. Green lines demark the access channel, Spoil Ground C and trunkline locations of the Wheatstone Project.

2.3 Metocean conditions

The southern part of the North West (NW) Shelf (south west of Barrow Island) has a tidal range (mean high water springs to mean low water springs) of 1.9 m at Onslow (Department of Transport 2017). Peak tidal currents occur during spring tide on the inner shelf but have a relatively low magnitude of up to 0.3 m/s. Localised areas of strong currents are present around islands and headlands.

Prevailing winds are from the southwest during the wet season (September to April) with winds shifting south easterly during the dry season (May to August) (Condie et al. 2006). Earlier work by Webster (1985a, 1985b) demonstrated that the inner shelf circulation was predominantly barotropic and associated with the excitation of continental shelf waves by the wind. Numerical modelling undertaken in Condie et al. (2006) also indicates that sub-tidal circulation on the shelf is driven by the wind.

Figure 5 presents an overview of the measured data obtained between May 2011 and February 2015. Daily depth-averaged currents at the Jetty AWAC location demonstrated a general seasonal pattern, eastward in the wet season and westward in the dry season but was punctuated by intermittent reversals that correlated with changes in the wind direction. This is particularly significant during cyclonic periods (Table 3) where tropical cyclones Lua, Narelle and to a lesser degree Mitchell generate strong south westerly currents during the wet season.

The NW Shelf is one of the most active regions for tropical cyclone occurrence in Australia with an average of 2-3 tropical cyclones per year occurring between November and April (Condie et al. 2009). Recent work by Dufois et al. (2017) has highlighted the importance of cyclones in driving a sediment pathway on the shallow inner shelf (< 20 m depth) towards the south west. This is highlighted in Figure 5 where the increased wave activity during the cyclonic periods drive strong increases in turbidity across all measurement sites, roughly in phase with the strong south-westerly currents. Sediment transport modelling undertaken in Margvelashvili et al. (2006) also indicate a general south-westward sediment transport pathway on the inner shelf and export of fine sediment off the shelf, which is roughly balanced by an intermittent input of fine sediment from the rivers on the NW Shelf. There is no clear correlation between rainfall and observed turbidity (Figure 5), with increases in wave height associated with cyclone activity being the dominant forcing process which results in up to two orders of magnitude increases in turbidity.

Table 3. Tropical cyclones passing within 550 km of Onslow during the baseline and dredging periods and distance, central pressure and cyclone wind speed at each cyclones closest position.

Name	Date	Distance (km)	Central Pressure (hPa)	Maximum mean wind speed (m/s)
Heidi	12/01/2012	331	990	20.6
Iggy	29/01/2012	418	975	25.7
Lua	13/03/2012	318	996	15.4
Mitchell	30/12/2012	501	989	23.2
Narelle	12/01/2013	405	941	48.9
Peta	23/01/2013	239	994	15.4
Rusty	26/02/2013	506	944	46.3
Christine	30/12/2013	207	973	30.9

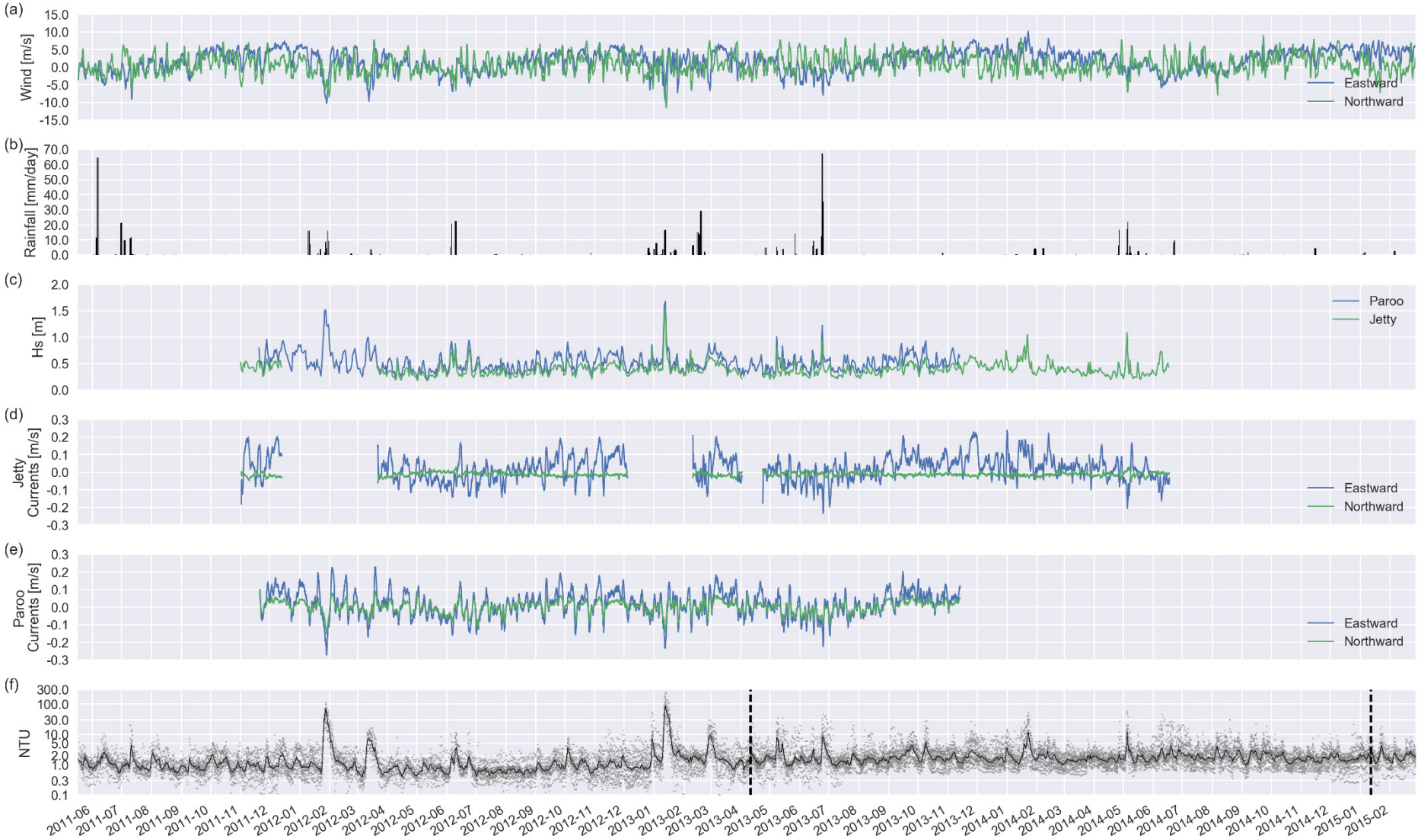

Figure 5. Overview of measured data obtained during the baseline and dredging periods. (a) Measured daily averaged winds at Onslow. (b) Measured daily rainfall at Onslow. (c) Significant wave height at Paroo and Jetty locations. (d) Daily mean depth-averaged currents at Jetty. (e) Daily mean depth-averaged currents at Paroo (f) Measured turbidity across all fixed monitoring stations. The black line is the median across all sites and the vertical dashed lines indicate the start and end of the period of the dredging campaign.

2.4 Numerical Model

2.4.1 Hydrodynamic and wave model

A coupled Delft3D/SWAN hydrodynamic and wave model was developed for the study site, with the Delft3D flow model two-way dynamically coupled to the SWAN wave model to allow for feedback between the wave and flow models. The Delft3D model has been applied to a broad range of systems to study sediment transport dynamics including, Columbia River Delta in the United States (Lesser et al. 2004), Ems Estuary in the Netherlands (van Maren et al. 2015 and van Maren & Cronin 2016) and extensively in the assessment of environmental impacts associated with dredging in Australia and overseas (e.g. Bettington & Miles 2009, Provis & Aijaz 2009, Aarninkhof & Luijendijk 2010).

A detailed description of the Delft3D model system is provided in Deltares (2014a, 2014b) and only a brief description of the model is provided here. Delft3D solves the unsteady shallow-water equations in two or three dimensions on a rectilinear or curvilinear boundary fitted grid. In 3D the vertical grid is defined using the σ coordinate approach. The model can be used to predict flow in shallow seas, coastal areas, estuaries, lagoons, rivers and lakes. The equations of motion are discretised using finite differences on an Arakawa C-grid and integrated in time using an Alternating Direct Implicit (ADI) method in the horizontal direction and a fully implicit method in the vertical to prevent time-step limitations in very shallow regions. It implements a range of horizontal advection schemes and turbulent closure models, with the cyclic advection scheme (Stelling & Leendertse 1992) and k-ε turbulence closure model utilised in this study.

The Simulating WAves Nearshore (SWAN) model is a third-generation spectral wave model that implements a fully implicit solution scheme (Booij et al. 1999). The SWAN model is based on the discrete spectral action balance equation and computes the evolution of random, short crested waves in coastal regions within deep, intermediate and shallow water including wave current interaction. The model accounts for the processes of refraction, wind growth, white capping, bottom friction, depth induced breaking and non-linear wave-wave interactions.

2.4.2 Sediment transport model

Delft3D provides numerous approaches to bed schematisation and sediment transport. The focus of this study is on nearshore cohesive fine sediment dynamics. The modelling of cohesive sediment transport is based on the Partheniades-Krone formulation (Partheniades, 1965) where the depositional flux of water column sediment to the bed is given by:

$$D_0 = w_s . c_b . S_d(\tau_{cw}, \tau_{cr,d}) \quad (1)$$

Where D_0 is the depositional flux [kg m^{-2} s^{-1}], w_s is the settling velocity, c_b is the average concentration in the near bottom computational layer (in 2D the entire water column) and S_d is a deposition step function given by:

$$S_d(\tau_{cw}, \tau_{cr,d}) = \begin{cases} \left(1 - \frac{\tau_{cw}}{\tau_{cr,d}}\right), & \tau_{cw} < \tau_{cr,d} \\ 0, & \tau_{cw} \geq \tau_{cr,d} \end{cases} \quad (2)$$

Where τ_{cw} is the combined wave-current bed shear stress and $\tau_{cr,d}$ is an empirically derived bed shear stress threshold above which no deposition occurs.

The erosive flux (E_0) from the bed to the water column is given by:

$$E_0 = M_0 . S_e(\tau_{cw}, \tau_{cr,e}) \quad (3)$$

Where E_0 is the erosive flux [kg m^{-2} s^{-1}], M_0 is the erosion parameter [kg m^{-2} s^{-1}] and S_e is an erosion step function given by:

$$S_e(\tau_{cw}, \tau_{cr,e}) = \begin{cases} 0, & \tau_{cw} < \tau_{cr,e} \\ \left(\frac{\tau_{cw}}{\tau_{cr,d}} - 1\right), & \tau_{cw} \geq \tau_{cr,e} \end{cases} \quad (4)$$

Where $\tau_{cr,e}$ is an empirically derived bed shear stress threshold below which no erosion occurs. If the bed shear stress threshold for deposition is set to be very large, deposition of sediment is allowed to occur continuously.

In addition, Delft3D has recently been extended to include the two-layer (2L) bed model of van Prooijen et al. (2007) and van Kessel et al. (2011). The 2L model implements an algorithm for the buffering of fines in a sandy seabed. The model consists of a thin upper layer of more easily erodible fine sediment (the fluff layer) and a single well-mixed under layer of sand (the buffer layer) into which fine sediment can infiltrate (see Figure 6). Equations 3 remain the same for erosion of fine sediment from the buffer layer. Erosion from the fluff layer is modelled by:

$$E_1 = M_f(\tau_{cw} - \tau_{cr,f}) \quad (5)$$

Where E_1 is the erosive flux from the fluff layer, $\tau_{cr,f}$ is a critical shear stress threshold for erosion of the fluff layer and M_f is the fluff layer erosion parameter given by:

$$M_f = \min(mM_1, M_2) \quad (6)$$

Where m is the mass of fine sediment in the fluff layer, $M_1$is the first order erosion parameter for the fluff layer and M_2 the zero-order erosion parameter for the fluff layer.

Deposition to the fluff and buffer layers is controlled by introducing parameter α which defines what percentage of deposition occurs to the different layers:

$$D_0 = \alpha . w_s . c_b \quad (7)$$

$$D_1 = (1 - \alpha) . w_s . c_b \quad (8)$$

Fine sediment is deposited predominantly to the fluff layer, as such $\alpha \ll 1$.

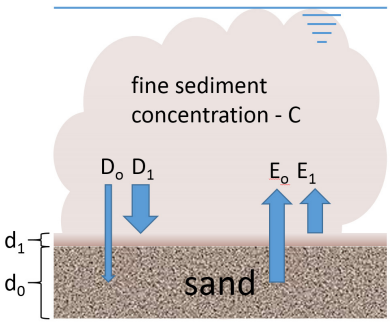

Figure 6. Schematic diagram of the two-layer model. Layer 1 is the thin fluff layer and layer 0 is the sandy seabed infiltrated with fines. d_i = thickness of layer, D_i = deposition flux towards layer i, E_i = erosion flux from layer i (i=0,1) and C = suspended solids concentration.

A key feature of the 2L model is the first order erosion rate of fine sediment from the fluff layer which scales with the mass available in the layer and transitions from first order to zero order at $m = M_2/M_1$ kg/m^2. The justification for this is that for small values of m the seabed is not completely covered with mud and will scale linearly with increasing mass up to a point where the seabed is fully covered and adding more fine sediment will not increase the erosion rate further.

A total of three sediment fractions were utilised in the model. One sand fraction with a median grain size of 200 µm, one cohesive sediment fraction for natural fine material already present in the system and one cohesive sediment fraction for fine material introduced due to dredging through the source terms defined in Section 4.1. The number of sediment fractions utilised in EIA studies varies widely, this study investigates the capacity to reproduce the modal sediment transport dynamics with a single fine sediment fraction. Additional sediment fractions further compound the complexity and data requirements of the sediment transport model which makes interpretation of the model results and dynamics increasingly difficult, often confounding model parameter estimates as the mass distribution between the fractions is difficult to establish.

3 Hydrodynamic model setup and results

3.1 Grid

The hydrodynamic model grid is curvilinear with a variable spatial resolution of approximately 200 m in the proximity of the dredging activities increasing smoothly to 1,500 m at the outer boundaries (Figure 7). The model grid extends approximately 300 km in the alongshore direction from North West Cape to the Dampier Archipelago and 100 km in the offshore direction with the offshore boundary approximately following the 150 m depth contour. The hydrodynamic grid has 10 sigma layers in the vertical direction with thicknesses 4%, 6%, 9%, 13%, 18%, 18%, 13%, 9%, 6% and 4%. The vertical resolution is refined near the bed and near the surface to better resolve the influence of bed shear stress and wind shear stress at the surface.

The wave model has two nested rectilinear girds, a 2500 m resolution outer grid to transfer wave energy from the Indian Ocean to the shelf and a 500 m resolution grid covering the inner shelf region, extending from North West Cape to Barrow Island (Figure 8).

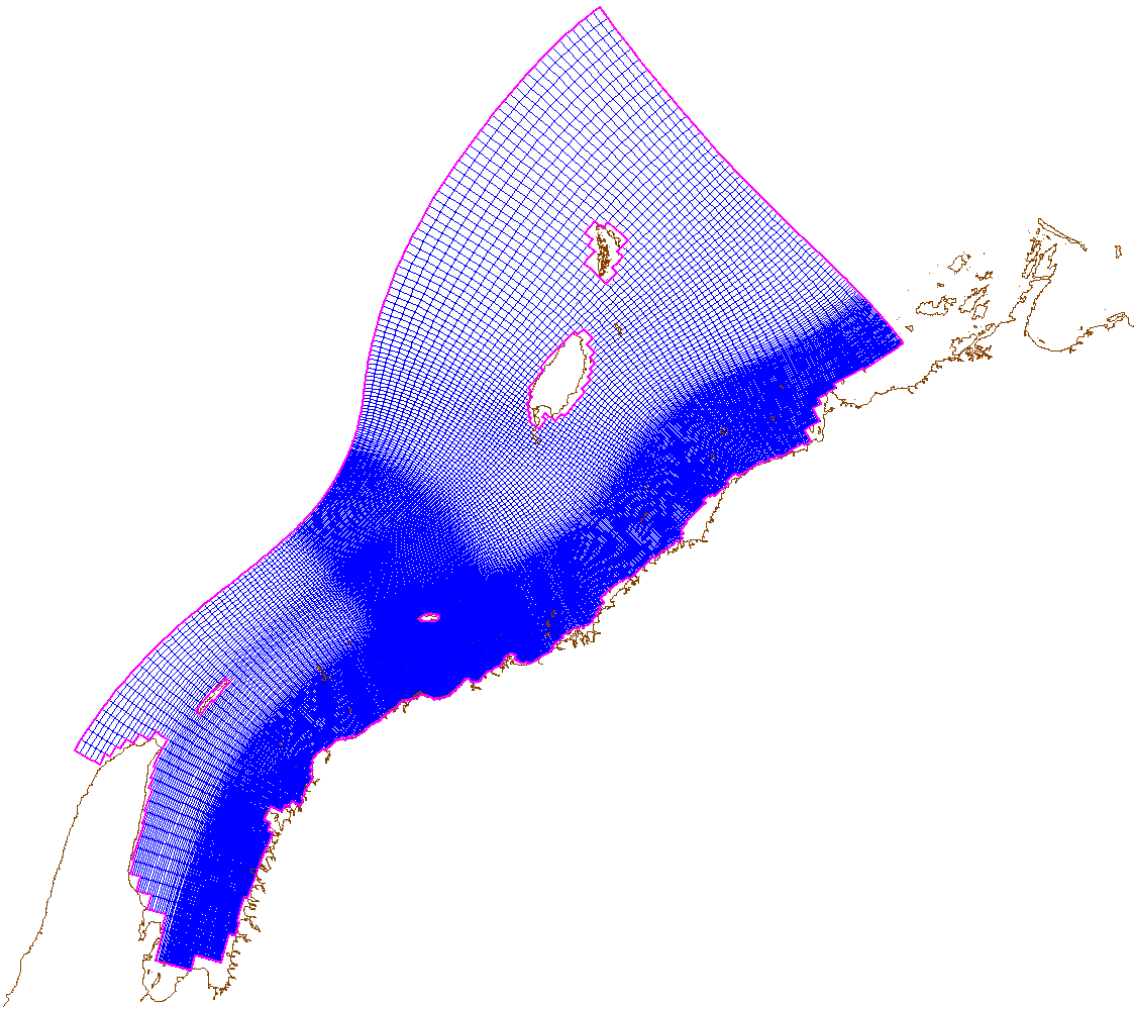

Figure 7. Overview of the curvilinear hydrodynamic model grid utilised in this study. The grid has a resolution of approximately 1500 m at the outer boundary and 200 m in the proximity of the dredging activities.

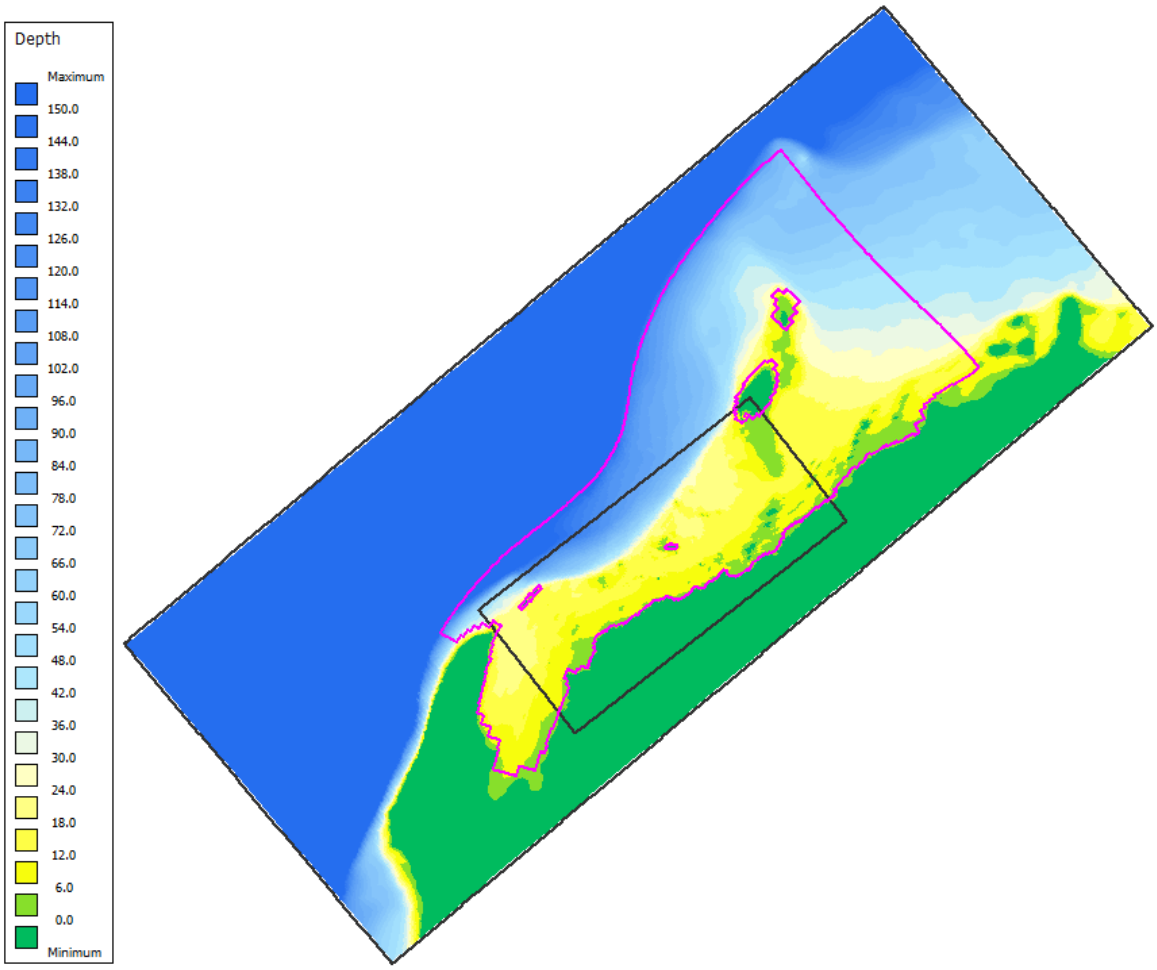

Figure 8. Model grid extents and bathymetry as depth below 0 m AHD (black – wave model grids, magenta – hydrodynamic model grid). Maximum depth has been truncated for display purposes only.

3.2 Bathymetry

A broad range of bathymetric datasets were obtained for the study in order to develop the best possible digital elevation model for the region (see Figure 9). These datasets include:

- Multibeam bathymetric survey data from Chevron along Wheatstone Project channel route;
- Coastal topographic survey from Entrance Point to Beadon Creek;
- Fugro airborne LiDAR bathymetry datasets of the NW Shelf of Australia;
- S57 Survey Data;
- Geoscience Australia Multi-beam Data;
- Australian Hydrographic Office Charts AUS064, AUS743 and AUS744;
- Geoscience Australia 250m Bathymetric Grid; and
- NASA SRTM (to fill in land elevations).

Data was corrected to consistent horizontal and vertical datums and the boundaries between datasets carefully buffered to ensure smooth transitions between datasets of different accuracy and resolution. In addition, to improve the representation of the numerous small islands, reefs and channels in the nearshore region, navigational charts were digitized to ensure appropriate grade break lines were incorporated to improve the representation of sudden depth changes, for example due to the presence of reef patches. The final digital elevation model had a resolution of 100 m (Figure 10) and was averaged onto the model grids.

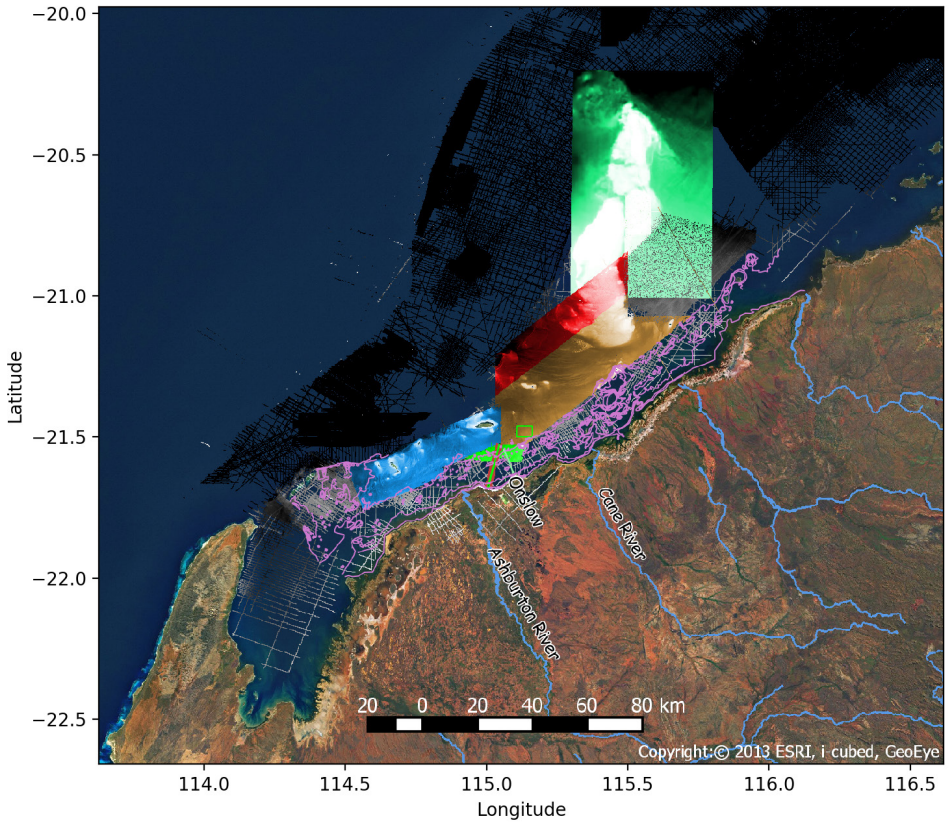

Figure 9. Overview of various bathymetric data sets compiled in the study.

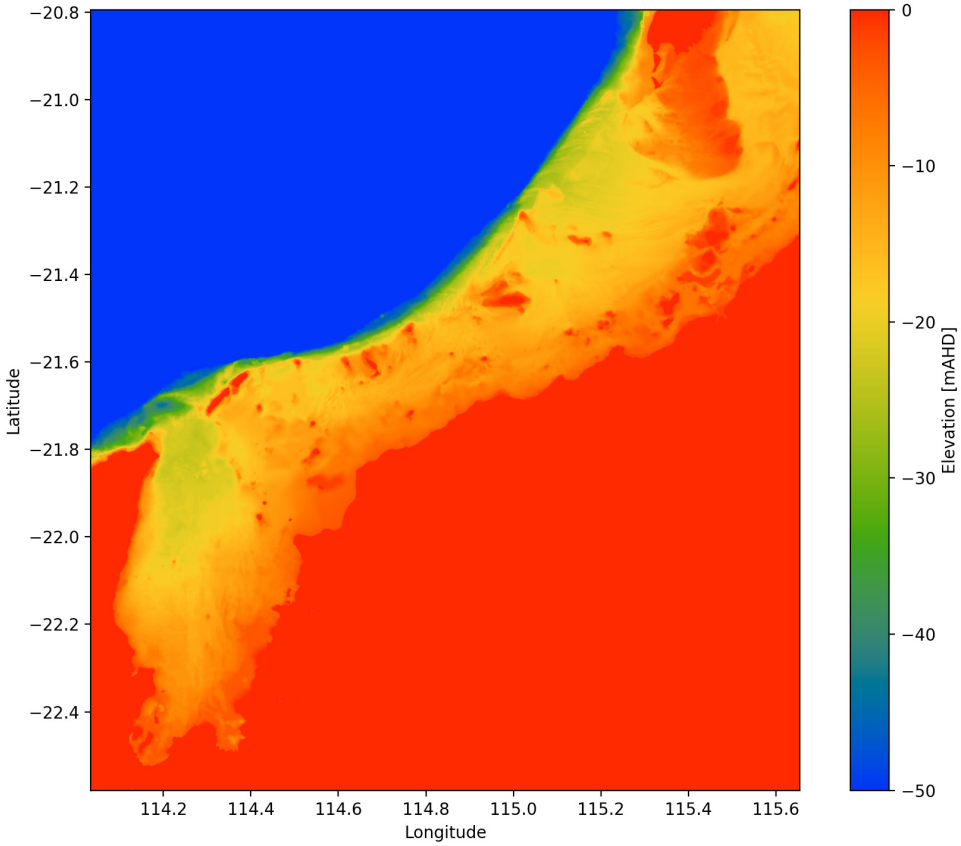

Figure 10. Example of the detailed 100 m resolution digital elevation model developed for the study. Elevation range is truncated to increase contrast of the shallow shelf region.

3.3 Forcing

The outer wave grid was forced using spatially variable frequency and directional spectra from the CAWCR Wave Hindcast (Durrant et al. 2014) at an hourly interval with winds applied from the Australian Bureau of Meteorology ACCESS-R model. Whilst the ACCESS-R model has a reasonable spatial resolution of 11 km, it did not resolve intermittent local wind events that generated local seas up to 1 m significant wave height.

Astronomic tide boundary conditions are provided by the Oregon State University inverse tide model (v8) (Egbert and Erofeeva 2002) with 13 constituents (M2, S2, N2, K2, K1, O1, P1, Q1, M4, MM, MF, MS4 and MN4) applied to 5 km segments on the outer boundary.

The hydrodynamic model is nested within the Bluelink Re-analysis model (BRAN2015) which has a horizontal resolution of 0.1° (~10 km) with 51 vertical z-depth layers (Oke et al. 2013). The BRAN2015 model provides the large-scale baroclinic forcing associated with the regional geostrophic flow at a daily interval. The 'ocean heat flux' model (Gill 1982, Lane 1989) is applied with hourly meteorological forcing (wind, sea level pressure, air temperature, relative humidity and cloudiness) from the ACCESS-R model. Fresh water input from terrestrial runoff was not readily available as model input and was not included.

3.4 Skill metrics

Statistical measures of model performance seek to provide a quantitative basis by which to compare models with observations. A recent review of model performance metrics (Willmott et al. 2012) identifies a general form of dimensionless measures of average error, $\rho = 1 - \delta/\mu$ where δ is the average error magnitude and μ is a basis of comparison. The selection of δ determines how well the average error will be represented, while the choice of μ determines the lower limit as well as the sensitivity of ρ to changes in δ. The upper limit of ρ is 1, indicating perfect agreement whilst the lower limit is typically 0, -1 or -∞. Different skill metrics can produce vastly different results depending on the distribution of errors and observations, with the consensus being that no single model skill metric provides a universal measure of the performance of a model. We apply several model skill metrics commonly utilised in hydrodynamic model validation in order to assess the performance of the models. We emphasize that model skill scores should not be used to replace other means of model-data comparison (such as spatial maps and time series) and professional judgement when assessing model performance.

Willmott (1981) index of agreement:

$$d = 1 - \frac{\sum_{i=1}^{n}(P_i - O_i)^2}{\sum_{i=1}^{n}(|P_i - \bar{O}| + |O_i - \bar{O}|)^2}$$

Willmott et al. (2012) refined index of agreement:

$$d_r = \begin{cases} 1 - \dfrac{\sum_{i=1}^{n}|P_i - O_i|}{2\sum_{i=1}^{n}|O_i - \bar{O}|}, \text{ when } \displaystyle\sum_{i=1}^{n}|P_i - O_i| \le 2\sum_{i=1}^{n}|O_i - \bar{O}| \\ \dfrac{\sum_{i=1}^{n}|O_i - \bar{O}|}{2\sum_{i=1}^{n}|P_i - O_i|} - 1, \text{ when } \displaystyle\sum_{i=1}^{n}|P_i - O_i| > 2\sum_{i=1}^{n}|O_i - \bar{O}| \end{cases}$$

Nash & Suttcliffe (1970) coefficient of efficiency:

$$NS = 1 - \frac{\sum_{i=1}^{n}(P_i - O_i)^2}{\sum_{i=1}^{n}(O_i - \bar{O})^2}$$

Mean squared error:

$$MSE = \frac{1}{n}\sum_{i=1}^{n}(P_i - O_i)^2$$

Model bias:

$$BIAS = \frac{1}{n}\sum_{i=1}^{n} P_i - \frac{1}{n}\sum_{i=1}^{n} O_i$$

and correlation coefficient:

$$CC = \frac{\sum_{i=1}^{n}(P_i - \bar{P})(O_i - \bar{O})}{\sqrt{\sum_{i=1}^{n}(P_i - \bar{P})^2}\sqrt{\sum_{i=1}^{n}(O_i - \bar{O})^2}}$$

where P are the model prediction and O are the observations.

It is noted that NS is also equivalent to the coefficient of determination and when compared to a reference experiment (as opposed to data) the skill score of Murphy (1992).

3.5 Hydrodynamic and wave model calibration

The hydrodynamic and wave models were calibrated for the January to June 2014 period. Sensitivity analysis was conducted on the key model processes and parameters that effect the modelled bed shear stress and residual currents, being the two critical processes driving the fate of the passive dredging plumes. For the SWAN wave model these included the wave bottom friction formulation, wave friction coefficient and white-capping model. For the hydrodynamic model the sensitivity to grid resolution, baroclinic forcing, sigma layer resolution, horizontal eddy viscosity and bed shear stress coefficient were assessed. Due to the focus of this study being the modelling of the passive dredging plumes the results of these sensitivity analyses are not presented. Table 4 presents a summary of the key model processes and parameters applied in the wave and hydrodynamic models.

The effect of alternative gridding strategies for the hydrodynamic model (domain decomposition versus single domain) is presented in Branson and Sun (2017). Whilst the water levels are better predicted with a higher resolution domain decomposition approach (due to a better resolved bathymetry) the sub-tidal currents in the near-shore region are reproduced equivalently well by the lower resolution single domain grid. Due to the different parallelisation implementations and the lower resolution the single domain model has approximately an order of magnitude better computational performance and was utilised in this study.

Due to the lack of freshwater input into the model it was considered that the inner shelf density dynamics would be poorly represented and earlier work by Webster (1985a and 1985b) demonstrated the inner shelf circulation is barotropic and driven predominantly by wind forced continental shelf waves. Therefore, the influence of baroclinic forcing was tested by comparing the model performance running in both baroclinic mode and barotropic mode (with the BRAN2015 model providing current and water level forcing only).

A key component of the error in a passive plume model is error in advection and how this error integrates over time. One approach to assess this error is the use of a progressive vector plot which takes the time integral of currents past a point and assesses the error in displacement after some time interval. An example for the period 20 May 2014 to 29 May 2014 at the Jetty AWAC location is presented in Figure 11 for a simulation with and without baroclinic forcing enabled. The displacement error after a given interval of time is dependent on the initial time and duration of integration. Figure 12 presents a violin plot of the advection error from 5000 randomly selected initial times and durations of integration for the calibration period (January to June 2014) at the Jetty AWAC location. The north/south error is reduced by excluding baroclinic forcing whilst the east/west error is increased. Assuming that fine material released during dredging has a settling velocity on the order of 0.1 mm/s (8.64 m/day, neglecting turbulent mixing) the timescale of persistence of initial plumes is likely in the order of 1 to 3 days for the 10 to 20 m deep inner shelf region. Over a 1 to 3-day timescale the east/west error associated with the exclusion of baroclinic forcing is reasonably comparable, however the north/south error is markedly reduced. On this basis and due to the reduced computational cost of a barotropic model, baroclinic forcing was excluded from the model.

Table 4. Overview of key wave and hydrodynamic model processes and parameters.

Description	Value/model applied
White capping model	Westhuysen (2007)
Wave bottom friction model	Collins (1972)
Wave bottom friction coefficient	0.015
Hydrodynamic bottom roughness formulation	White-Colebrook (z_0)
Bottom roughness coefficient	0.001 m
Horizontal eddy viscosity coefficient	5 m^2/s
Vertical turbulence closure model	k-ε
Model for bottom shear stress due to waves and currents	van Rijn (2007)

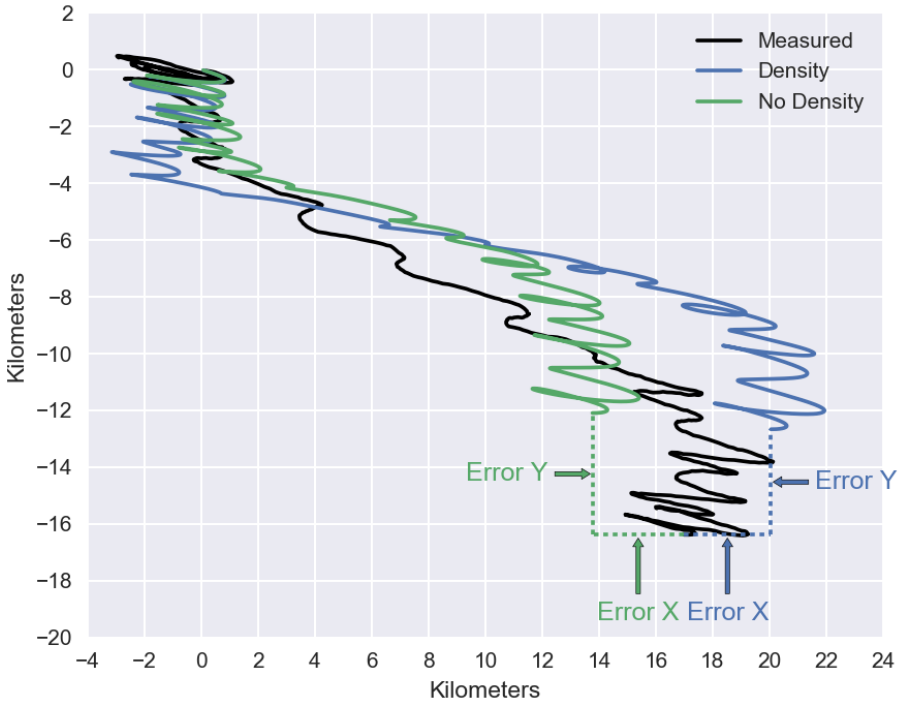

Figure 11. Progressive vector plot of time integrated depth-averaged currents for the period 20 May 2014 through 29 May 2014 at the Jetty AWC location. The baroclinic simulation is labelled 'Density' and the barotropic simulation 'No Density' with the east/west (X) and north/south (Y) errors in displacement calculated against the measured data.

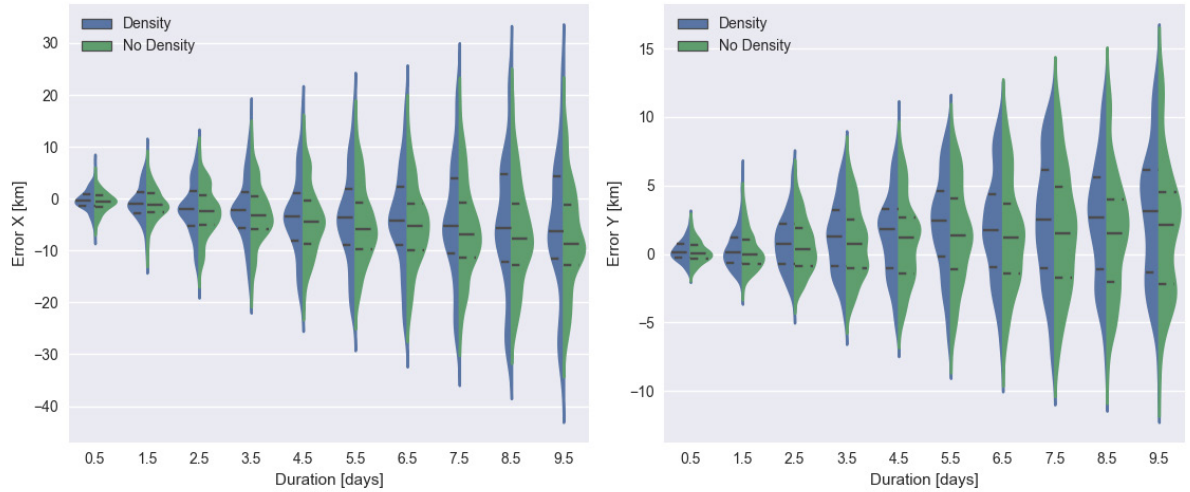

Figure 12. Violin plot of east/west (left) and north/south (right) advection error at the Jetty AWAC location from 5000 randomly selected starting times and integration durations for the simulation period 10 January 2014 through 14 June 2014. Solid lines indicate the median of each PDF and dashed lines the interquartile range. The north/south error is reduced in the nearshore when baroclinic forcing is excluded from the model, however the east/west error is increased.

3.6 Wave simulation result

Figure 13 presents a time series comparison of the modelled and measured significant wave height (Hs) and peak wave period (Tp) at the Jetty AWAC location for the period January 2014 through June 2014. Figure 14 presents a quantile-quantile comparison and scatter density plot of the modelled versus the measured Hs and mean wave period (T_{m01}) at the Jetty AWAC location. A quantile-quantile plot compares the cumulative probability distribution of the measured data to the model. Overall agreement between the model and measurements is very good. Wave heights have a slight positive bias, particularly in the upper percentiles. As indicated by the plots of wave period, the site is predominantly exposed to locally generated seas, with the broad continental shelf and numerous islands providing significant sheltering from ocean swell.

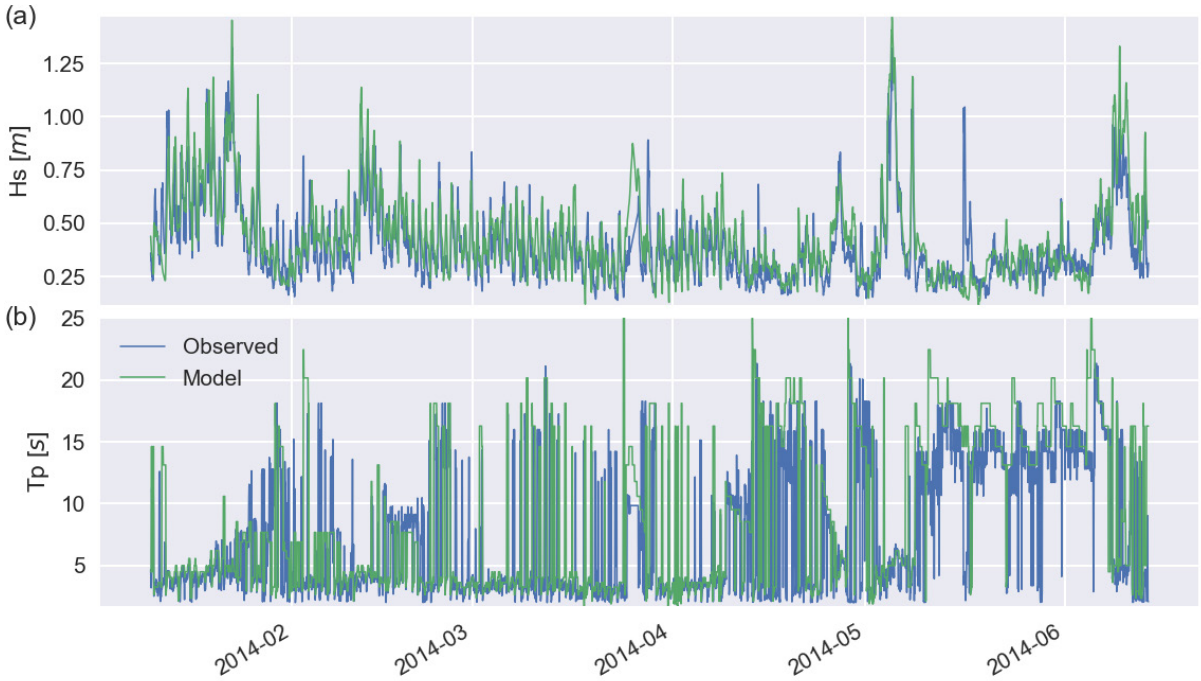

Figure 13. Comparison of modelled and measured time series of (a) significant wave height (Hs) and (b) peak wave period at the Jetty AWAC location.

The negative bias in the mean wave period is likely somewhat due to contribution from higher frequency energy resolved in the model (1 Hz) compared to the measured data (2 Hz). Investigation of individual mismatches suggest that error in the modelled wind contribute significantly to errors in wave height (i.e. 16 May 2014), which is to be expected in situations where strong locally generated wind events occur that are not resolved by the ACCESS-R model gird (11 km resolution).

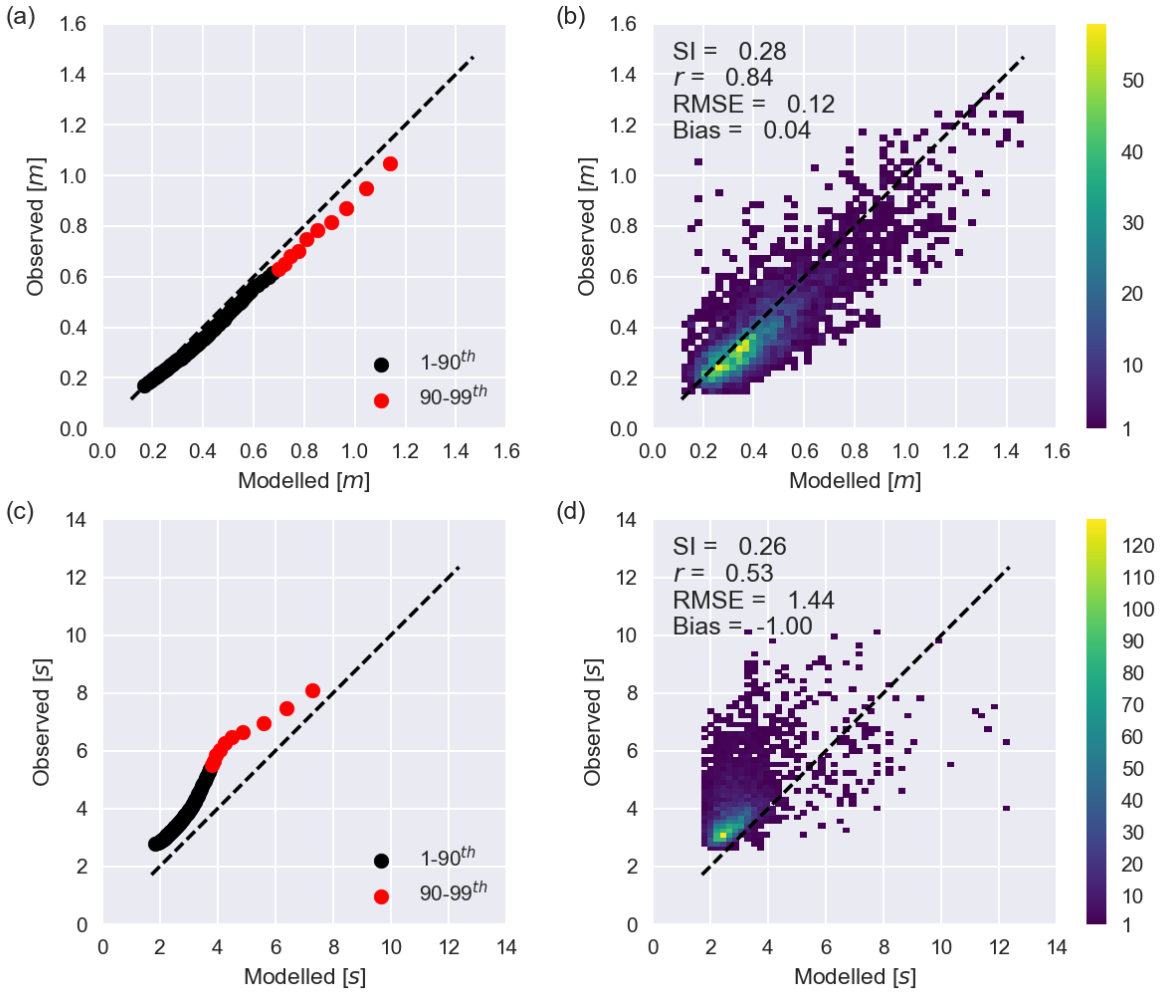

Figure 14. Comparison of modelled and measured wave conditions. (a) QQ-plot and (b) scatter density plot for significant wave height. (c) QQ-plot and (d) scatter density plot for mean wave period (Tm_{01}) at the Jetty AWAC location. A Quantile-Quantile plot compares the cumulative probability distributions of the measured data to the model. The colour bar indicates the number of samples within each bin of the scatter density plot.

3.7 Currents and water levels simulation results

Figure 15 presents a time series comparison of the modelled and measured water levels and depth-averaged currents at the Jetty AWAC location. Figure 16 presents a quantile-quantile comparison and scatter density plot of the modelled and measured water level and depth-averaged currents at the Jetty AWAC location. Measured water level is reproduced very well by the model with high skill (Nash-Sutcliffe skill score (NS) of 0.93), no bias and low root mean squared error (RMSE of 0.13 m).

Peaks in the depth-averaged currents were under estimated however with little overall bias. Depth-averaged current model skill is very good in the east-west (along shore) direction (0.9) and reasonable (0.48) in the north-south (cross shore) direction with strong correlation. It should be noted that the measured north-south depth-averaged current is strongly influenced by high-frequency variability that is not present in the model. This observed high-frequency variability could be due to measurement noise or an unresolved cross shelf process (Figure 17), however the dominant tidal circulation is reproduced very well.

Figure 18 presents the subtidal east-west and north-south depth-averaged currents at the Jetty AWAC location. Subtidal depth-averaged currents were calculated by a fifth order low pass Butterworth filter with a cut off period of 23.5 hours. The phasing and magnitude of the dominant east-west subtidal currents is reproduced well with very strong correlation (0.93) and high skill (NS = 0.82). The model tends to underestimate peaks in the eastward currents. The north-south subtidal current is reproduced less well, however it is noted that the Jetty AWAC location is close to shore (approximately 3 km) resulting in the magnitude of the north-south subtidal current typically being very small (< 0.05 m/s).

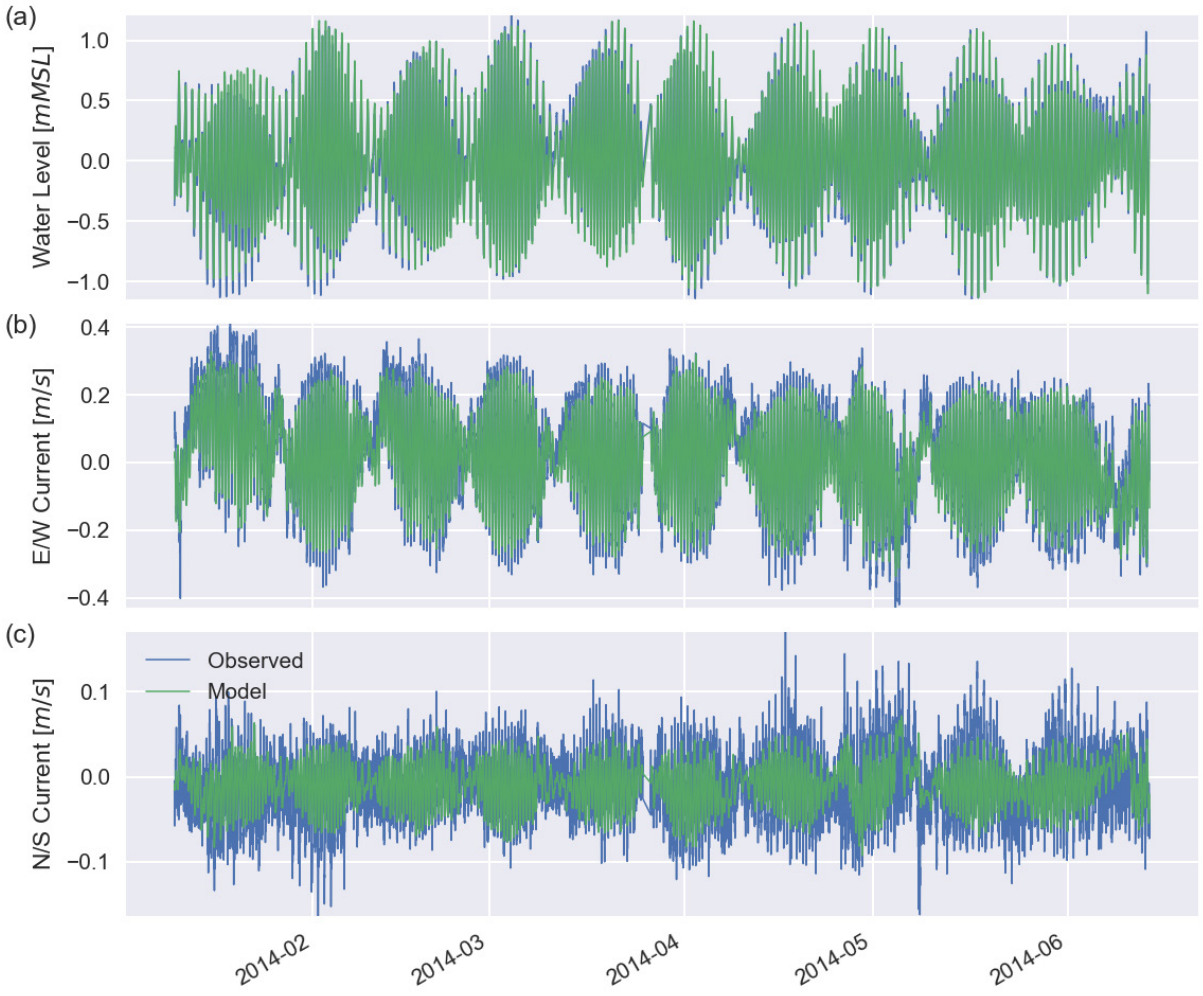

Figure 15. Comparison of modelled and measured time series of (a) water level, (b) depth-averaged east/west currents and (c) depth-averaged north/south currents at the Jetty AWAC location. Note the y-scale is different in (b) and (c).

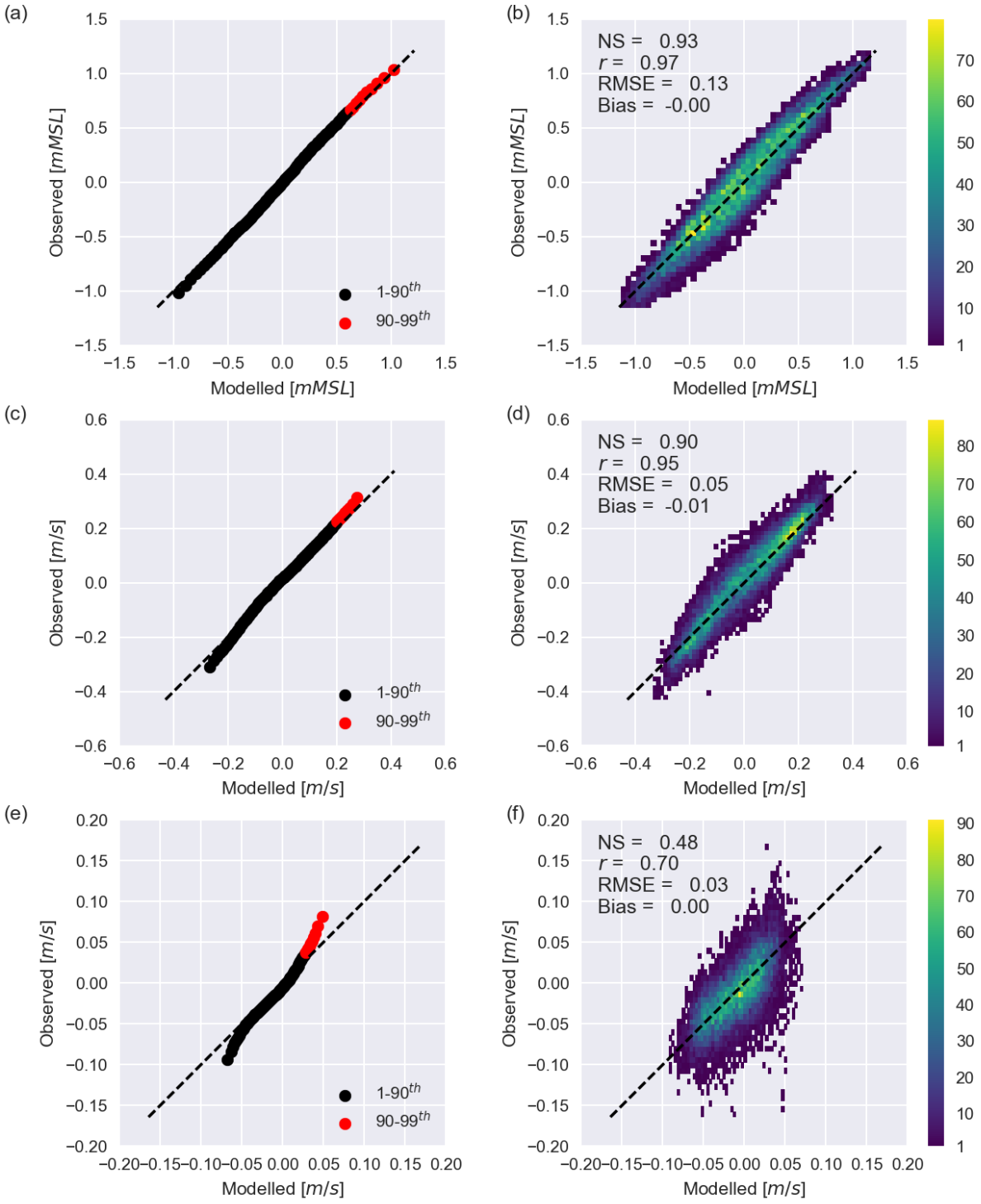

Figure 16. Comparison of modelled and measured hydrodynamics. (a) QQ-plot and (b) scatter density plot for water level. (c) QQ-plot and (d) scatter density plot for east/west depth-averaged currents. (e) QQ-plot and (b) scatter density plot for north/south depth-averaged currents at the Jetty AWAC location. A Quantile-Quantile plot compares the cumulative probability distributions of the measured data to the model. The colour bar indicates the number of samples within each bin of the scatter density plot.

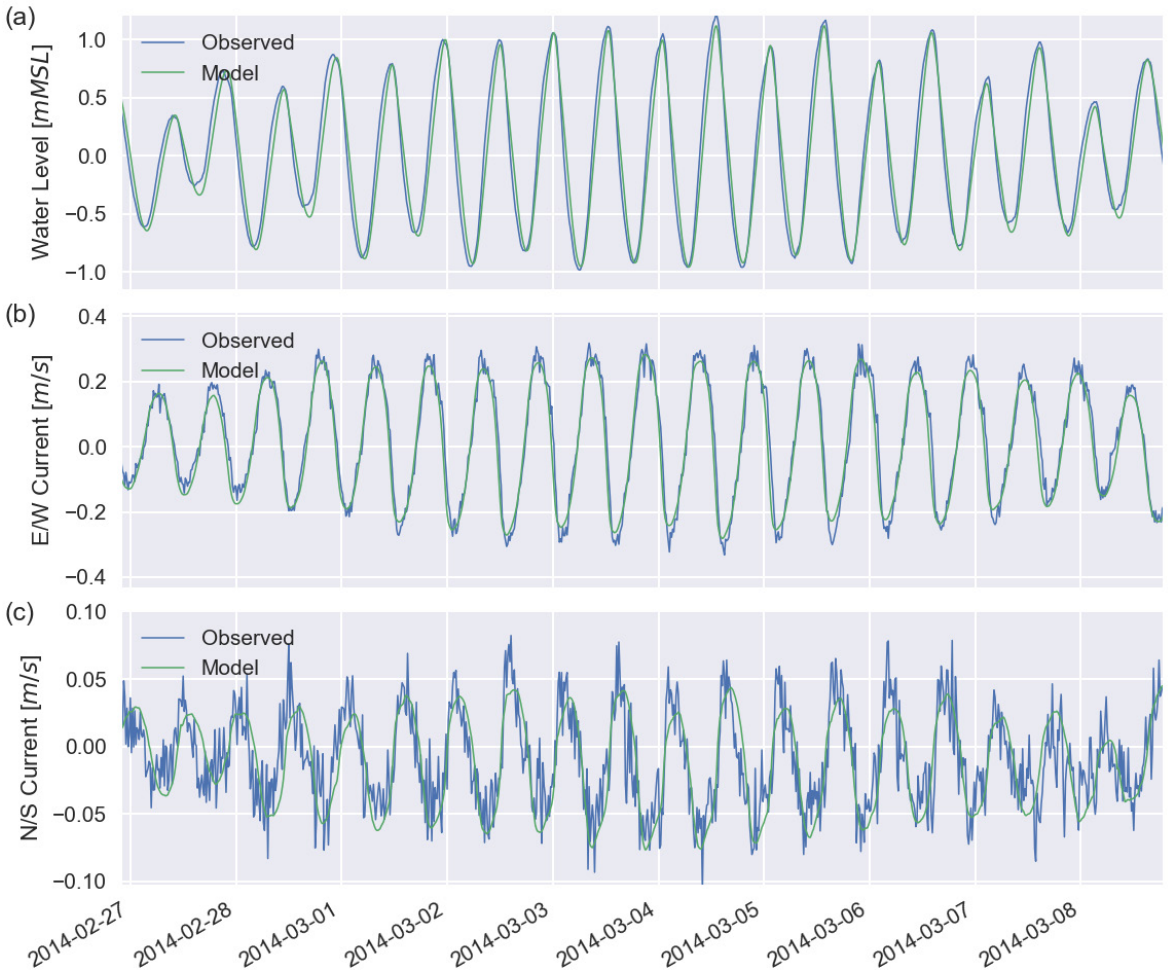

Figure 17. Comparison of modelled and measured time series of (a) water level, (b) depth-averaged east/west currents and (c) depth-averaged north/south currents at the Jetty AWAC location for the period 27 February 2014 through 8 March 2014. Note the y-scale in (c) is much smaller than in (b).

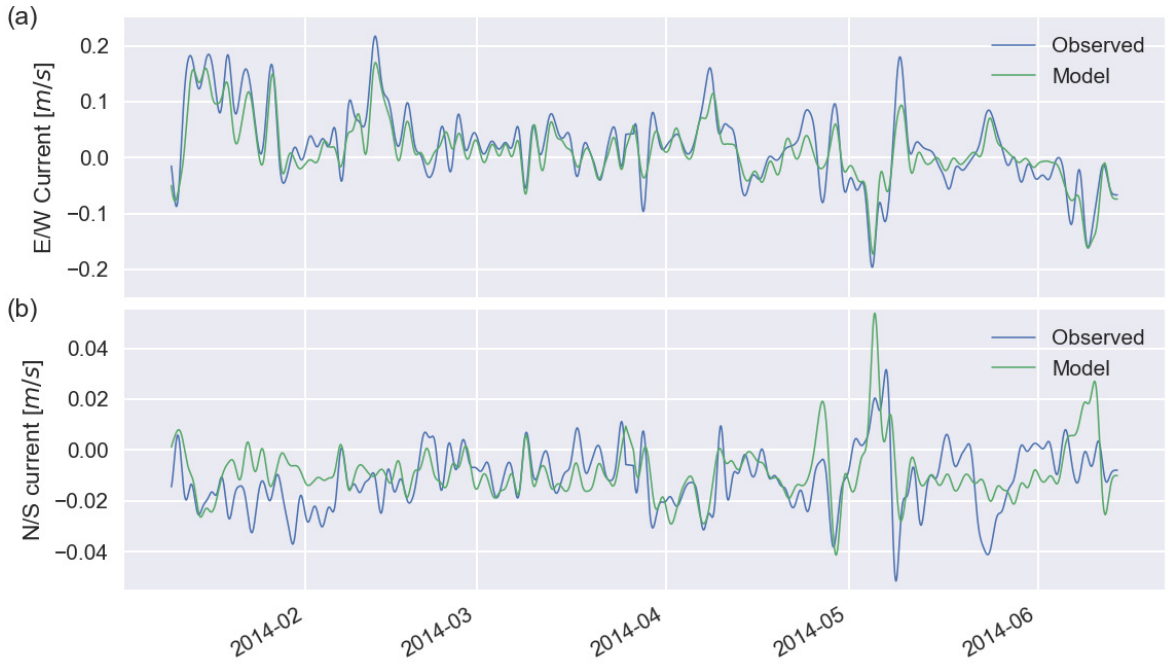

Figure 18. Comparison of modelled and measured subtidal currents obtained from a fifth order low pass Butterworth filter with a cut off period of 23.5 hours. (a) East-west and (b) north-south depth-averaged subtidal currents at the Jetty AWAC location. Note the y-scale in (b) is much smaller than in (a).

3.8 Combined wave-current bed shear stress climate

Whilst the inner shelf region around Onslow is significantly sheltered from long period swell due to the broad shelf and numerous islands, as demonstrated in Section 2.3, wave activity is still the primary driver of turbidity dynamics in the region. The bed shear stress due to waves on the sea bed is a function of wave conditions and water depth. Figure 19 presents the modelled mean combined wave-current bed shear stress over the period April 2013 through December 2013. The magnitude of bed shear stress is strongly correlated with water depth. Figure 20 presents a time series and cumulative probability density of bed shear stress at the EndOfChannel and Jetty AWAC locations. Due to the wave forcing being predominantly short period the bed shear stress climatology changes significantly, particularly for percentiles greater than 70%. The bed shear stress climatology is particularly important when defining bed shear stress thresholds for erosion of the fluff and buffer layers.

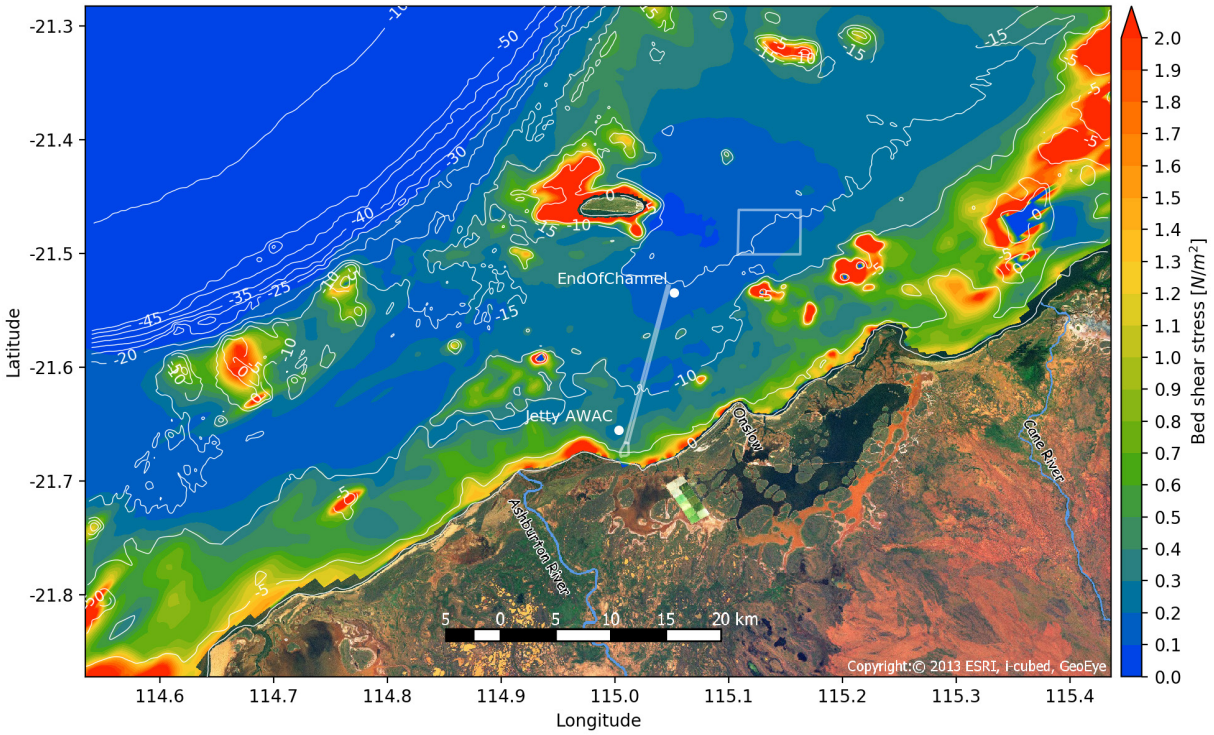

Figure 19. Filled contour plot of modelled mean bed shear stress over the period 1 April 2013 through 31 December 2013. The mean modelled bed shear stress is highly correlated with the bed level on the inner shelf.

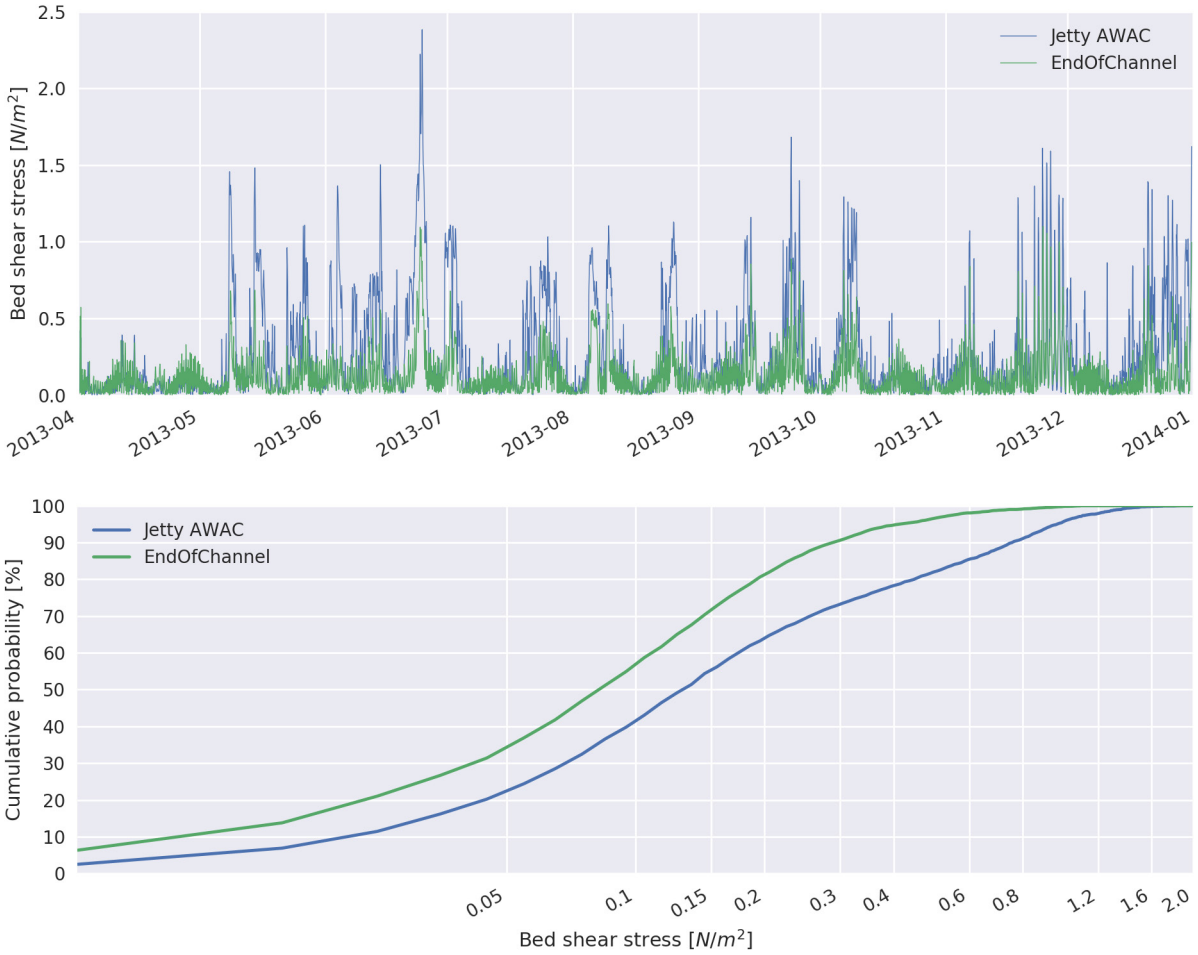

Figure 20. Time series (top) and cumulative probability density (bottom) of the modelled wave current bed shear stress at the Jetty AWAC and EndOfChannel locations highlighting the significant increase in shear stress climatology from 14 m depth to 8 m depth.

4 Sediment transport model setup

In this section, we first present our analyses on source term estimates, using the dredging log analysis to determine where and when dredging happened, and applying the Becker et al. (2015) model to determine the flux of fines released into the water column. We then present the results on the relationship between TSS and turbidity (NTU) derived from field measurements, the relationship between deposition and sedimentation, and analysis of sediment trap accumulation data to derive an estimated settling velocity.

4.1 Source term

The specification of dredge plume source terms is a critical step in the assessment of the environmental impacts associated with the underwater handling of sediment. It defines the amount of fine material input into a modelled far field dredging plume and requires that the location, time and magnitude of the dredging related flux of fine material be defined.

In order to define the time and location of the dredging source terms the electronic dredging logs were analysed and validated against PDF daily dredging reports. Each daily dredging report contained a summary of the daily activity for each piece of dredging equipment operating as well as records of the overall progress of the excavation and placement. During the Wheatstone Project the Cutter Suction Dredge (CSD) completed the majority of the excavation and loaded several barges of various sizes via a pipeline. In addition, three Trailing Suction Hopper Dredges (TSHDs) were utilised both as a dredge and as a large barge loaded by the CSD. Based on the EIA and the environmental approval granted in Ministerial Statement 873 (MS, 873), two overflow control

zones were defined where overflow would be restricted. In total 8 different modes of operation were identified: with and without overflow for the TSHD dredging and the CSD loading three different sizes of barge (one of which was the TSHD operating in a barge mode). Whilst a Back-hoe dredge was also mobilised for the project it only excavated approximately 150,000 m^3 (of the > 25 Mm^3) and plumes associated with this dredge were not included in the model.

Typically for large scale dredging projects the magnitude of fines released by dredging is estimated by the dredging contractor based on an assessment of the dredging program, type of dredging equipment and any geotechnical data available for the excavation location. Becker et al. (2015) outlines one such approach for the estimation of source term magnitude that is based on a mass balance approach with several empirically derived coefficients that fractionates the available fine material across the various material handling stages associated with dredging. Becker et al. (2015) advocate that a more uniform approach to source term estimation will improve environmental impact assessment in general and provide a table of 'reasonable' ranges for the various empirical fractions utilised in their model. This study applies the approach outlined in Becker et al. (2015) to the Wheatstone dredging campaign to a) validate the approach through practical application to a hindcast model of a large capital dredging project; and b) gain insight into the crucial steps required to ensure mass balance between the Becker et al. (2015) model and its application to a numerical model.

4.1.1 Dredging log analysis

Electronic dredging logs from the 11 pieces of dredging equipment were also provided. All files were text based with roughly one file provided per day for each piece of equipment. The file formats and available fields varied across equipment and in time. The various data files were parsed into a standardised data-structure so that a minimum set of variables could be identified to establish the operating activity (dredging or placement) of the various equipment utilised. Major gaps in the electronic logs were identified through cross referencing with PDF daily dredging reports and where possible backfilled, in particular for large gaps in the Cutter Suction Dredge (CSD) record, the dredging activity was inferred from barge records. The processed dredging logs were averaged to a consistent 5-minute time step and comprised of the following data fields: time, spatial coordinates and a bit flag (0/1) to indicate if the given piece of equipment was dredging or placing material.

A critical step in the application of moving source terms is to ensure that the source is correctly distributed across the computational grid cells given the computational time step. To achieve this, the processed dredging logs were interpolated to 10x the model time step (24 seconds) and grid cell averaged on the computational grid to obtain the correct discharge per computational cell at each model time step.

Table 5 presents a validation of the processed dredging logs where the number of placement events identified from the electronic logs between 1 April 2013 and 20 December 2014 is compared against the number of placement events recorded in the daily dredging report on 20 December 2014 (Chevron Australia 2014a). The agreement between the analysed electronic records and daily dredging report is very good. Underestimates for the TSHD equipment are due to gaps in the electronic logs that could not be easily filled.

Table 5. Recorded number of placement events as at 20 December 2014 compared to modelled placement events.

Vessel	Recorded Spoil Ground C placement events	Modelled Spoil Ground C placement events
TSHD Brabo	2894	2795
TSHD Breydel	2956	2905
TSHD Gateway	2325	2209
SHB Sloeber	1452	1453
SHB Pagadder	1493	1503
SHB Trinidad	422	422
SHB Santiago	445	449
SHB GL-501[a]	29	-
SHB GL-502[a]	27	-

a SHB GL-501 and GL-502 were not processed

4.1.2 Source term estimates

The first step in the application of the Becker et al. (2015) model (henceforth B2015) is the establishment of the mass of fines available in the excavation. A detailed geotechnical investigation is provided in Chevron (2010a) which presents an assessment of the material to be dredged. Whilst results varied across the different geological units and with depth the dry bed density was in the range 1,500 kg/m^3 and 2,500 kg/m^3. The daily dredging reports provide estimates of the excavated volume and total mass of placed solids, based on the data reported on 20 December 2014 a reasonable estimate of average dry bed density of 1,860 kg/m^3 is utilised to convert the excavation volume to an excavation mass (Chevron, 2014a). Particle size analysis of the excavation material presented in Chevron (2010a) indicated significant variability in the percentage of fines (< 75 µm) available across the excavation (from 10% to 86%) with an average value 36%. A representative value of 33% fines was utilised in this study. This results in an estimated total mass of fines of 1.56 x 10^{10} kg to be handled during the dredging excavation.

Based on the 20 December 2014 daily dredging report the average excavated volume per loading cycle (production rate) for each size of barge was calculated and the total mass of fines handled per cycle calculated for each barge according to Equation 9:

$$m_t = \rho_d . f_f . V \quad (9)$$

where m_t is the mass of fines handled per cycle, ρ_d is the dry bed density (1,860 kg/m^3), f_f is the fraction of fines (0.33) and V is the cycle production rate (m^3). Next the factors for each stage of the dredging process were estimated. The factor TSHD drag head stir-up (σ_d) was estimated at 0.01 and the CSD cutter head stir-up (σ_d) as 0.05. It was noted in earlier plume characterisation work (Chevron, 2014) that due to the shallow water, dynamic positioning thrusters and ancillary vessels there was a significant source of fine material resuspension due to propeller wash. This was accounted for through applying the upper limit of the 'reasonable' range for the cutter head stir-up factor. The factors for trapping (f_{trap}) and settlement (f_{sett}) in the hopper can be established through the use of a hopper settlement model (i.e. Van Rhee, 2002; Spearman et al., 2011); however, in this instance values of 0.025 and 0.3 were utilised respectively based on the examples and ranges provided in B2015.

When the hopper is full, loading continues, and excess sediment laden water is released as an overflow. Some proportion of the sediment flowing through the overflow is released into the passive plume (σ_o) and B2015 suggest a reasonable range for this factor of 0 – 0.2. A recent detailed parametric computational fluid dynamics (CFD) study of the dynamic overflow was undertaken by De Witt (2014) and establishes a set of empirical relationships that can be utilised to estimate the proportion of fines released from the overflow to the passive plume and the vertical structure of the passive plume. Through application of the relations set out in De Witt (2014) a value of 0.3 was estimated for σ_o in this study. Similarly, during placement some proportion of the fines retained in the hopper are released to the passive plume some distance from the placement location (σ_p), for this study the upper limit of the reasonable range (0.1) defined in B2015 is used.

An example of the calculation table utilised is provided in Table 6 for the CSD loading the TSHD as a barge with overflow (the primary operating mode that was utilised). For the scenario outlined in Table 6, 18% of the fines production rate is released during dredging and 5% during placement. A summary of all source terms applied in the study is provided in Table 7.

The cycle loading time for each combination of dredge and barge was estimated based on visual inspection of the electronic dredging records. It was not possible to consistently establish when overflow was occurring based on the data available in the electronic records, primarily due to the loading of the barges by the CSD via a pipeline. This introduced a phase lag between the activation of the dredge pump and changes in the hopper volume that changed throughout the excavation, presumably due to varying length of pipe as the pipe velocity tended to be reasonably consistent. Therefore, it was assumed that any dredging that took place within the overflow control zones was conducted without overflow and dredging that occurred outside these zones included overflow. In addition, it was not possible to establish a different source term for initial loading prior to the commencement

of overflow, therefore the total release of fines during the dredging phase of the cycle was averaged across the period that the dredge pump was running.

Table 6. Example calculation table (based on Becker et al. 2015) utilised to derive source term estimate for the CSD loading the TSHD as a barge.

Operating mode - CSD loading TSHD as barge		Value	Units	Factor[a]	Value applied	Lower Bound[a]	Upper Bound[a]
Cycle Loading Time (t2-t0)		6600	s				
Overflow Time (t2-t1)		4200	s				
Placement Time		900	s				
Cycle Volume		3000	m^3/cycle				
Number of Cycles		8.47E+03	cycles				
Production rate		0.45	m^3/s				
Mass of fines (cycle)		1.84E+06	kg/cycle				
Cutter-head stir up	m_d	9.21E+04	kg/cycle	σ_c	0.05	0.01	0.05
Mass to hopper	m_h	1.75E+06	kg/cycle				
Mass settled in hopper				f_{sett}	0.3	0	1
Mass trapped in hopper				f_{trap}	0.025	0.01	0.05
Mass to overflow	m_o	7.60E+05	kg/cycle				
Mass of overflow to passive plume	m_{op}	2.28E+05	kg/cycle	σ_o	0.3	0	0.2
Mass of overflow to dense plume	m_{od}	5.32E+05	kg/cycle				
Mass retained in hopper	m_r	9.90E+05	kg/cycle				
Mass of placement to passive plume	m_{pp}	9.90E+04	kg/cycle	σ_p	0.1	0	0.1
Mass of placement to dense plume	m_{pd}	8.91E+05	kg/cycle				
To Passive Plume							
Flux of fines - drag head		14.0	kg/s				
Flux of fines - overflow		54.3	kg/s				
Flux of fines - placement		110.0	kg/s				
Flux of fines - dredging		48.5	kg/s				
Loading - % Fines Production	P_{fl}	17%					
Placement - % Fines Production	P_{fp}	5%					

a Factor labels and reasonable bounds as reported in Becker et al. (2015)

Table 7. Far-field source terms estimated for various modes of operation utilised by the dredging equipment in the Wheatstone project.

Operating Mode	Hopper Capacity [m^3]	Loading			Placement		
		Duration [min]	Source Term [kg/s]	% Fines Production Rate	Duration [min]	Source Term [kg/s]	% Fines Production Rate
TSHD Trailing with overflow	12,000	55	78	14	15	115	6
CSD loading TSHD as barge with overflow	12,000	110	48	17	15	115	5
CSD loading 2,735 m^3 barge with overflow	2,735	45	48	21	20	22	4
CSD loading 1,800 m^3 barge with overflow	1,800	40	48	22	10	35	4
TSHD Trailing without overflow	12,000	55	6	1	15	198	10
CSD loading TSHD as barge without overflow	12,000	110	14	5	15	198	10
CSD loading 2,735 m^3 barge without overflow	2,735	45	14	5	20	49	10
CSD loading 1800 m^3 barge without, overflow	1,800	40	14	5	10	83	10

4.1.3 Validation of modelled source term

An estimate of the production rate (rate of excavation) can be estimated from the modelled fines production rate using Equation 10:

$$P_m = \frac{\varphi_f}{\rho_d \cdot f_f \cdot p_f} \tag{10}$$

where P_m is the excavation rate ($m^3.s^{-1}$), φ_f is the flux of fines released in the model ($kg.s^{-1}$) and p_f is the weighted average fines production rate estimated using the B2015 model. The fines production rates presented in Table 7 are weighted by the reported volume of material placed for each barge on 20 December 2014 (Chevron, 2014a), resulting in the average p_f being approximately 23.6% in this study. This calculation is used to validate that the assumptions utilised in the B2015 model calculations are reflected in the volume of fines applied to the model which were derived from the electronic dredging records. Ultimately it requires that the assumed loading and placement durations used in the B2015 calculations are consistent with the average loading and placement times calculated from the electronic dredging records. Table 8 compares the modelled cumulative production to the cumulative production reported in the daily dredging reports on 31 December 2013 and 20 December 2014. It is noted that this is a somewhat circular calculation and as expected there is good agreement between the modelled and reported cumulative production with the discrepancy being due to gaps in the electronic dredging logs. Table 8 demonstrates that that the assumptions utilised in the B2015 are reflected in the passive plume model and the moving source terms have been correctly applied to the model grid, but it does not demonstrate that factors applied in the B2015 model and the calculated source terms are correct. Figure 21 presents a time series of the modelled production rate and fines release rate. The gap at the end of December 2013 was due to a shutdown associated with Tropical Cyclone Christine.

Table 8. Recorded and modelled cumulative production at two times in the dredging campaign.

Cumulative Production	Recorded at 31 December 2013[a]	Modelled at 31 December 2013	Recorded at 20 December 2014[b]	Modelled at 20 December 2014
In situ Volume [Millions m^3]	9.37	8.53	25.38	24.93
Total Dumped Solids [Millions Tonnes]	16.46	15.87	47.32	46.38
Fines Released to Passive Plume [Millions Tonnes]	-	1.24	-	3.61

a Daily Dredge Report (WS1-0000-CNS-RPD-BEC-CMD-00450-000.pdf) (Chevron, 2013)
b Daily Dredge Report (WS1-0000-CNS-RPD-BEC-CMD-00804-000.pdf) (Chevron, 2014a)

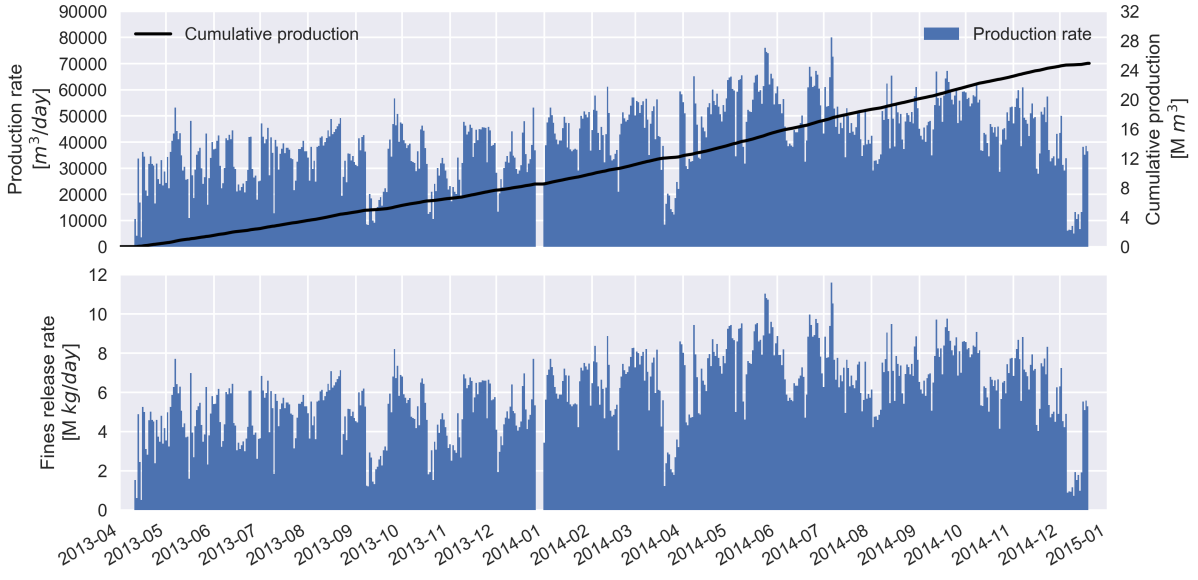

Figure 21. Time series of estimated daily production rate and cumulative dredging volume derived from the electronic dredging logs and applied in the model.

4.2 Sediment characteristics

4.2.1 Relationship between total suspended solids and turbidity

Turbidity as quantified by a Nephelometer measures the scattering of light by suspended particles (commonly in the infrared wavelength range). This scattering process is influenced by a number of properties of the suspended particles, including their size, shape and colour. This in turn influences the relationship between NTU and TSS, with the slope of the relationship integrating the various influences across the distribution of suspended particles.

As part of Project 3.2, CSIRO and Curtin University collaborators undertook two field data collection exercises during the inshore and offshore dredging in October 2013 and June 2014 respectively. Data collected during these campaigns included *in situ* optical properties required for calibration of remote sensing reflectance to total suspended solids (TSS) (Dorji et al. 2016), water samples collected within the passive dredging plumes (analysed for TSS), vertical profiles of turbidity and ADCP transects.

An *in situ* relationship between TSS and factory calibrated Campbell Scientific OBS3 NTU was established in in Fearns et al. (2017a) and is reproduced in Figure 22. It is noted that the slope of the relationship, 1.07, is in good agreement with the slope utilised in the Wheatstone Project dredge plume model validation where a value of 1.1 was assumed (Chevron, 2014). Surficial sediment cores were collected during the field exercises and were subsequently utilised in tank experiments to investigate the variability in measurements between different optical instruments (Fearns et al. 2017b). The TSS to NTU relationship derived for the Campbell Scientific OBS3 and Wetlabs ECO NTU were compared across five different samples with a range of particle size distributions. The root mean squared error in the linear slope of regression between the instruments was 0.1 highlighting the remarkably good agreement between the two instruments (Fearns et al. 2017b). A value of 1.07 was utilised in this study to convert from NTU to TSS.

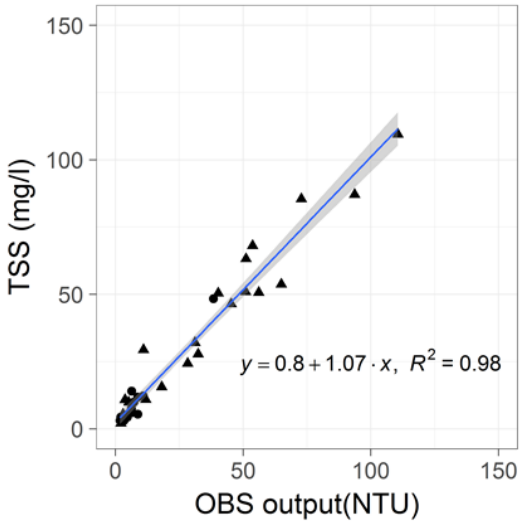

Figure 22. Relationship between TSS and NTU developed from *in situ* water column samples of passive dredging plumes during the Wheatstone dredging campaign (Mortimer et al. 2015).

4.2.2 Relationship between deposition and sedimentation

The impact thresholds associated with sediment deposition can be defined as some thickness of sedimentation over a given time interval or a deposition mass per unit area. Numerical models can quantify the bed sediment fluxes in mass per unit area (typically kg/m^2) or in terms of a change in bed level (i.e. sedimentation thickness). As such it is necessary to convert from a deposition mass to a deposition thickness and this depends on some assumed dry density of freshly deposited material. The Wheatstone Project EIA utilised a dry bed density of 400 kg/m^3 '…based on DHI's extensive monitoring experience of sedimentation…' (Chevron, 2010). This is consistent with a commonly applied default value of 500 kg/m^3 for cohesive sediment (Deltares, 2014a), however, this

should be considered indicative of fully consolidated cohesive sediment. Experimental investigations of consolidation indicate that initial sedimentation from suspensions of mud from the river Scheldt have a dry bed density of approximately 50 kg/m^3 which increases to approximately 125 kg/m^3 after 14 days of self-weight consolidation (Toorman & Berlamont 1991). The density at the base of the settling tube reached approximately 225 kg/m^3 after 14 days. Whilst the sand content has a significant influence on the measured dry bed density, sand fractions rapidly settle to the bed close to the dredging activity and likely don't contribute appreciably to sedimentation from a passive dredging plume. Grasso et al. (2015) note that in most estuarine deposits, dry bed densities do not exceed 100 kg/m^3 and this value can be considered a '...fresh deposit…' in sediment transport modelling. In this study, TSS was also related to the total volume concentration measured by a LISST instrument in Fearns et al. (2017) (see Figure 23). The slope of the relationship provides some indication of the excess density (or dry density) of the suspended material. A slope of 0.23 suggests a dry density of approximately 230 kg/m^3 and this appears a reasonable upper limit estimate for conversion from deposition (kg/m^2) to sedimentation (m) and is subsequently utilised in this study.

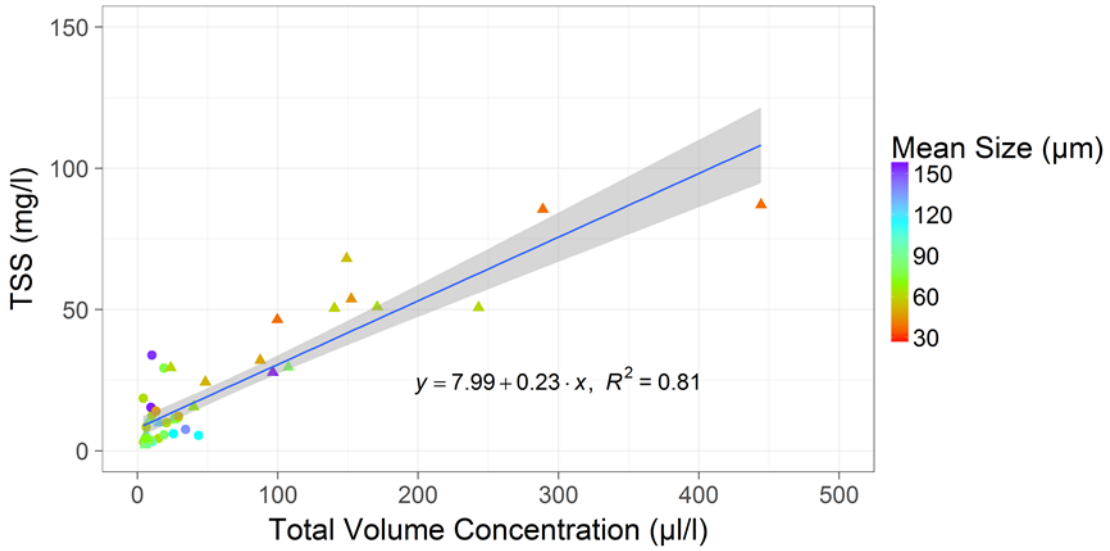

Figure 23. Relationship between TSS and LISST Total Volume Concentration developed from *in situ* water column samples of passive dredging plumes during the Wheatstone dredging campaign (Fearns et al. 2017a).

4.2.3 Sediment trap accumulation and fine sediment settling velocity

Sediment trap data was grouped in Nearshore, Inner Shelf, Eastern Islands and Offshore in accordance with Table 1 for comparison across time and location. The grouping highlights distinct regions with respect to sediment trap median grain size (D50) and accumulation rates (Figure 24 a and b, respectively). Nearshore sites generally had the highest trap accumulation rates with the smallest median grain size; D50 consistently between 5 – 10 µm. Trap accumulation rates and mean TSS decreased generally in the cross-shore direction, with increasing D50. Offshore sites tended to be located close to islands in shallow water (< 10 m depth) subjected to a relatively high bed shear stress climatology and this likely accounts for the increased D50 of the trapped material. Trap accumulation rates increased by an order of magnitude across all groups during cyclonic periods (Figure 24), however there is no clear increase in trap accumulation during the dredging period compared to the baseline period. Average TSS for deployments impacted by cyclonic activity were also an order of magnitude higher than non-cyclonic periods.

There is indication of an increase in the mean TSS across all sites during dredging of approximately 1 mg/L compared to non-cyclonic periods during the baseline period. It is not known if this is due to changes in the instrument configuration/calibration associated with instrument servicing or a shift in the background TSS due to dredging. An increase of ~1 NTU is consistent with the analysis of Fisher et al. (2015) who assessed water quality measurements obtained during three other major capital dredging projects on the NW Shelf and Wahab

et al. (2017) who undertook more detailed analysis of water quality during the Wheatstone dredging project (the same dataset as used in this study).

Despite the noted shortcomings of sediment traps in measuring sedimentation (e.g. Storlazzi et al, 2011) it is possible to obtain an estimate of the settling velocity of suspended material that is advected past the sediment trap. The conversion from turbidity to TSS discussed in Section 4.2.1 is applied to all sites and for both the baseline and dredging periods. Assuming that the trap accumulation rate (D) is given by:

$$D = w_s.C.A.t \quad (1)$$

where w_s is the sediment settling velocity, C is the suspended solids concentration A is the cross sectional area of the trap and t is the duration of the deployment. Neglecting the influence of turbulent diffusivity across the trap entrance, the settling velocity is estimated by simply re-arranging Equation 1. Figure 24d presents the estimated settling velocity for the baseline and dredging periods. Overall, a general decrease in estimated settling velocity during the dredging period was observed. In this simplified model the decrease is due to the increase in the mean TSS. The estimate of settling velocity with this method is sensitive to measurement of the low background TSS (due to the relatively long averaging period over a 40-day deployment). This can be influenced by changes in instrument zero point calibration, or by small shifts in the background TSS and it is unclear if the increase in the low TSS observations shown in Figure 24c (see also Figure 5f) is due to instrument changes or dredging activity.

The position of the sediment traps being approximately 1.1 m above the seabed will preferentially sample the more slowly settling portion of the resuspended particle size distribution. This is supported by analysis of the baseline sediment trap data which demonstrated that approximately 80% of the trapped material was mud (< 63 µm), despite the seabed being comprised of only 9% mud (Dufois et al, 2017). As such a TSS to NTU relationship derived based on sampling of the passive dredging plume (which is predominantly comprised of mud) is reasonable for this region of the shelf.

Despite the differences in D50 across the groups, there was no clear trend of increasing settling velocity with increasing D50. It is possible that this is due to changes in the TSS to NTU relationship, associated with changes in sediment type (colour) or suspended particle size distribution. NTU has an inverse sensitivity to particle size distribution (Campbell Scientific, 2017), so a larger particle size distribution leads to a larger slope in the TSS to NTU relationship, i.e. a larger TSS for a given measured NTU. This in turn would result in lower estimates of settling velocity using Equation 1. Suspended sediment of increasing 'whiteness', increases NTU sensitivity for a given concentration (Campbell Scientific, 2017) which would lead to a smaller slope in the TSS to NTU relationship. It is likely that the increasing presence of carbonate sands and reduction in terrigenous mud around the islands in the Offshore group results in an overestimation of the TSS derived from NTU using a slope of 1.07 and as such an under estimation of settling velocity at these sites. Therefore, the estimates of settling velocity likely have greatest validity for the Nearshore and Inner Shelf sites.

It is important to note that the settling velocity estimated from the sediment traps is somewhat higher than the Stokes settling velocity (0.09 mm/s for a particle size of 10 µm) calculated for the median captured grain size, suggesting that flocculation processes may still have been occurring to some degree despite the generally low TSS concentration. It is informative to calculate the Stokes settling velocity based on the range in mean particle size measured by the LISST (45–90 µm) and the estimated density of the particles (approximately 1,255 kg/m^3) presented in Figure 23. On the basis of the LISST data the range in settling velocity is 0.25 mm/s to 1.0 mm/s which is in good agreement with the settling velocity estimated from the sediment traps for non-cyclonic periods (between 0.2 mm/s to 1.0 mm/s), providing additional evidence of a reasonable range for the fine sediment fractions in the passive plume model.

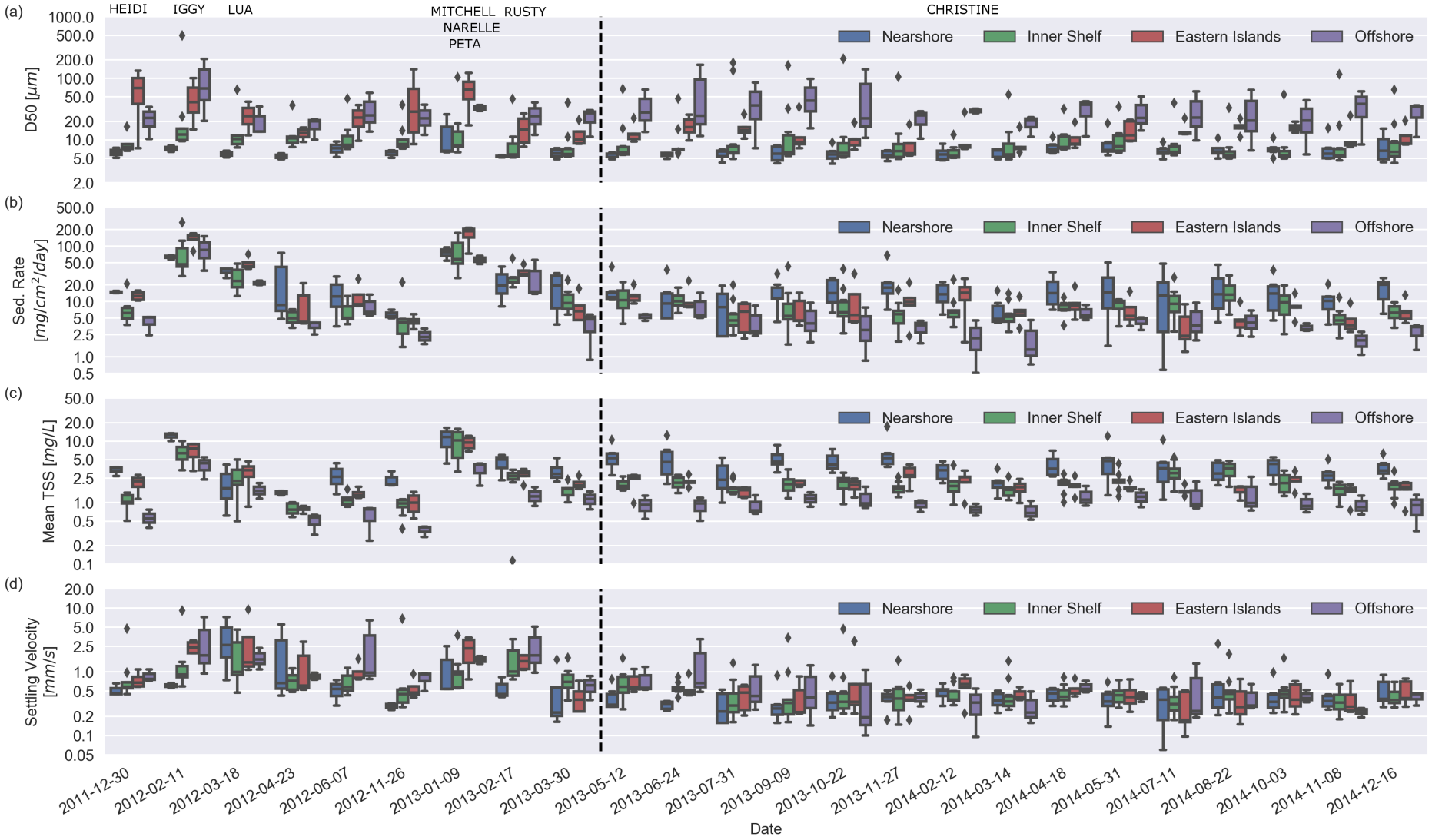

Figure 24. Overview of sediment trap data collected over 24 deployments at the fixed monitoring stations. Dates indicate mid-point of each deployment and the vertical dashed line marks the commencement of dredging. Names indicate approximate periods of cyclones affecting the region. (a) Box plot of median particle size of material captured in the trap. (b) Average trap accumulation rate for each deployment. (c) Average TSS derived from the co-located Turbidity sensor (assuming TSS = 1.07 * NTU). (d) Estimated sediment trap settling velocity.

5 Sediment transport model sensitivity analysis

In this section, we present the sediment transport model sensitivity analysis to investigate how model parameters influence the initial settling and dispersion of dredge plumes, the distribution of deposited dredged material, and resuspension in the nearshore and inner-shelf regions, and distribution of fines in the buffer layer. A table of key sediment transport model parameters is provided (Table 10)

On the basis of the available data and analysis of the processes governing the dispersion and resuspension of passive dredging plumes a sensitivity analysis of model parameters was undertaken. A total of 15 model parameters were identified which influence the dynamics of the modelled passive dredging plumes. A preliminary 'best estimate' model and upper and lower bounds for each parameter was established based on data analysis and professional judgement. It is noted that several of the parameters cannot be considered in isolation, in particular, the fluff layer zero- and first-order erosion parameters as their combination influences the erosion flux from the fluff layer. All simulations assumed an initial seabed (buffer layer) sediment distribution of 30% natural fines, 70% sand and that deposition occurred continuously (the shear stress threshold applied for deposition $\tau_{cr,d}$ was set to 1000 N/m^2). Table 9 provides a summary of the model parameters (their best estimates, lower and upper bounds) to assess sediment transport model sensitivity.

A total of 30 simulations were completed for the period 1 May 2013 to 8 July 2013 which includes a resuspension event on 25 June 2013 and a general south westerly residual current. Model sensitivity was assessed quantitatively through comparison of near bed TSS concentration time series and model skill metrics at the fixed monitoring sites (Figure 1) and qualitatively through comparison of the spatial distribution of TSS in the surface layer against selected MODIS TSS maps; on 21 May 2013 during a period of low shear stress and 26 June 2013 during a period of relatively high bed shear stress.

In general, the dynamics of the fluff and buffer layers are most strongly influenced by their respective bed shear stress thresholds, as this governs the initiation of erosive sediment fluxes and subsequently the erosion rate and deposition parameters. Due to the strong dependence of bed shear stress on depth, the shear stress thresholds significantly influence the spatial extent of local resuspension. Results of the sensitivity analysis will be described in the following six subsections, addressing: 1) parameters influencing the initial spreading and settlement of the plumes from source, 2) parameters influencing the distribution of deposited dredging material, 3) parameters influencing resuspension in the higher dynamic nearshore, 4) parameters influencing resuspension on the lower dynamic inner shelf, 5) influence of the initial distribution of fines in the buffer layer, and 6) calibrated key sediment transport model parameters.

Table 9. Overview of model parameters varied to assess sediment transport model sensitivity. Parameter bounds and estimates were established based on data analysis and literature where available and professional judgement otherwise.

Parameter description	Sediment Fraction	Units	Lower Bound	Best Estimate	Upper Bound
Horizontal eddy diffusivity	All	$m^2.s^{-1}$	0.1	1	10
Background vertical eddy diffusivity	All	$m^2.s^{-1}$	1.00E-08	1.00E-06	1.00E-04
Fluff layer 0th-order erosion parameter (M_2)	All	$kg.m^{-2}.s^{-1}$	1.00E-05	1.00E-03	1.00E-02
Fluff layer 1st-order erosion parameter (M_1)	All	s^{-1}	1.00E-06	1.00E-04	1.00E-03
Fluff layer critical shear stress threshold for erosion ($\tau_{cr,f}$)	All	$N.m^{-2}$	0.05	0.2	0.4
Burial fraction on deposition (α)	All	-	0.02	0.1	0.2
Settling velocity (w_s)	Dredging	$m.s^{-1}$	5.00E-05	0.2	1.00E-03
Buffer layer critical shear stress threshold for erosion ($\tau_{cr,e}$)	Dredging	$N.m^{-2}$	0.3	0.8	1.5
Buffer layer erosion parameter (M_0)	Dredging	$kg.m^{-2}.s^{-1}$	1.00E-06	1.00E-05	1.00E-04
Fluff layer initial mass (m)	Dredging	$kg.m^{-2}$	0	5.00E-04	2.00E-03
Settling velocity (w_s)	Natural	$m.s^{-1}$	2.00E-04	5.00E-04	2.00E-03
Buffer layer critical shear stress threshold for erosion ($\tau_{cr,e}$)	Natural	$N.m^{-2}$	0.3	0.8	1.5
Buffer layer erosion parameter (M_0)	Natural	$kg.m^{-2}.s^{-1}$	1.00E-06	1.00E-05	1.00E-04
Fluff layer initial mass (m)	Natural	$kg.m^{-2}$	0	5.00E-04	2.00E-03
Buffer layer thickness (d_0)	All	m	0.05	0.1	0.2

5.1 Effect of 2D v 3D modelling

An important decision to make when modelling passive dredging plumes for the EIA is whether or not 3D modelling is needed. To employ a 2D model is attractive because it reduces computational cost significantly. The rational is based on the idea that if the circulation and plume dispersion are well mixed vertically (especially in shallow waters) then 2D modelling might be sufficient. It is recognised that the sediment transport model calibration parameters for a 2D model are different from those for a 3D model. It is important to note that deposition fluxes are a function of the sediment concentration in the computational grid cell closest to the seabed, which in a 2D model is the full water column. Due to this no vertical gradient, or 'Rouse-like' profile in sediment concentration is present in a 2D model. This results in deposition flux being artificially reduced and lateral flux artificially increased. An example of this effect is shown in Figure 25 when the model was executed in both 2D and 3D mode. The 3D model produced a more realistic vertical profile in TSS, with lower sediment concentration in the water column due to the higher depositional flux than the 2D model for the same settling velocity. The reader is referred to Tuinhof (2014) for a more detailed idealised assessment of the effects of 2D v 3D modelling in the context of dredging plume models.

In addition to 3D effects on the sediment transport model, potentially significant differences in the modelled circulation can result due to the manner in which friction at the seabed and sea surface are modelled in a 2D model. The shallowness of the coastal zone is often used as justification for applying 2D models, however wind stress (a primary driver of residual circulation in the coastal zone) establishes circulation that is inherently three-dimensional. In this study it was found that the 2D model was incapable of reproducing a weak (but important) wind driven over turning secondary circulation, which was the measured in the nearshore Jetty ADCP data, however, this was better resolved by the 3D model. This outcome is supported by a recent paper that demonstrated, in locations where the water depth is much smaller than the Ekman layer thickness, the top and bottom boundary layers interact, the bottom stress had direct dependence on the surface wind stress (Cushman-Roisin & Deleersnijder, 2017). Dredging requirements, by their very nature, take place in shallow water locations, frequently in locations where wind and wave activity are import drivers of circulation and sediment transport, therefore 3D models are essential in order to resolve these inherently 3D processes.

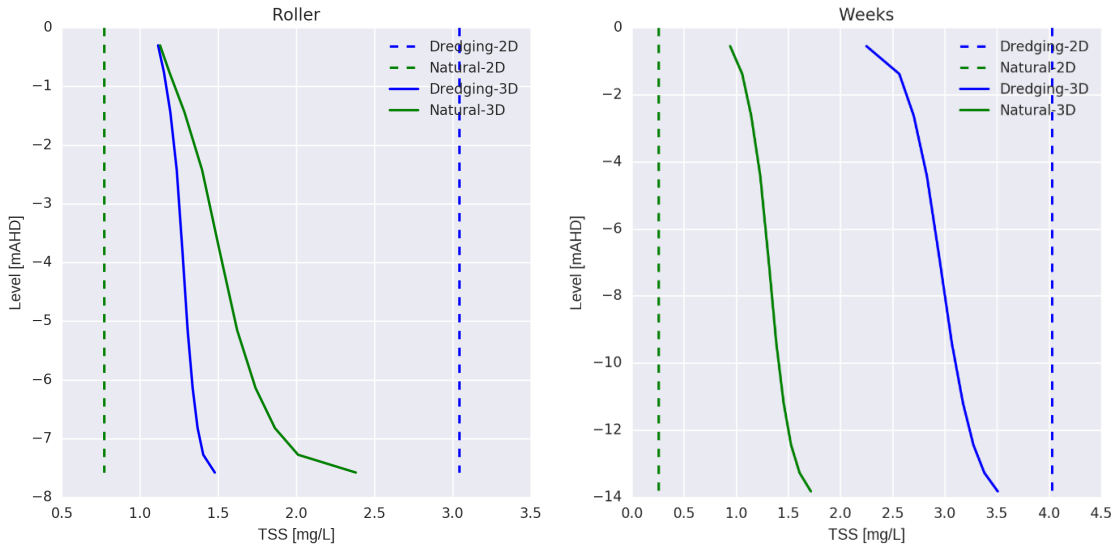

Figure 25. Time averaged vertical profile of TSS at the Roller and Weeks locations derived from an 8-week simulation with a 2D and 3D model with the same parameter settings. Notice the significant vertical structure present, in natural TSS at the shallower Roller site which has greater exposure to wave activity. At both sites the 2D model produced higher in water column dredging TSS due to the reduced deposition rates for the same settling velocity.

5.2 Importance of the fluff and buffer layer model

The need for the two layer (2L) bed model of van Prooijen et al. (2007) and van Kessel et al. (2011) was assessed on the basis of 27 additional model simulations (not shown) that attempted to reproduce the resuspension dynamics across the large dynamic range in shear stress climatology that is present between the nearshore and inner shelf region of the study area. Without the use of the more easily erodible fluff layer it was not possible to reproduce the observed resuspension dynamics of freshly deposited dredging fines on the inner shelf at the same time as resuspension in the nearshore. An alternative approach would be to utilise a spatially variable bed shear stress threshold based on the seabed particle size distribution as was applied in Dufois (2018, submitted).

5.3 Parameters influencing the initial settling and dispersion of dredging plumes

In the water column the transport of the passive plume is governed by the advection-diffusion equation. The horizontal advection and turbulent mixing is superimposed on downward gravitational settling and the balance between gravitational settling and vertical turbulent mixing is described by the Peclet number (Equation 9):

$$P_e = \frac{w_s H}{K_s} \tag{9}$$

where w_s is the settling velocity, H is the water depth and K_s is the vertical turbulent eddy diffusivity. If $P_e \gg 1$ gravitational settling dominates, and the dredging plume rapidly settles to the bed. If the $P_e \ll 1$ the passive plume persists in the water column for a longer duration and is subjected to increased horizontal advection and diffusion.

The background vertical eddy diffusivity had limited influence for the parameter values tested as the modelled vertical eddy diffusivity (from the k-ε model) typically always exceeded 1.00E-3 $m^2.s^{-1}$ in the study area. The average modelled vertical turbulent eddy diffusivity at mid depth for the period April 2013 to December 2013 was 1.25E-2 $m^2.s^{-1}$ and 6.39E-3 $m^2.s^{-1}$ at the EndOfChannel and Jetty AWAC locations, respectively. For the lower settling velocity of 0.05 mm/s, $P_e \approx$ 6.0E-2 and for the higher settling velocity of 1 mm/s, $P_e \approx 1$ highlighting the significantly greater influence of gravitational settling for the higher settling velocity case. The higher settling velocity significantly reduced the passive plume extent and concentration and on the basis of comparison with MODIS imagery, unrealistically so. Similarly, the lower bound significantly increased the extent and concentration of the passive plume also unrealistically so, supporting the estimates of settling velocity established in Section 4.2.3.

The horizontal eddy diffusivity had a significant influence on the extent and concentration of the passive dredging plume. Using the lower bound resulted in concentrated, laterally constrained plumes that extended further in the down flow direction, while using the upper bound resulted in lower concentration, laterally spread plumes but with reduced down flow extent. Based on comparison with the MODIS TSS the upper value of 10 $m^2.s^{-1}$ was clearly too high for the roughly 200 m resolution grid utilised in this model. For the lower value of 0.1 $m^2.s^{-1}$ the dredging plume maintained its concentration for too great a distance in the down flow direction. The best estimate value of around 1 $m^2.s^{-1}$ for the horizontal eddy diffusivity appears to be a reasonable estimate.

5.4 Parameters influencing the distribution of deposited dredging material

In the model applied in this study no bed shear stress threshold for deposition was applied, such that a dynamic balance between erosion and deposition is established in the model to maintain suspended sediment concentrations. In the two-layer model presented here deposition of fine material primarily occurs to the fluff layer, however with some (small) fraction depositing to the buffer layer (α). A consequence of the approach to infiltration from the fluff layer to the buffer layer via the water column is that it introduces a dynamic dependence on the bed shear stress thresholds for erosion. Where the fluff layer threshold is exceeded more frequently deposited material infiltrates to the buffer layer more rapidly which in turn has a significant influence on rate at which dredging fines mix with natural fines in the buffer layer. In addition, the fluff layer shear stress threshold alters the spatial distribution as upon each resuspension event the fine material is subjected to additional

advection. A higher threshold for erosion of the fluff layer results in accumulation of fines in the fluff layer, closer to the source, which when the threshold is subsequently exceeded results in significant resuspension.

5.5 Parameters influencing resuspension in the nearshore

The nearshore region (shallower than 8 m depth) is a relatively high dynamic environment with bed shear stress exceeding 0.8 N/m^2 (the best estimate threshold for erosion of the buffer layer) approximately 10% of the time and 0.2 N/m^2 (the best estimate threshold for erosion of the fluff layer) approximately 35% of the time at the Jetty AWAC location, primarily due to the action of locally generated seas. As a consequence, both the fluff layer and buffer layer are active in the nearshore region.

Resuspension of natural fines in the nearshore was very sensitive to the buffer layer shear stress threshold for erosion, with the lower value significantly increasing the extent and concentration of nearshore resuspension. By extension natural fines were also very sensitive to the buffer layer erosion parameter (M_0) and settling velocity.

Resuspension of natural and dredging fines in the nearshore was less sensitive to the fluff layer bed shear stress threshold due to the range of values tested (0.05 N/m^2 to 0.4 N/m^2) all being relatively frequently exceeded. Resuspension of natural fines in the nearshore exhibited low sensitivity to the lower bound in M_2 (the fluff layer zero-order erosion parameter) and no sensitivity to the upper bound. Resuspension of natural fines in the nearshore was very sensitive to M_1 (the fluff layer first order erosion parameter). This is in contrast to van Kessel (2011) who indicate that the two-layer model is relatively insensitive to changes in M_1. The high sensitivity to M_1may indicate that the 'best estimate' M_2 was too high and it is noted that the combinations of M_1 and M_2 tested in the sensitivity analysis resulted in quite different equilibrium mass being present in the fluff layer. The spatial distribution was strongly driven by gradients in bed shear stress, with the fluff layer accumulating fines in low shear stress areas.

In contrast to natural fines, dredging fines exhibited greater sensitivity to the lower bound in M_2 in the nearshore, with resuspension of the dredging fines being more concentrated with reduced spatial extent due to differences in manner in which fines accumulated in the fluff layer over the course of the simulation. Dredging fines also exhibited sensitivity to M_1, once again due to the distribution of dredging fines available in the fluff layer for resuspension. The lower bound significantly reduced the extent of resuspended dredging fines in the nearshore whilst the upper bound increased the concentration whilst having less of an influence on the extent.

Both dredging fines and natural fines were very sensitive to the burial fraction on deposition (α) parameter. This was the most sensitive parameter for resuspension of dredging fines in the nearshore. The lower bound resulted in significant accumulation of fines in the fluff layer across a broad spatial extent which were subsequently resuspended during the high shear stress period resulting in extensive and concentrated plumes of dredging fines. The upper bound significantly reduced the concentration and extent of resuspension of dredging fines due to greater infiltration to the buffer layer.

In summary, in the nearshore, resuspension of natural fines was most sensitive to the parameterisation of the buffer layer and dredging fines were most sensitive to the parameterisation of the fluff layer. There exists a complex interaction between the various fluff layer parameters which significantly influences the spatial distribution of dredging fines.

5.6 Parameters influencing resuspension on the inner shelf

The inner shelf region around the channel and spoil ground is a low dynamic environment with the modelled bed shear stress only exceeding 0.2 N/m^2 approximately 20% of the time and rarely exceeding 0.8 N/m^2. Consequently, resuspension on the inner shelf region is most sensitive to the parameterisation of the fluff layer with the buffer layer being mostly inactive except for around the peak of the larger resuspension events. Due to the lower shear stress environment the dynamics of natural fines on the inner shelf is also strongly influenced by

advection from adjacent nearshore and shallow regions around islands, which introduces some sensitivity to the buffer layer parameters as outlined in Section 5.4.

Like the nearshore, the resuspension of dredging fines exhibit sensitivity to the fluff layer erosion parameters, directly through altering the flux from the fluff layer and indirectly by altering the spatial distribution of fines in the fluff layer prior to a large resuspension event occurring (by altering the dynamics of frequent small magnitude resuspension events). The lower bound of M_2 shifts the peak concentration of the resuspended dredging plume closer to the source, with the upper bound exhibiting no difference to the 'best estimate' due to the zero-order erosion parameter not being reached. Both the upper and lower bounds of M_1 significantly reduce the magnitude of dredging resuspension on the inner shelf, for the lower bound due to significantly reducing the erosion flux from the fluff layer, and for the upper bound by rapidly diffusing the dredging fines in the fluff layer across the shelf and infiltrating into the buffer layer.

As described in Section 5.4 the shear stress threshold for erosion of the fluff layer plays a significant role in altering the distribution of dredging fines across the shelf and infiltration into the buffer layer. The lower bound results in the dredging fines having a reduced mass in the fluff layer (due to being distributed broadly across the shelf) and subsequently reduced concentration upon resuspension. The higher threshold results in the fluff layer close to the source having greater mass and more concentrated resuspension during high shear stress. Similarly, a reduction in the burial parameter (α) also increases the mass in the fluff layer and both the extent and concentration of resuspension on the inner shelf.

5.7 Distribution of fines in the buffer layer

The initial distribution of fines in the sea bed (buffer layer) has a significant influence on the modelled TSS dynamics. The uniform initial map specified for the sensitivity analysis simulations (30% natural fines, 70% sand) is only appropriate for the inner shelf and nearshore region that was sampled in the geotechnical study (Chevron, 2010a). Regions of frequent exposure to high shear stress and limited supply of fine sediment would naturally have much lower availability of fines for resuspension. The thickness of the buffer layer strongly influences how quickly fines are flushed from regions of high shear stress (due to the mass available being proportional to the buffer layer thickness). A buffer layer thickness of 0.05 m resulted in fines being flushed off in regions of high shear stress around the offshore islands (< 5 m depth) by the end of the 10-week simulation, however there was limited change in the nearshore region. The final map of natural fines availability in the fluff and buffer layers were utilised from the sensitivity simulation with a buffer layer thickness of 0.05 m as the initial condition for the final hindcast simulation. It is noted that 10 weeks is likely not sufficient time to 'warm up' the fines distribution across the entire shelf region within the model. However, after an extended period time (multiple years), as the model does not include natural sources of fine sediment from the regional rivers, the model would eventually flush all fines from the nearshore due to the model predicting a net transport of fines off the shelf, consistent with previous work by Margvelashvili et al. (2006).

5.8 Sediment transport calibration parameters

Several additional model simulations were conducted to further tune the model parameters. The significant challenge in calibrating the model was identifying a combination of model parameters that adequately reproduced the resuspension dynamics of the near shore and inner shelf regions for both consolidated natural fines and recently deposited, more easily erodible dredging fines. Numerous additional model simulations were completed to examine various combinations of fluff layer parameters and assess their influence on the spatial distribution of dredging fines and resuspension. The final set of key sediment transport model parameters is provided in Table 10

Table 10. Overview of key sediment transport model parameters.

Description	Value applied
Horizontal eddy diffusivity	0.5 m^2/s
Background vertical eddy diffusivity	1.00E-6 m^2/s
Fluff layer 0th-order erosion parameter (M_2)	2.00E-5 m^2/s
Fluff layer 1st-order erosion parameter (M_1)	1.00E-4 m^2/s
Fluff layer critical shear stress threshold for erosion ($\tau_{cr,f}$)	0.15 N/m^2
Burial fraction on deposition (α)	0.15
Settling velocity (w_s) – dredging fines	0.2 mm/s
Settling velocity (w_s) – natural fines	0.5 mm/s
Buffer layer critical shear stress threshold for erosion ($\tau_{cr,e}$)	1.0 N/m^2
Buffer layer erosion parameter (M_0)	2.00E-5 m^2/s
Buffer layer thickness (d_0)	0.05 m

6 Passive dredging plume model results

In this section, modelled TSS results near the surface were compared with MODIS, and modelled TSS results near the bed were compared with *in situ* mobile near bed TSS measurements both qualitatively and quantitatively. Modelled deposition and sedimentation maps were also presented. First the broad trends in modelled near surface TSS will be described with reference to the MODIS TSS product. Subsequently a quantitative comparison of the model to the various observations of TSS will be described with a range of model skill metrics and time series comparison. It is particularly important to compare the probability distributions of observed and modelled TSS, as this will reflect the likelihood of a given threshold TSS being exceeded. The Quantile-Quantile plots (QQ-plot) will be presented to compare these distributions. Finally, indicative maps of potential water quality and deposition will be presented to inform assessment of ecological pressure or highlight the likelihood of ecological impact.

6.1 Qualitative comparison with MODIS TSS

Figure 26, Figure 27 and Figure 28 present comparisons of the modelled near surface TSS and MODIS TSS at 26 June 2013, 27 August 2013 and 26 September 2013.

A significant wave driven resuspension event occurred on the 26 June 2013 in conjunction with an extended period of south westward residual current (Figure 26). The concentration of the initial dredging plume is reproduced reasonably well, albeit with a small westerly offset. The location and concentration of plumes at the spoil ground are reproduced quite well. The resuspension extents and concentration in the nearshore region southwest of the dredging is also reproduced reasonably well, however the resuspension in the nearshore between Roller and Locker is somewhat over-estimated. The resuspension to the east, around the Mangrove location is significantly overestimated, a feature that is persistent through-out the simulation, likely due to a combination of poor bathymetry, over-estimated fines availability and coarser grid resolution throughout this region. Also, in the offshore region, to the north west of Serrurier, Bessieres and Thevenard Islands the model over-predicts resuspension. Along the 50 m shelf break a band of elevated fines mass accumulates in the fluff layer at a depth where the fluff layer shear stress threshold for resuspension is infrequently exceeded. In subsequent larger wave events, the model predicts that this material will be bought into suspension, however this feature is not visible in the MODIS data.

During 27 August 2013, a time of lower bed shear stress following a period of somewhat elevated bed shear stress, an intense dredging plume is visible in the nearshore region that is reasonably well reproduced by the model (Figure 27). The plumes in the proximity of the spoil ground are quite well reproduced, however TSS levels to the east of Mangrove are overestimated similar to Figure 26. The general background level TSS between 1-3 mg/L that is present on the inner shelf is under estimated by the model. The magnitude of TSS in the nearshore

around Fly and Tubridgi is reasonably well reproduced in the model, however is under-estimated in the proximity of Locker.

Figure 28 presents a comparison for a period of strong north eastward residual current and a period of extensive dredging in the nearshore zone. The model appears to over predict the surface TSS in the nearshore between Ward and the berth pocket, however reproduces the general extent in the nearshore quite well. The nearshore TSS to the south west is well reproduced from the Roller to Fly locations. The plumes extending from the spoil ground to the north-west are reproduced reasonably well albeit with an overall more diffuse character. The modelled plumes extending from the channel are more pronounced than in the MODIS TSS. The region to the east around the Mangrove and West locations is over estimated and the low TSS concentration on the inner shelf is underestimated in the model similar to Figure 26 and Figure 28.

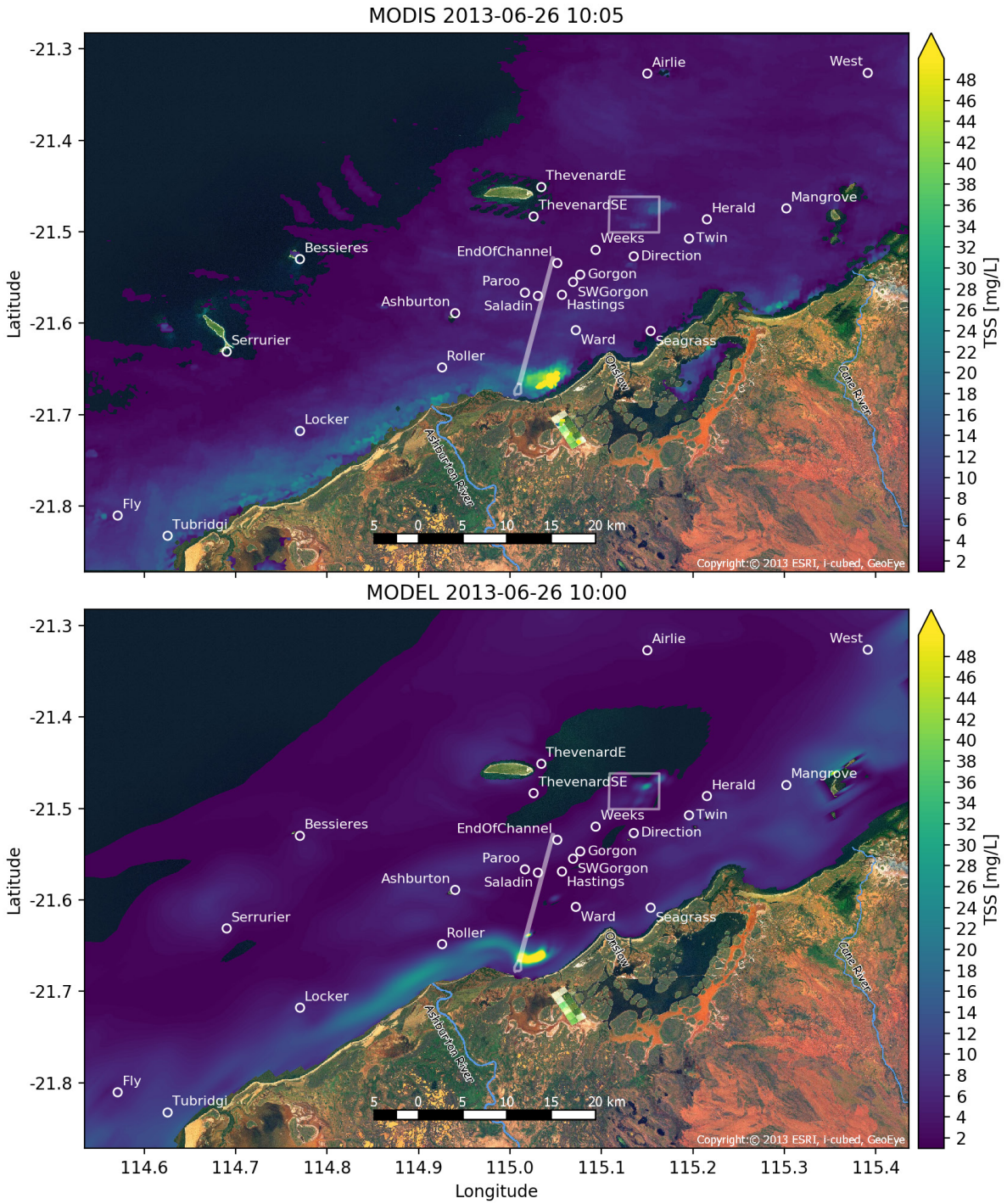

Figure 26. Comparison between MODIS TSS and modelled near surface TSS on 26 June 2013 during a resuspension event with net south-westerly drift.

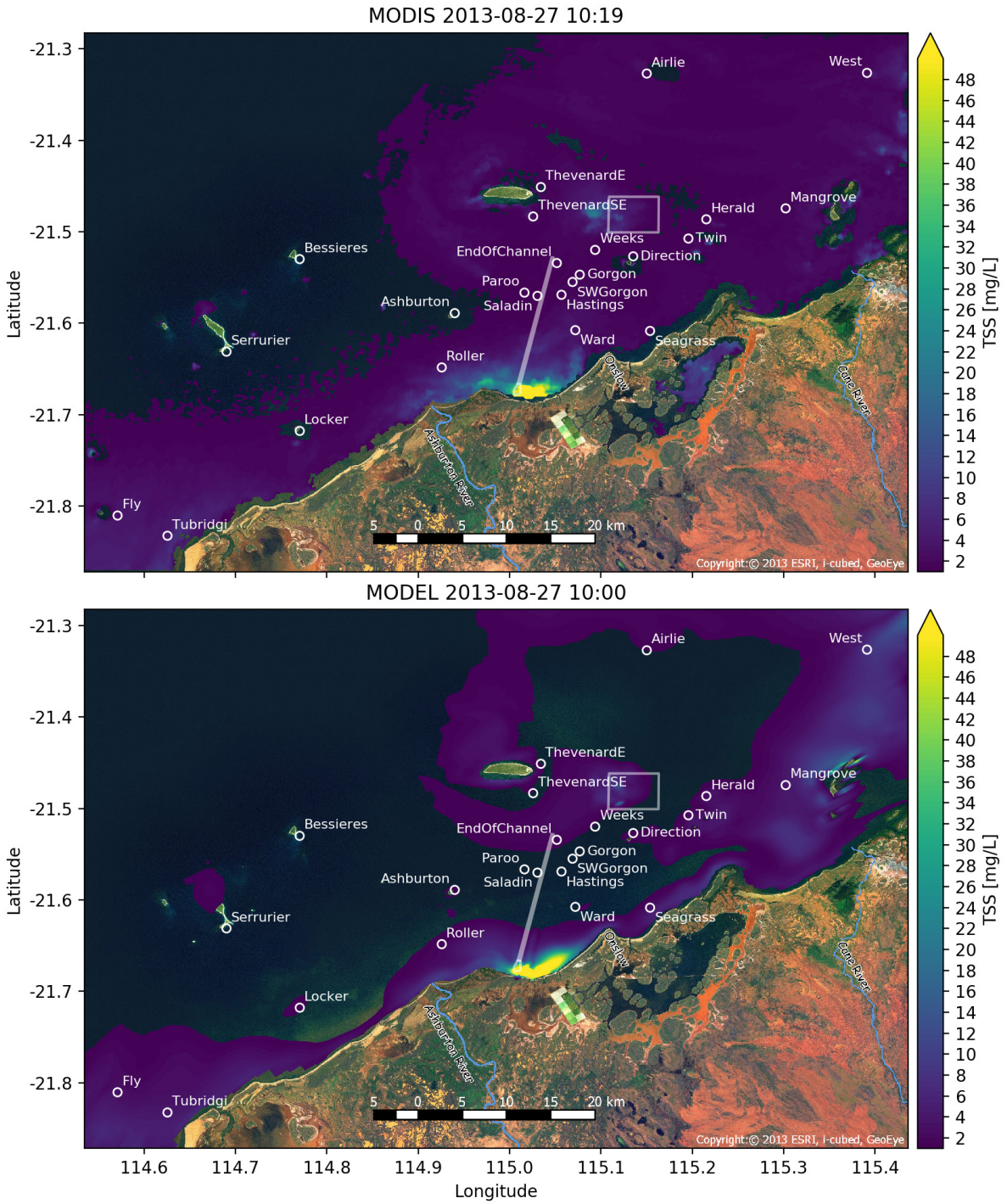

Figure 27. Comparison between MODIS TSS and modelled near surface TSS on 27 August 2013 during intense nearshore dredging and net north easterly drift

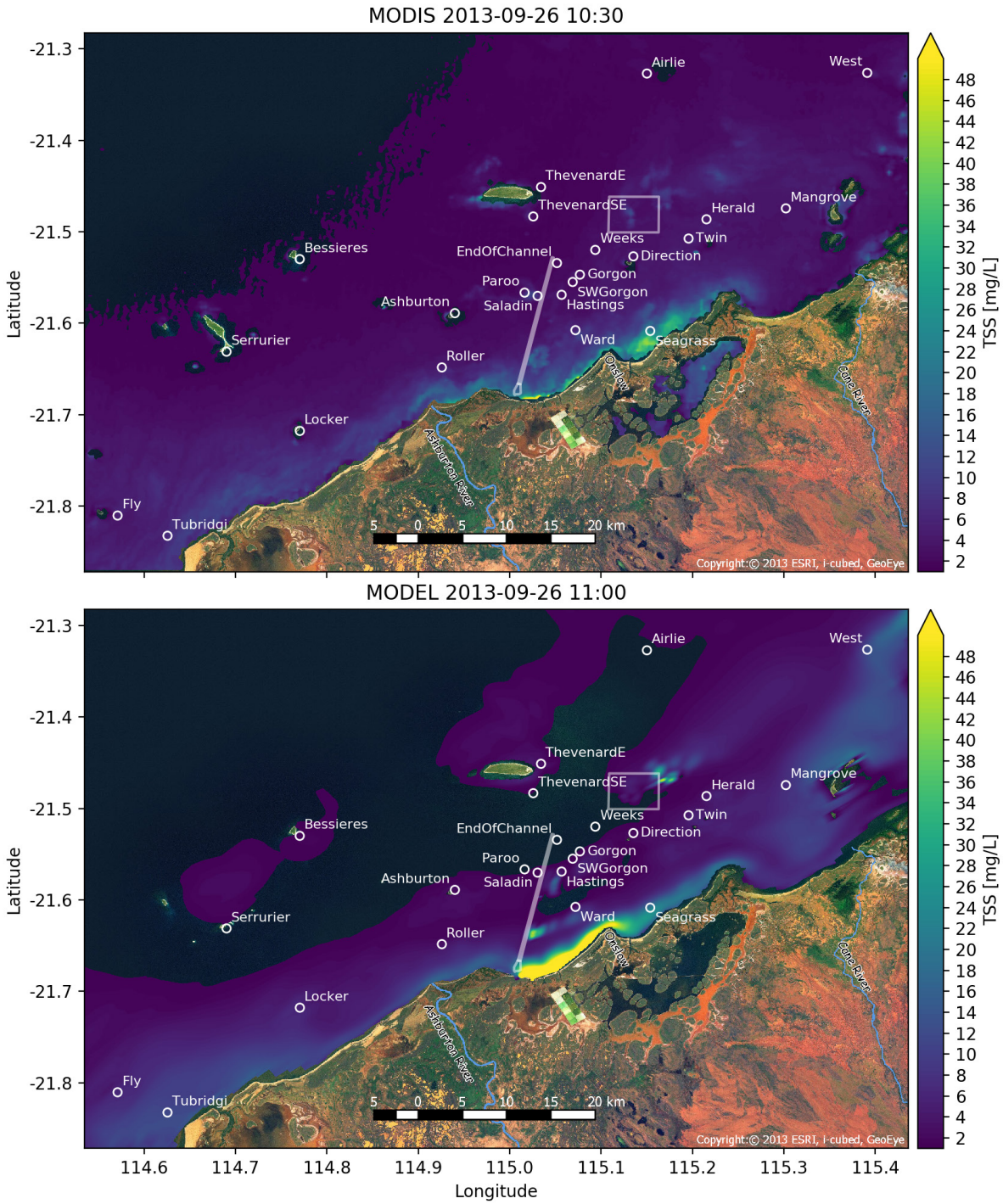

Figure 28. Comparison between MODIS TSS and modelled near surface TSS on 26 September 2013 during strong net north easterly drift.

6.2 Quantitative comparison with MODIS TSS and *in situ* measurements

Table 11 presents a summary of the model skill metrics for the daily averaged TSS at the Nearshore locations. The comparison with MODIS TSS is over the polygons denoted NearshoreEast1, NearshoreEast2 NearshoreWest1, NearshoreWest2. Figure 29 presents a time series comparison of the modelled and measured daily averaged TSS at the nearshore location and Figure 30 presents quantile-quantile plots for the same period and locations. Overall the model reproduces the dynamics of TSS in the nearshore well, with the phasing of modelled peaks in TSS being reasonably consistent with measured peaks. The model has an overall negative bias of ~2 mg/L at the fixed monitoring stations, which increases in magnitude to negative 8 mg/L for the mobile stations, which were generally located closer to the source dredging plumes. The negative bias is most pronounced during low TSS periods. In general, the magnitude of TSS peaks observed at the mobile monitoring stations (TEWL##) are underestimated by up to 50% and this is highlighted further in the QQ plots presented in Figure 30. The exception are the MODIS areas and the Locker location for which the modelled and measured percentiles are reasonably consistent. Model skill was generally good, with some locations and areas having very high skill and strong correlation (i.e. NearshoreEast2, TEWL01 and Seagrass).The worst model skill and greatest error occurred at TEWL07 which was located initially on the inner shelf to the west of the channel (from April to June 2013) and subsequently was moved to the mouth of the Ashburton river from mid-June through December 2013 resulting in the model having significant negative bias as no source was specified for the Ashburton river.

Table 11. Overview of model skill metrics for Nearshore locations, MODIS polygons are in *italics* other locations are *in situ* measurements of TSS approximately 1 m above the sea bed. d = Willmott (1981) index of agreement, dr = Willmott et al. (2012) refined index of agreement, NS = Nash & Suttcliffe (1970) coefficient of efficiency, BIAS = difference between modelled and measured mean, CC = Correlation Coefficient and MSE = Mean Squared Error.

Site/Polygon	d	dr	NS	BIAS	CC	MSE
NearshoreEast1	0.68	-0.17	-0.51	0.42	0.51	31.95
NearshoreEast2	0.87	0.25	0.42	-0.44	0.78	6.11
NearshoreWest1	0.65	-0.26	-0.32	-1.83	0.47	17.45
NearshoreWest2	0.68	-0.45	-0.16	-1.41	0.60	5.10
TEWL01	0.81	0.45	0.46	-8.82	0.76	374.89
TEWL04	0.71	0.30	0.21	-6.27	0.61	209.19
TEWL05	0.67	0.22	0.14	-7.54	0.57	267.64
TEWL07	0.55	-0.24	-0.66	-14.06	0.49	366.38
TEWL08	0.53	0.00	-0.14	-4.31	0.39	75.46
TEWL10	0.63	0.02	-0.08	-4.78	0.57	61.87
Fly	0.72	0.00	0.09	-2.28	0.71	11.71
Locker	0.73	-0.10	-0.01	-1.32	0.61	6.62
Roller	0.64	0.13	0.13	-2.68	0.61	26.32
Seagrass	0.86	0.49	0.64	-1.41	0.83	36.43
Tubridgi	0.66	0.08	0.11	-2.32	0.50	51.75
Ward	0.75	-0.19	0.10	-2.74	0.77	13.99

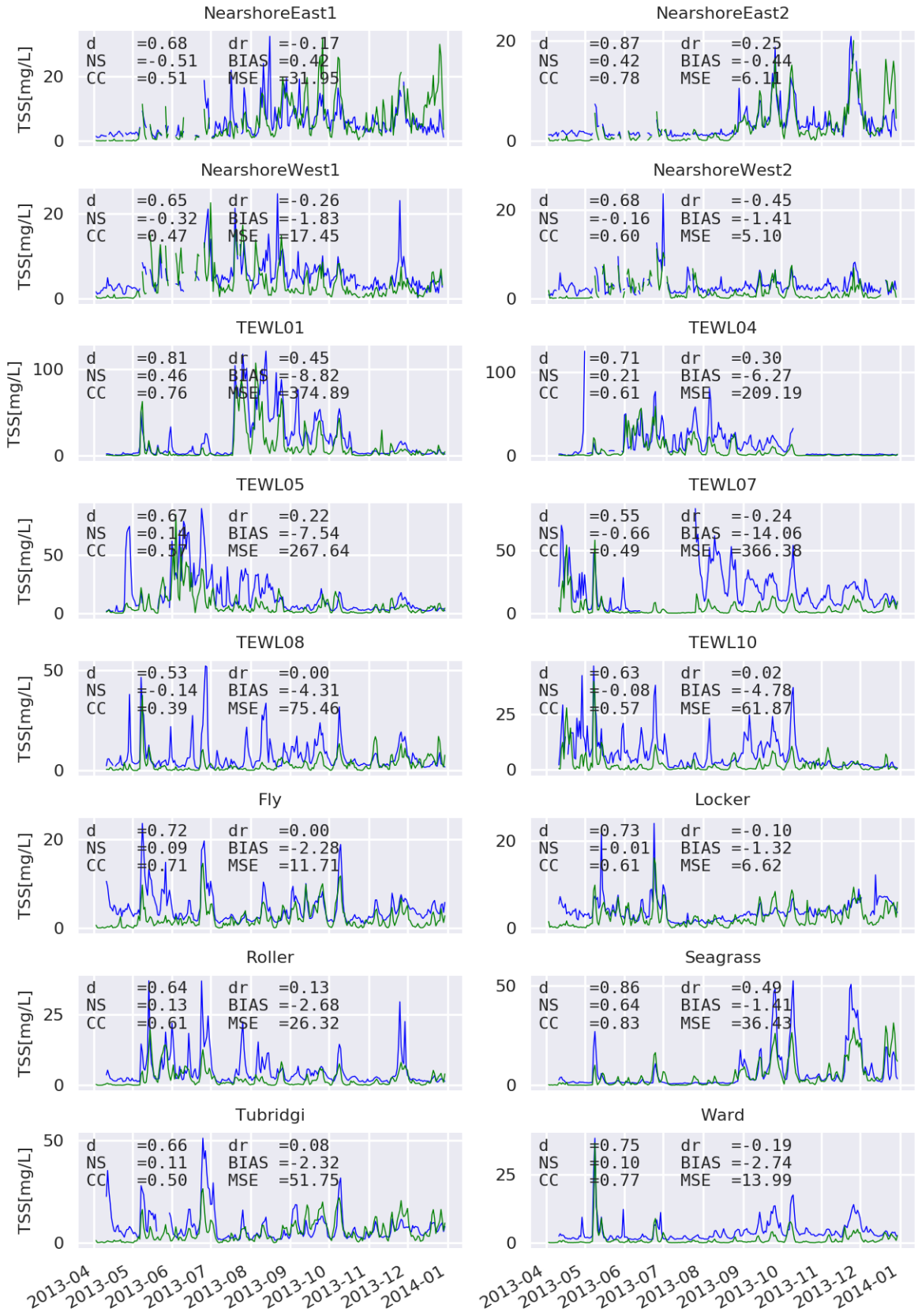

Figure 29. Time series comparison of observed (blue) and modelled (green) daily mean TSS for Nearshore locations. d = Willmott (1981) index of agreement, dr = Willmott et al. (2012) refined index of agreement, NS = Nash & Suttcliffe (1970) coefficient of efficiency, BIAS = difference between modelled and measured mean, CC = Correlation Coefficient and MSE = Mean Squared Error.

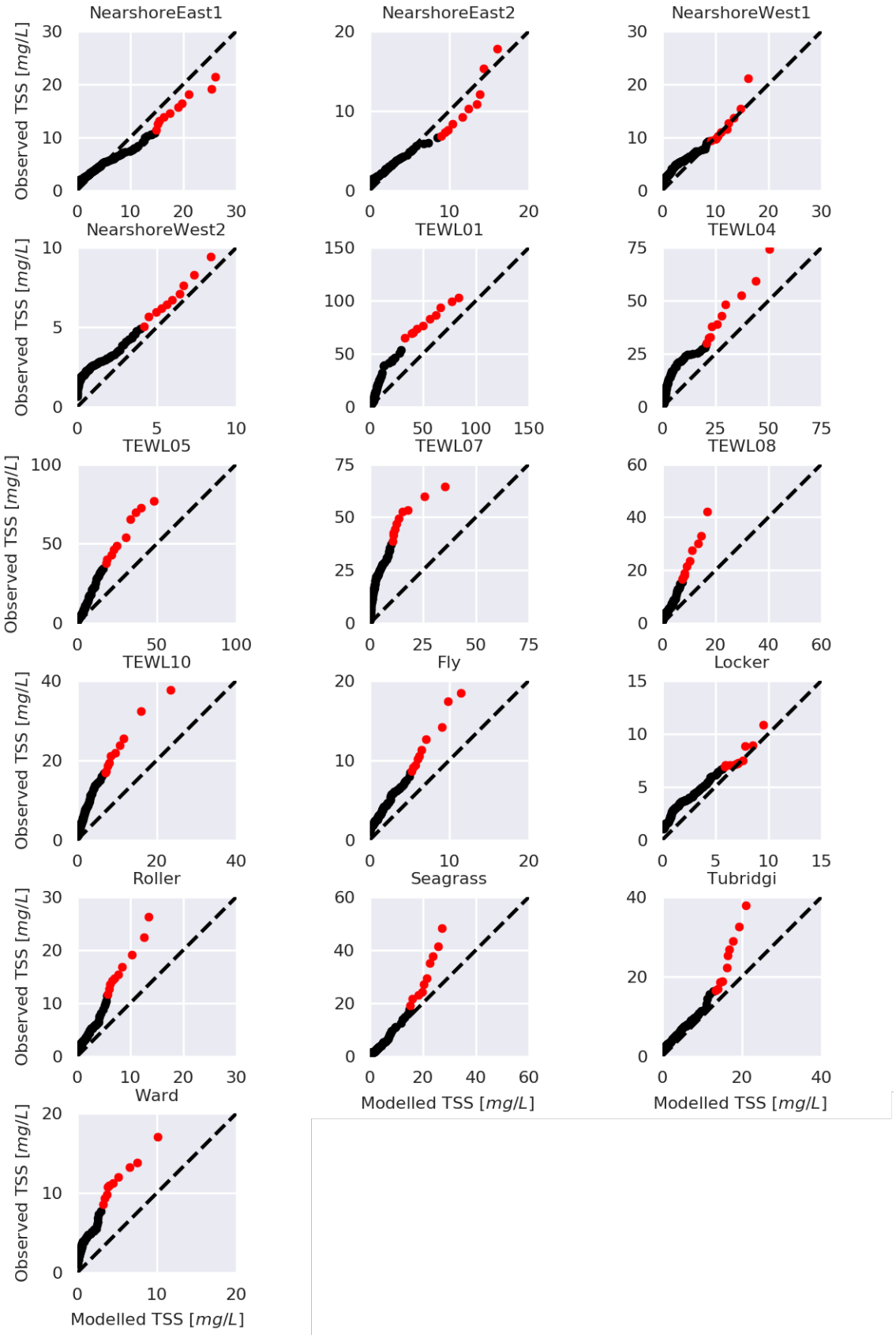

Figure 30. QQ-plots of observed and modelled daily mean TSS at Nearshore locations. Black dots indicate percentiles from 1 to 90, red dots indicate percentiles from 90 to 99.

Table 12 presents a summary of the model skill metrics for the daily averaged TSS at the Inner Shelf locations. Figure 31 presents a time series comparison of the modelled and measured daily averaged TSS at the Inner Shelf location and Figure 32 presents quantile-quantile plots for the same period and locations. TSS is generally an order of magnitude lower on the Inner Shelf than the Nearshore and this cross-shore reduction is reproduced in the model well. A negative bias of ~1 mg/L is present across the inner shelf sites and this is exhibited in Figure 32 with the percentiles up to 90% being underestimated by approximately 1 mg/L in the model however percentiles greater than 90% are reasonably consistent with measurements. Model skill and correlation is generally lower compared to the nearshore, however this is partly due to the smaller overall magnitude of the TSS variability.

Table 12. Overview of model skill metrics for Inner Shelf locations, MODIS polygons are in *italics* other locations are *in situ* measurements of TSS approximately 1 m above the sea bed. d = Willmott (1981) index of agreement, dr = Willmott et al. (2012) refined index of agreement, NS = Nash & Suttcliffe (1970) coefficient of efficiency, BIAS = difference between modelled and measured mean, CC = Correlation Coefficient and MSE = Mean Squared Error.

Site/Polygon	**d**	**dr**	**NS**	**BIAS**	**CC**	**MSE**
ChannelEast1	0.51	-0.93	-1.34	-1.54	0.44	3.94
ChannelWest1	0.41	-0.55	-2.48	-0.93	0.17	1.57
ChannelEast2	0.41	-0.55	-1.78	-1.03	0.21	2.06
ChannelWest2	0.47	-0.93	-2.21	-0.78	0.28	0.99
Airlie	0.70	-0.45	-0.85	-0.33	0.60	1.64
Ashburton	0.66	-0.56	-1.60	0.25	0.57	2.85
EndOfChannel	0.61	-0.55	-1.32	-1.14	0.47	5.33
Paroo	0.63	-0.95	-0.59	-0.92	0.50	2.86
Saladin	0.60	-0.51	-0.40	-0.87	0.42	3.20
Hastings	0.69	-0.57	-0.74	-0.96	0.59	3.48
SWGorgon	0.68	-0.61	-0.21	-0.90	0.56	2.89
Gorgon	0.60	-0.54	-0.86	-1.27	0.54	3.53
ThevenardSE	0.42	-0.69	-5.78	-1.06	0.45	1.47
Weeks	0.50	-0.55	-2.53	-0.72	0.29	5.32

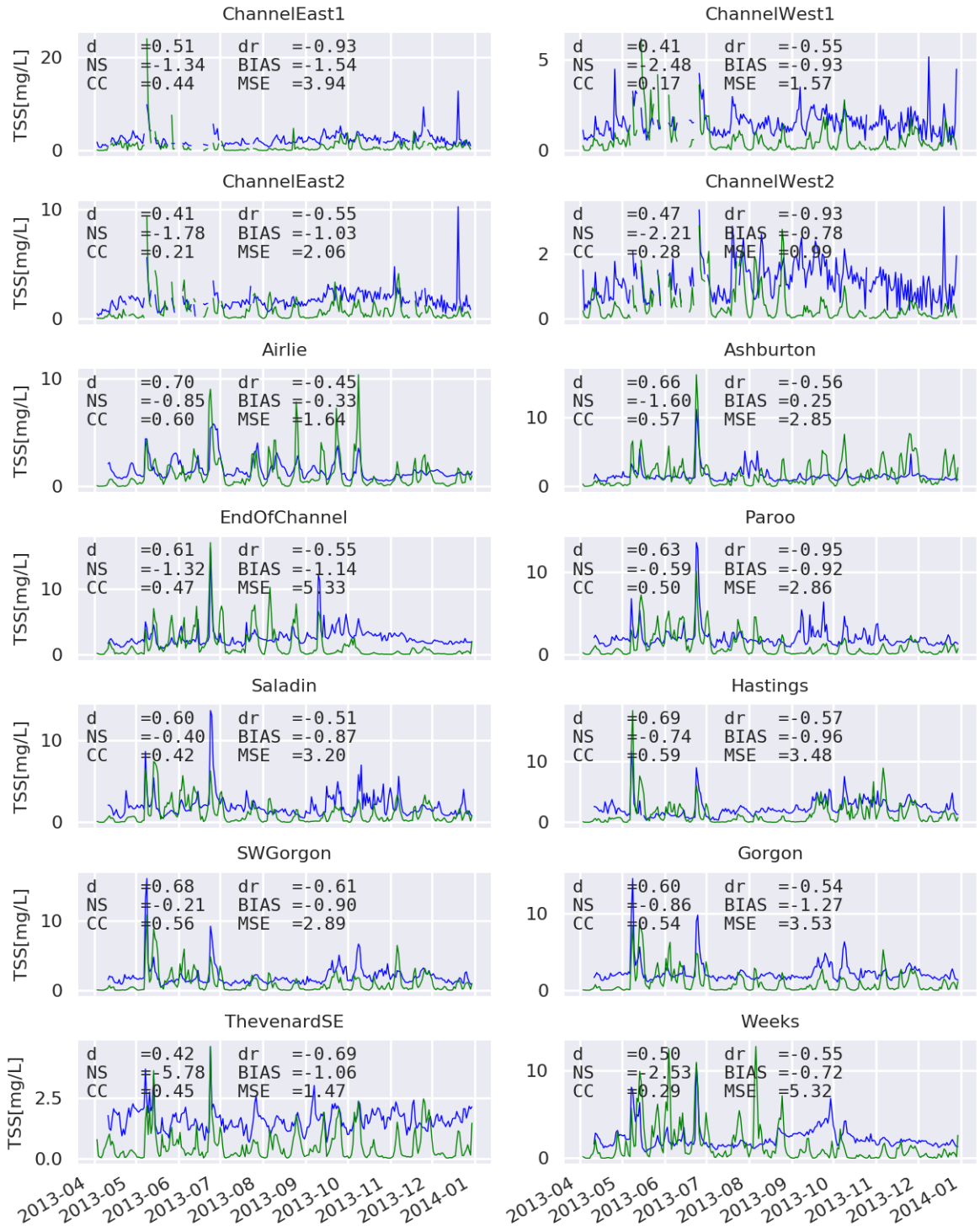

Figure 31. Time series comparison of observed (blue) and modelled (green) daily mean TSS for Inner shelf locations. d = Willmott (1981) index of agreement, dr = Willmott et al. (2012) refined index of agreement, NS = Nash & Suttcliffe (1970) coefficient of efficiency, BIAS = difference between modelled and measured mean, CC = Correlation Coefficient and MSE = Mean Squared Error.

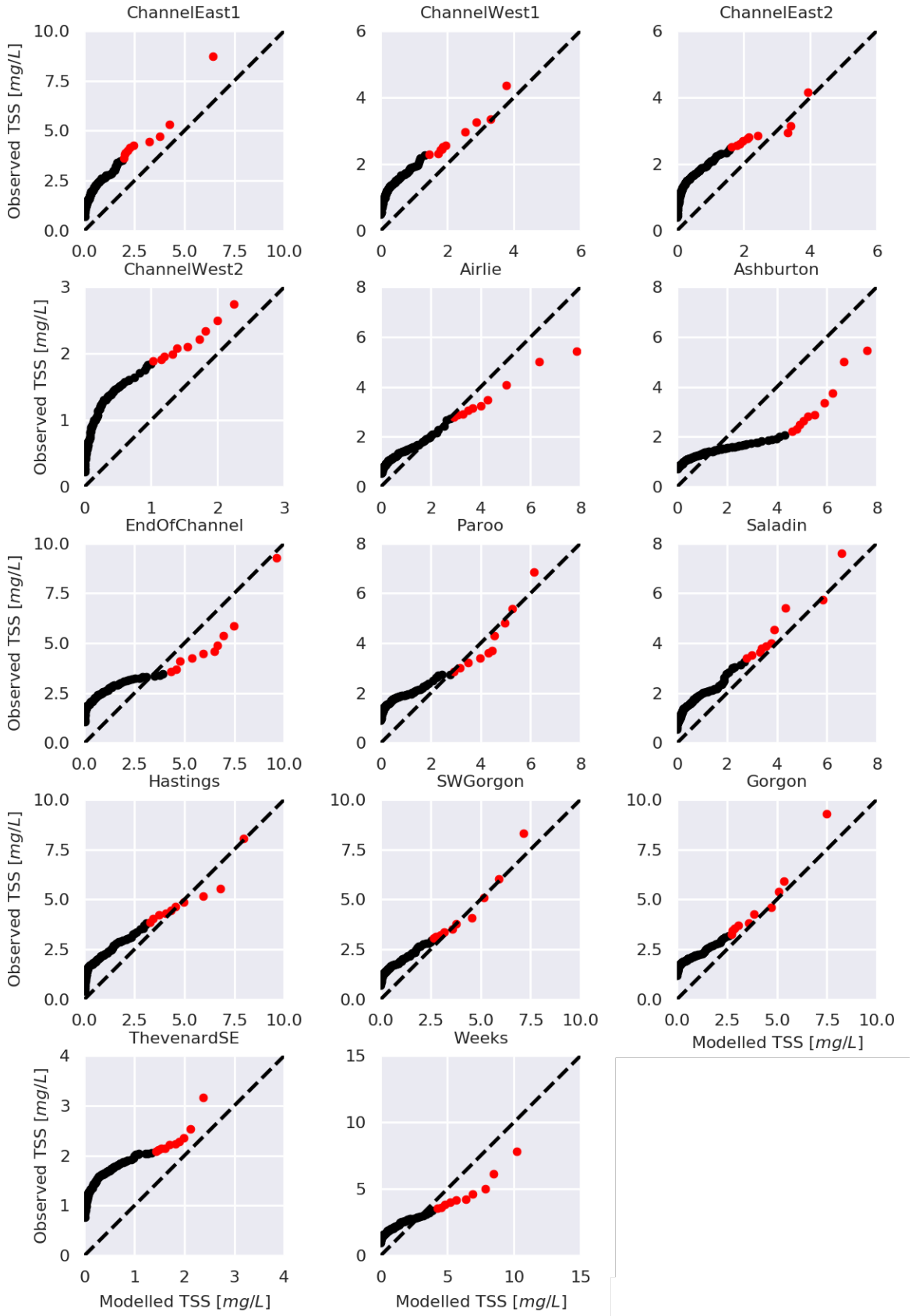

Figure 32. QQ-plots of observed and modelled daily mean TSS at Inner shelf locations. Black dots indicate percentiles from 1 to 90, red dots indicate percentiles from 90 to 99.

Table 13 presents a summary of the model skill metrics for the daily averaged TSS at the Offshore locations. Figure 33 presents a time series comparison of the modelled and measured daily averaged TSS at the Offshore location and Figure 34 presents quantile-quantile plots for the same period and locations. TSS is generally an order of magnitude lower on the Offshore location than the Nearshore and this cross-shore reduction is reproduced in the model well. A negative bias of less than 1 mg/L is present across the Offshore sites. The region around the spoil ground is modelled quite well, with the SpoilGroundEast and TEWL09 locations having good model skill and strong correlation. Similarly, there is good agreement between the modelled and measured TSS percentiles for the location near to the Spoil Ground (Figure 34). At locations near to the offshore islands, measured TSS peaks were overestimated despite having a reasonable degree of correlation. This is consistent with the results from qualitative comparison with MODIS TSS presented in Section 6.1 and is highlighted by overestimation of the upper percentiles at the fixed monitoring stations presented in Figure 34.

Table 13. Overview of model skill metrics for Offshore locations, MODIS polygons are in *italics* other locations are *in situ* measurements of TSS approximately 1 m above the sea bed. d = Willmott (1981) index of agreement, dr = Willmott et al. (2012) refined index of agreement, NS = Nash & Suttcliffe (1970) coefficient of efficiency, BIAS = difference between modelled and measured mean, CC = Correlation Coefficient and MSE = Mean Squared Error.

Location	d	dr	NS	BIAS	CC	MSE
SpoilGroundWest	0.39	-0.62	-0.91	-0.72	0.12	1.93
SpoilGroundEast	0.75	-0.17	-0.18	-0.36	0.63	1.35
TEWL06	0.59	-0.39	-1.10	-0.33	0.40	10.08
TEWL09	0.81	0.08	0.37	-0.83	0.79	1.75
Bessieres	0.59	-0.61	-4.68	0.13	0.65	0.80
Serrurier	0.68	-0.57	-2.22	-0.30	0.72	0.69
ThevenardE	0.49	-0.60	-3.44	-0.45	0.33	1.22

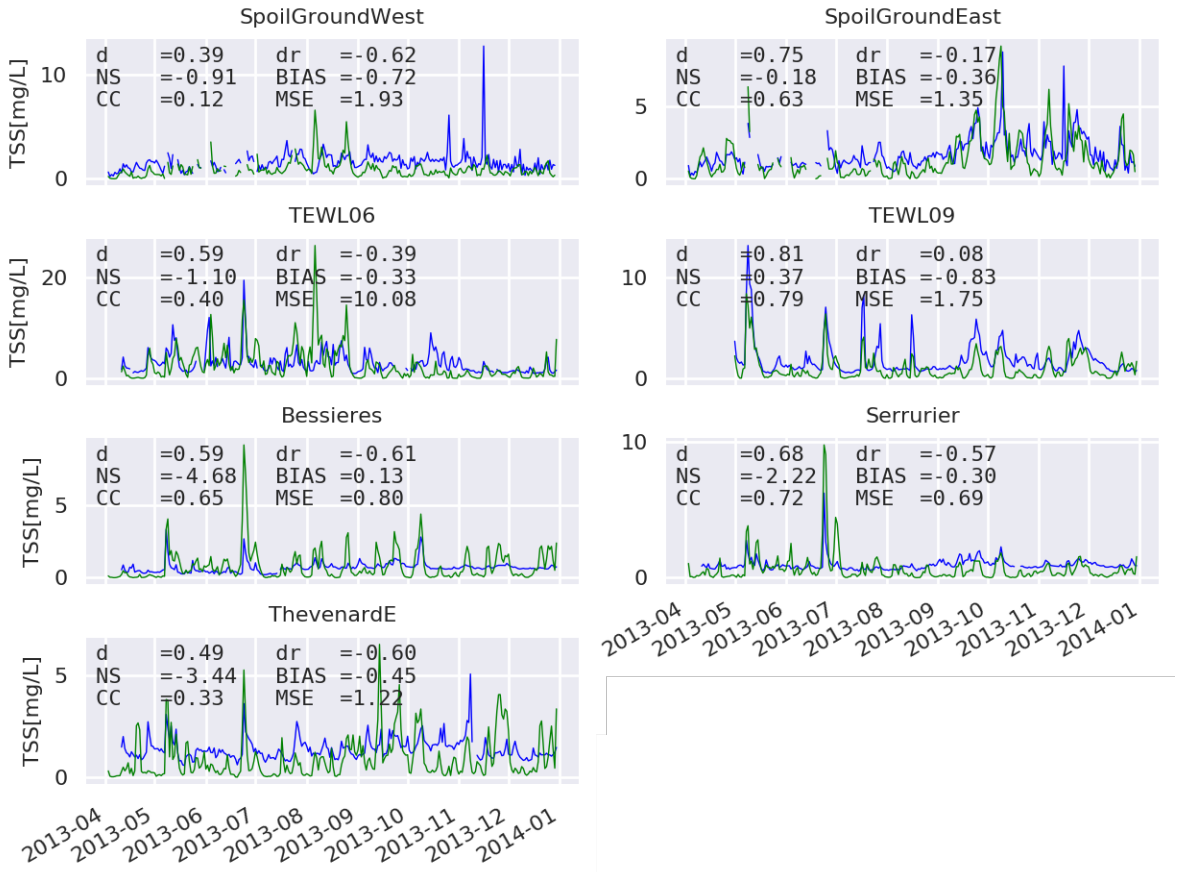

Figure 33. Time series comparison of observed (blue) and modelled (green) daily mean TSS for Offshore locations and the Spoil Ground. d = Willmott (1981) index of agreement, dr = Willmott et al. (2012) refined index of agreement, NS = Nash & Suttcliffe (1970) coefficient of efficiency, BIAS = difference between modelled and measured mean, CC = Correlation Coefficient and MSE = Mean Squared Error.

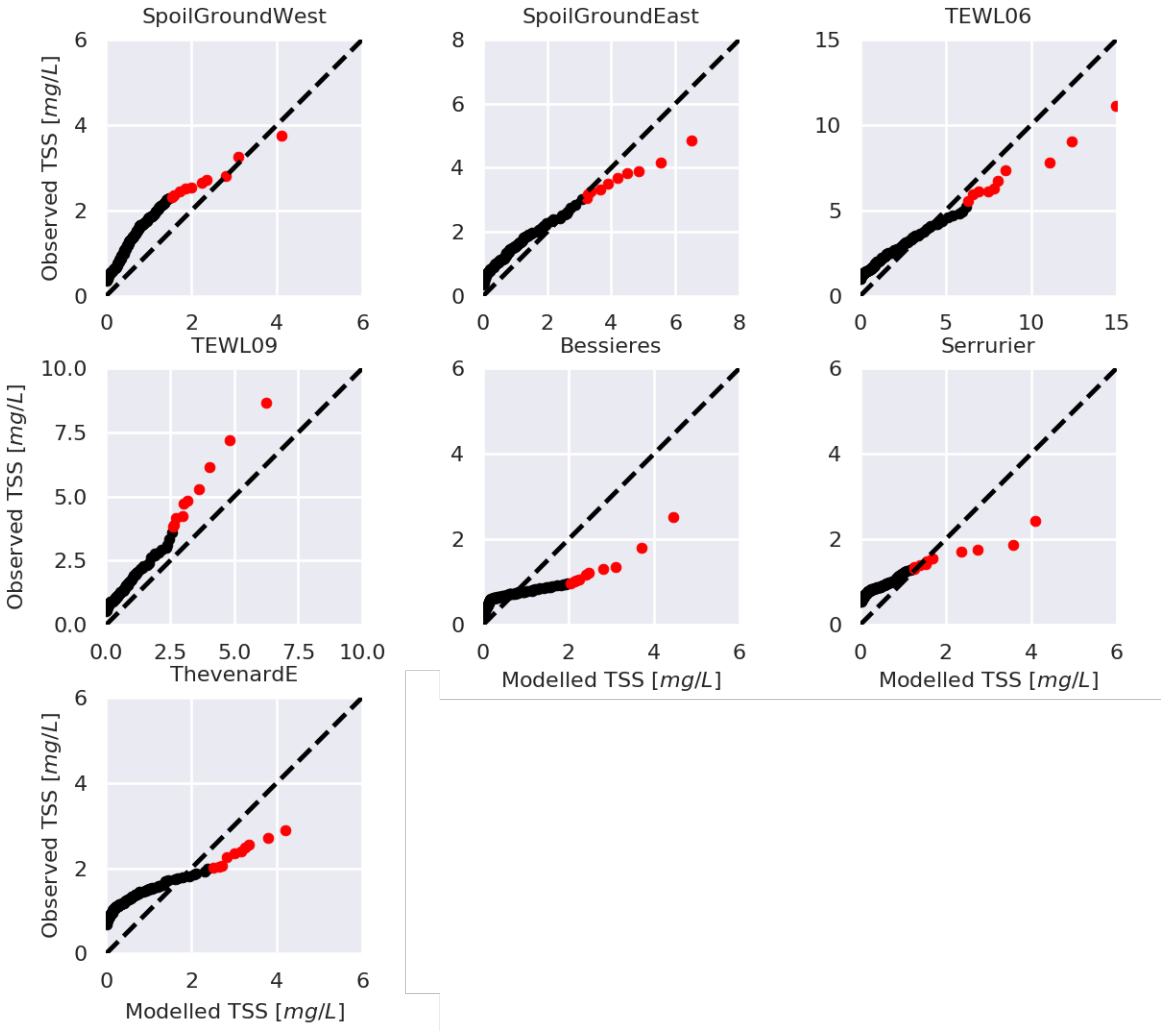

Figure 34. QQ-plots of observed and modelled daily mean TSS at Offshore locations. Black dots indicate percentiles from 1 to 90, red dots indicate percentiles from 90 to 99.

Table 14 presents a summary of the model skill metrics for the daily averaged TSS at the Eastern Islands locations. Figure 35 presents a time series comparison of the modelled and measured daily averaged TSS at the Eastern Islands locations and Figure 36 presents quantile-quantile plots for the same period and locations. TSS is generally higher at the Eastern Islands locations than the Inner Shelf and Offshore locations, but lower than the Nearshore locations. The model has a positive bias across these sites of approximately 2 mg/L with the exception of the Direction location which has a negative bias, particularly during the low TSS periods. Observed peaks in TSS are significantly over-estimated at the Twin, Herald and West locations, consistent with the qualitative comparison of modelled TSS with MODIS TSS presented in Section 6.1.

Table 14. Overview of model skill metrics for Eastern Islands locations, MODIS polygons are in *italics* other locations are *in situ* measurements of TSS approximately 1 m above the sea bed. d = Willmott (1981) index of agreement, dr = Willmott et al. (2012) refined index of agreement, NS = Nash & Suttcliffe (1970) coefficient of efficiency, BIAS = difference between modelled and measured mean, CC = Correlation Coefficient and MSE = Mean Squared Error.

Site/Polygon	d	dr	NS	BIAS	CC	MSE
Direction	0.75	-0.28	-0.12	-0.69	0.65	2.29
Twin	0.53	-0.57	-6.84	1.66	0.67	24.34
Herald	0.44	-0.64	-9.38	1.96	0.55	30.11
Mangrove	0.75	-0.15	-0.51	0.34	0.65	7.92
West	0.55	-0.65	-5.47	2.55	0.71	14.30

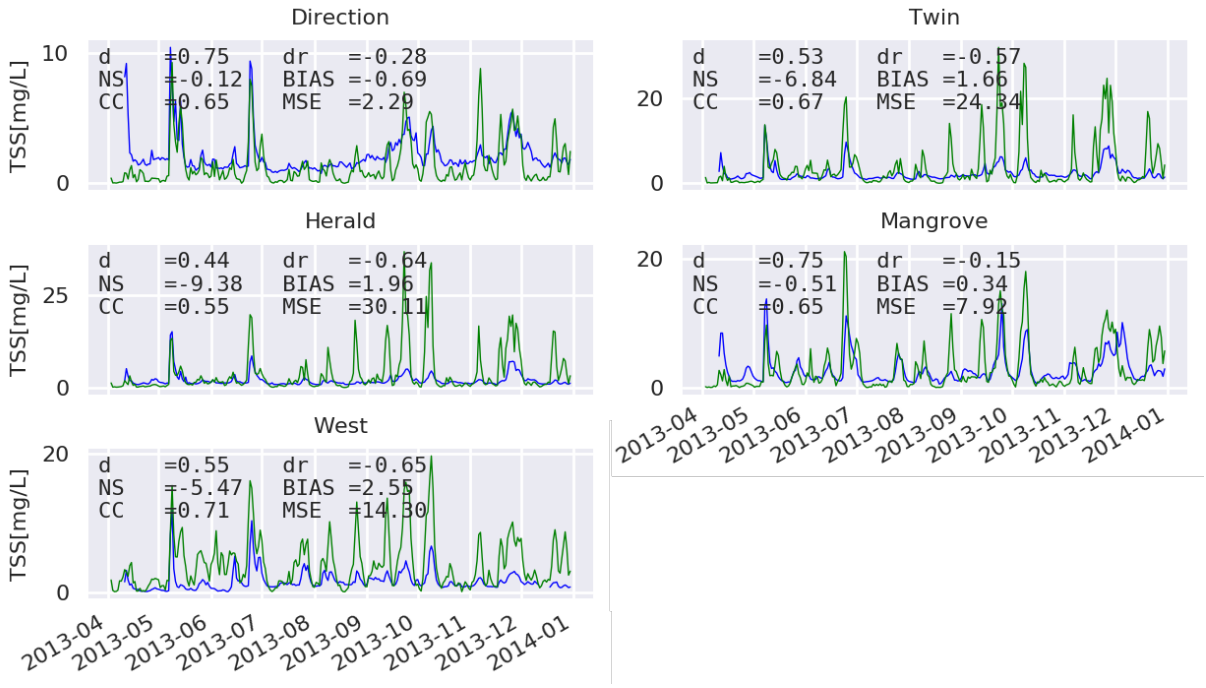

Figure 35. Time series comparison of observed (blue) and modelled (green) TSS for Eastern Islands locations. d = Willmott (1981) index of agreement, dr = Willmott et al. (2012) refined index of agreement, NS = Nash & Suttcliffe (1970) coefficient of efficiency, BIAS = difference between modelled and measured mean, CC = Correlation Coefficient and MSE = Mean Squared Error.

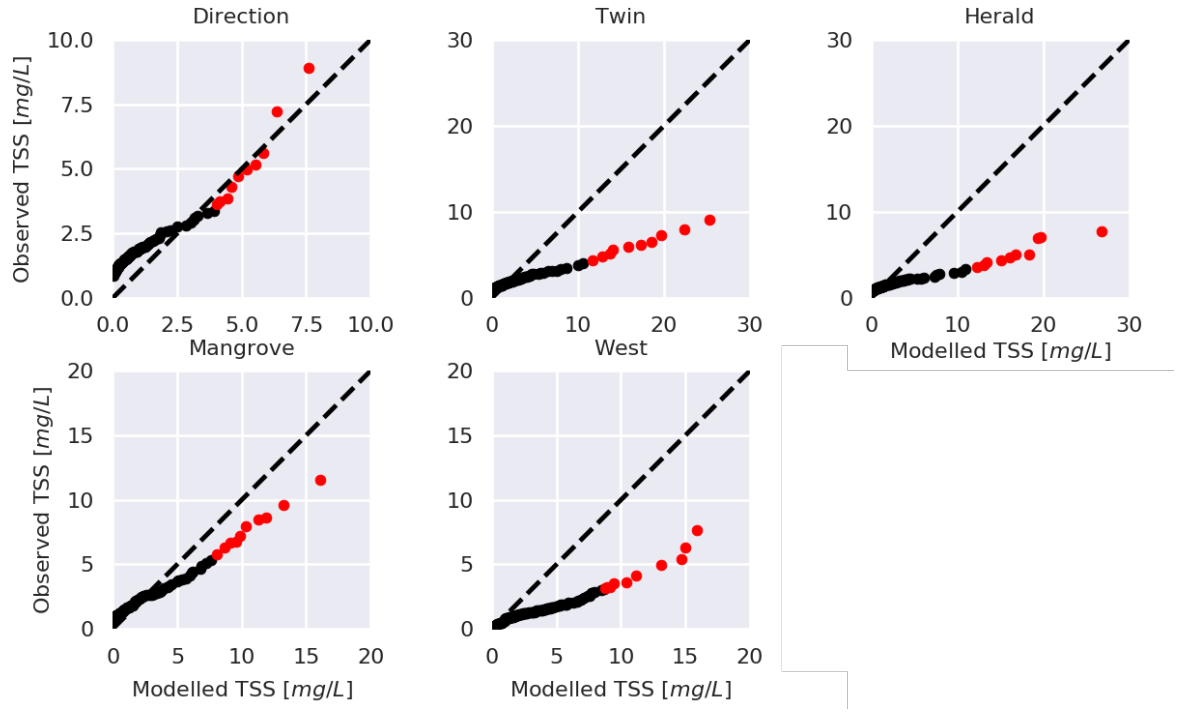

Figure 36. QQ-plots of observed and modelled TSS at Eastern Islands locations. Black dots indicate percentiles from 1 to 90, red dots indicate percentiles from 90 to 99.

6.3 Translating plume model results into ecological pressure fields

In environmental impact assessment it is necessary to translate model output into ecologically relevant pressure fields that assist in delineating management zones. However, this task is not straightforward and finding effective and robust methods to translate model output into pressure fields remains a significant challenge in EIA modelling. Here we demonstrate some useful methods to derive pressure fields. Fisher et al. (2017) presents a detailed analysis of water quality and coral health data from a large dredging project at Barrow Island, which is a clear water environment. They developed dose-response relationships and estimated thresholds for corals with three cause-effect pathways: deposition, TSS and light attenuation. They found that deposition has the greatest statistical power in predicting coral mortality, however, deposition cannot be reliably measured in the field with current technology. Therefore, light and TSS are the best choice despite their lower statistical power. A detailed analysis of the challenges associated with the development and application of pressure field thresholds for environmental management of dredging is provided in Fisher et al. (2018), titled "Deriving and operationalizing thresholds for managing dredging impacts on coral reefs."

These thresholds for corals in a clear water environment are applied to our passive plume model results as a demonstration on how model results could be translated into ecologically relevant pressure fields. Note these thresholds are hypothetical in this study with no consideration of the actual presence of coral or other benthic habitats within the study area. The purpose of this exercise is to demonstrate the following: 1) the challenge in translating thresholds from one location to another; 2) the difficulty of utilising a single fixed threshold across a system with a wide range in TSS (and near bed light) climatology and 3) the advantages of modelling the combined dredging and ambient TSS. When carrying out an actual environmental impact assessment, the modeller should use the habitat map and apply relevant thresholds in the particular environment for different benthic ecosystems, such as corals, seagrasses and sponges.

6.3.1 Deposition and sedimentation

Fisher et al. (2017) identified that deposition provided the greatest power in predicting impacts, however, the difficulty of measuring deposition in a robust, repeatable manner in the field makes utilising deposition as a management indicator difficult. In addition, it is a difficult measure to calculate from the numerical model due to repeated resuspension and reworking of dredging material. Whilst this may be the case with respect to monitoring it remains informative to examine the modelled sedimentation of dredging fines in order to highlight the fate of the dredging fines across the system and assist in identifying which receptors may potentially be impacted and which are likely not.

Figure 37 presents the total sedimentation thickness on 31 December 2013 (modelled total sedimentation over the period 1 April through 31 December) and shows the distribution of dredging fines transported in the passive plume deposited to the seabed. The figure does not show the sedimentation due to directly placed material or due to density currents in the dynamic plume phase. Daily deposition was calculated by calculating the difference in modelled sedimentation from one day to the next.

The 60-day running mean of the daily deposition of dredging fines was calculated and is presented in Figure 38 for various contour intervals. Similarly, Figure 39 presents a range of contours for the percentage of days where deposition exceeded 0.04 mg/cm^2/day. Figure 40 presents a range of contours for the maximum number of consecutive days where the modelled daily deposition was greater than 0.19 mg/cm^2/day. It is important to note that these values are used hypothetically for demonstration purpose and they should not be compared to thresholds derived in Fisher et al. (2017) due to the differences in the environment (turbid water in our case study vs very clear water in Fisher's case), and the inherent difficulty in measuring sediment deposition in situ and converting Settled Sediment Surface Density (SSSD) to a deposition rate (Stark et al, 2017). As such these results can only be considered qualitatively to provide insight into the modelled spatial distribution of net deposition. As concluded in Fisher et al (2017) the relative ease with which light and TSS can be measured in a reliable and repeatable manner make light and TSS more appropriate for quantitative assessment than sediment deposition rate, which cannot be reliably measured at the present.

6.3.2 Total suspended solids

The 14-day running mean TSS may be a useful operational management trigger (Fisher et al. 2017). Figure 41 presents a spatial plot of the modelled peak 14-day running mean near bed TSS (combined natural and dredging) for the period April to December 2013. Contour lines indicate the percentage of the peak TSS that is contributed by dredging fines to provide context to the influence of dredging. It is noted that it is the combined stress of dredging and natural TSS forcing that result in ecological impacts. Therefore, the approach of only considering suspended sediments due to dredging activities without taking ambient sediments into account is inadequate when evaluating ecological impacts.

Fisher et al. (2017) establish management thresholds for corals based on the 80th and 95th percentile values derived from the baseline water quality data collected in the relatively clear offshore waters around Barrow Island. To apply these thresholds to modelled TSS, the NTU thresholds defined in Fisher et al. (2017) were converted to TSS using a factor of 1.8 (i.e. TSS = 1.8 x NTU) – the best estimate conversion factor for that site (Fisher *pers. comm.*). Figure 42 presents the percentage of days where the modelled daily mean near bed TSS exceeded 3.2 mg/L with the strict and permissive thresholds of 45% and 64% shown. Figure 43 presents the maximum number of consecutive days where the modelled daily near bed TSS exceeded 8.6 mg/L between 1 April 2013 and 31 December 2013. It is noted that these thresholds define a very limited spatial extent around the spoil ground and a significantly broader extent in the nearshore.

The Fisher et al. (2017) TSS thresholds are likely to have some relevance for the clearer offshore waters in this study area, however, they are likely too low for the more turbid nearshore region. In an ideal EIA study, the modelling results would be assessed against an appropriate benthic habitat map for the region and relevant thresholds for each benthic system applied. Here the TSS thresholds applied are hypothetical for the purpose of demonstrating how model results may be translated into pressure fields. An advantage of having modelled the natural dynamics of TSS in addition to the passive dredging plume dynamics is that it is possible to analyse the model results excluding the dredging fine fraction. A spatially variable threshold is developed by calculating the 80th and 95th percentile modelled daily averaged TSS excluding dredging fines. It is noted that such an approach will not be identical to a simulation without dredging included due to the erosion rates being proportional to the mass fractions in the buffer and fluff layers. This will be most significant where the mass of dredging fines in the respective layers becomes the dominant fraction, resulting in a reduction in the resuspension of natural fines as a greater proportion of the erosion demand is satisfied by the dredging fraction.

Figure 44 and Figure 45 present spatial contour plots of the 80th and 95th percentile TSS excluding dredging. There is no clear indication of a significant influence from dredging fines on the erosive fluxes of natural fines, likely due to the temporally variable location in the supply of dredging fines, compared to the dominant natural processes in the nearshore and the naturally lower concentrations of fines in the fluff layer offshore. Figure 46 presents a spatial plot of the percentage of days where the modelled daily average TSS exceeded the 80th percentile of the modelled daily average natural TSS. Figure 47 presents a spatial plot of the maximum number of consecutive days where the modelled daily average TSS exceeded the 95th percentile of the modelled daily average natural TSS.

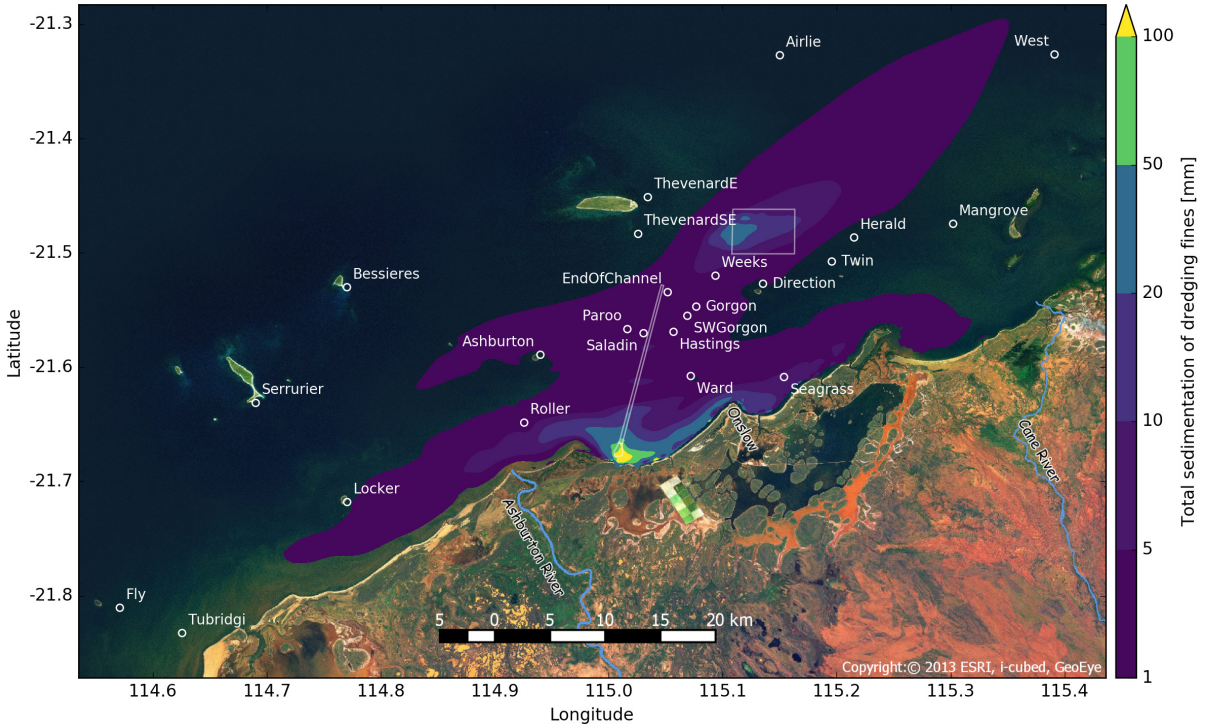

Figure 37. Spatial plot of the modelled total sedimentation from passive dredging plumes over the period 1 April through 31 December 2013. Note: this figure does not include direct deposition to the seabed due to placement or due to density currents associated with the dynamic phase of the dredging plume.

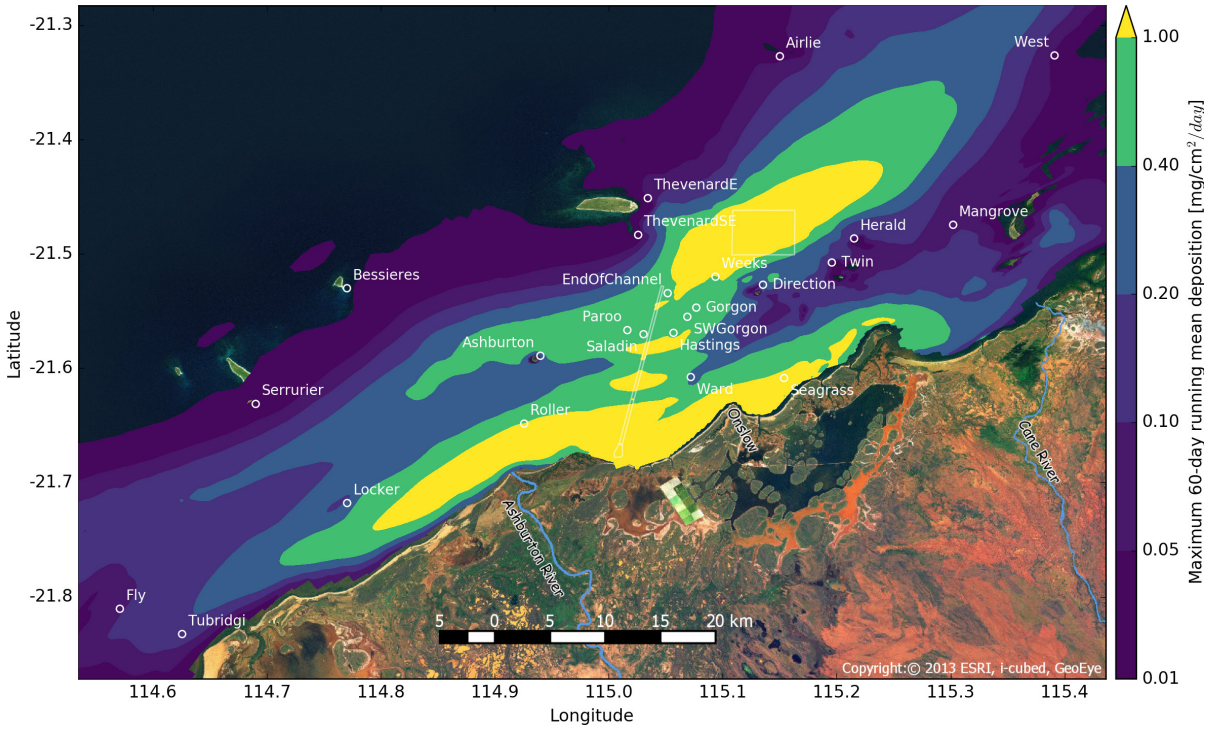

Figure 38. Spatial plot of the modelled peak 60-day running mean daily deposition of dredging fines between 1 April 2013 and 31 December 2013.

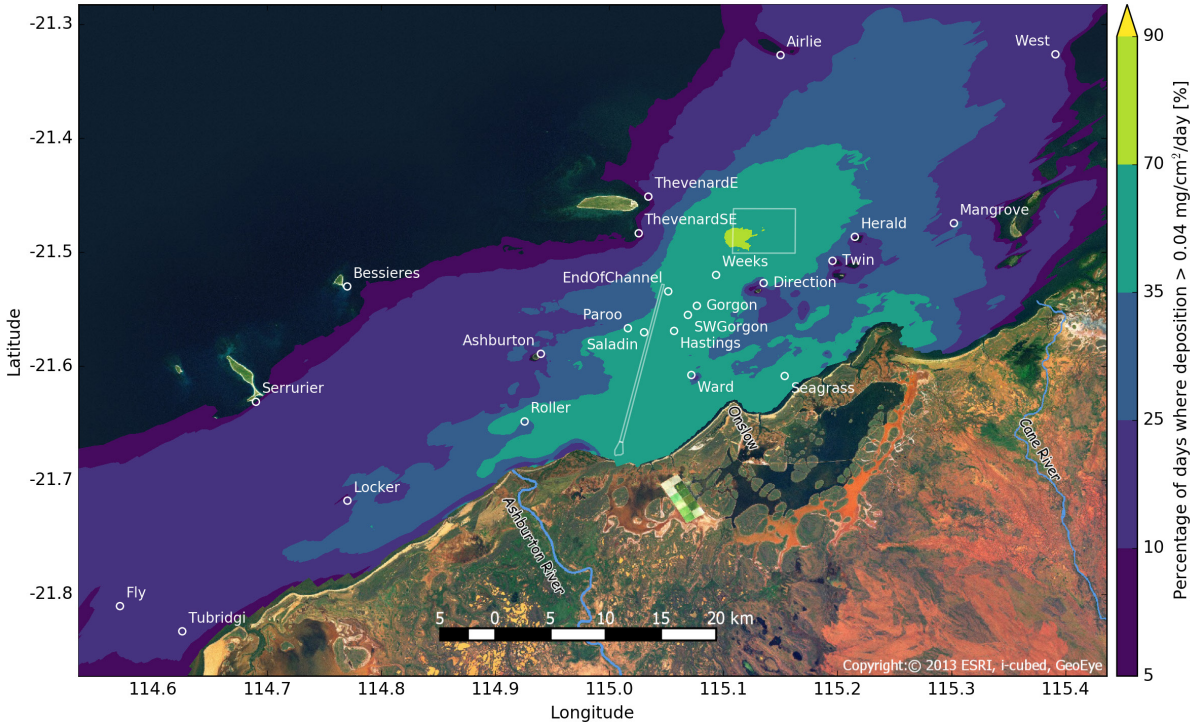

Figure 39. Spatial plot of the percentage of days where the modelled daily deposition of dredging fines was greater than 0.04 mg/cm²/day between 1 April 2013 and 31 December 2013. Note this threshold of 0.04 mg/cm²/day is hypothetical and used for demonstration purpose only.

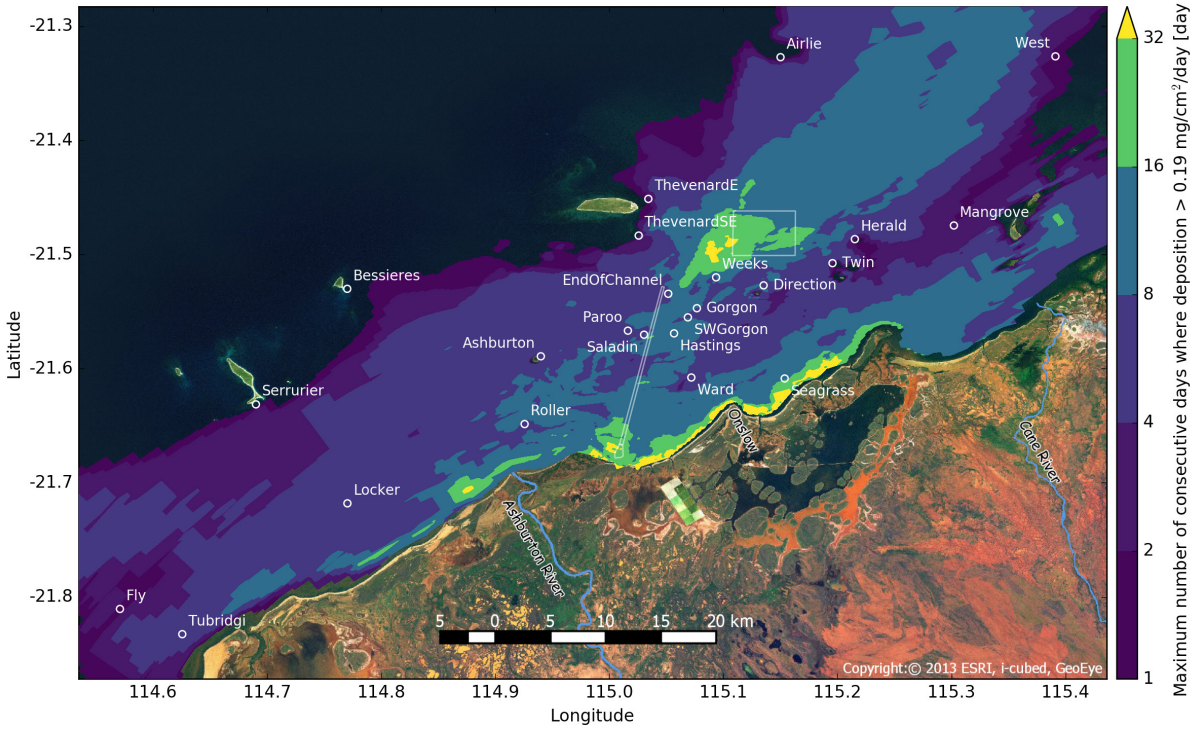

Figure 40. Spatial plot of the maximum number of consecutive days where the modelled daily deposition of dredging fines was greater than 0.19 mg/cm²/day between 1 April 2013 and 31 December 2013 . Note this threshold of 0.19 mg/cm²/day is hypothetical and used for demonstration purpose only.

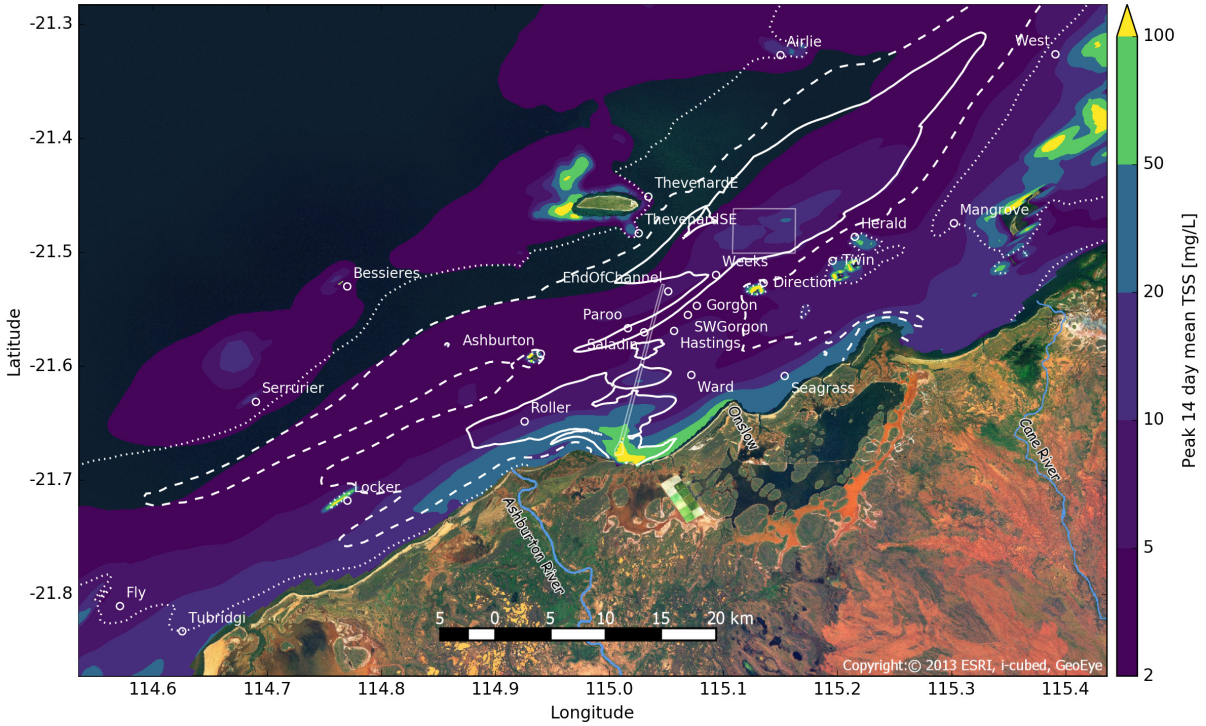

Figure 41. Spatial plot of the peak 14 day running mean near bed total TSS (combined dredging and natural fines). White lines demark regions where dredging fines contribute a given percentage to the total TSS: dotted = 10%, dashed = 50% and solid = 90%.

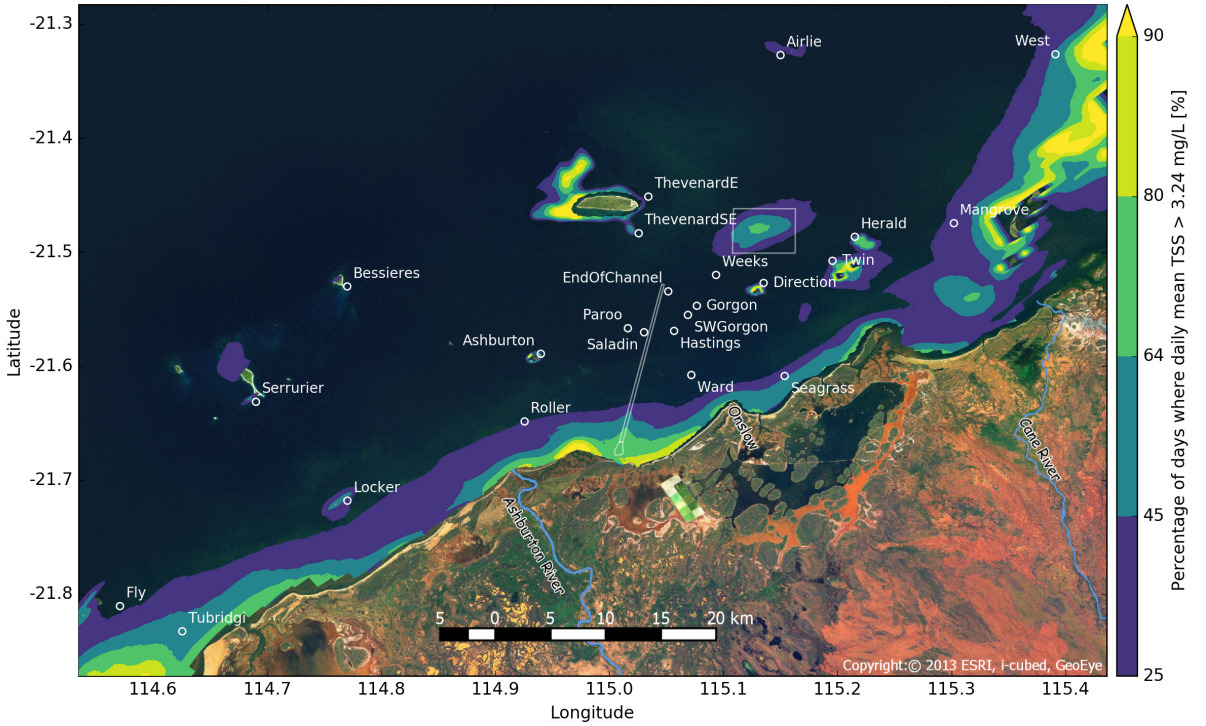

Figure 42. Spatial plot of the percentage of days where the modelled daily mean near bed TSS exceeded 3.2 mg/L between 1 April 2013 and 31 December 2013.

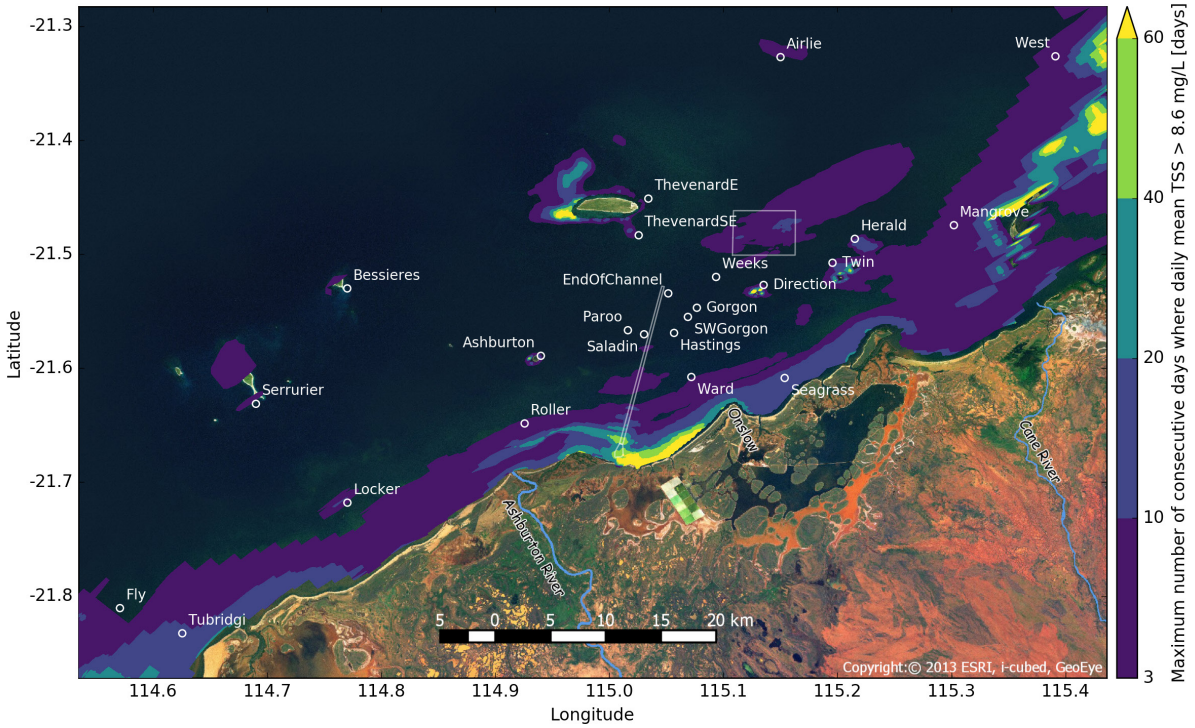

Figure 43. Spatial plot of the maximum number of consecutive days where the modelled daily mean near bed TSS exceeded 8.6 mg/L between 1 April 2013 and 31 December 2013.

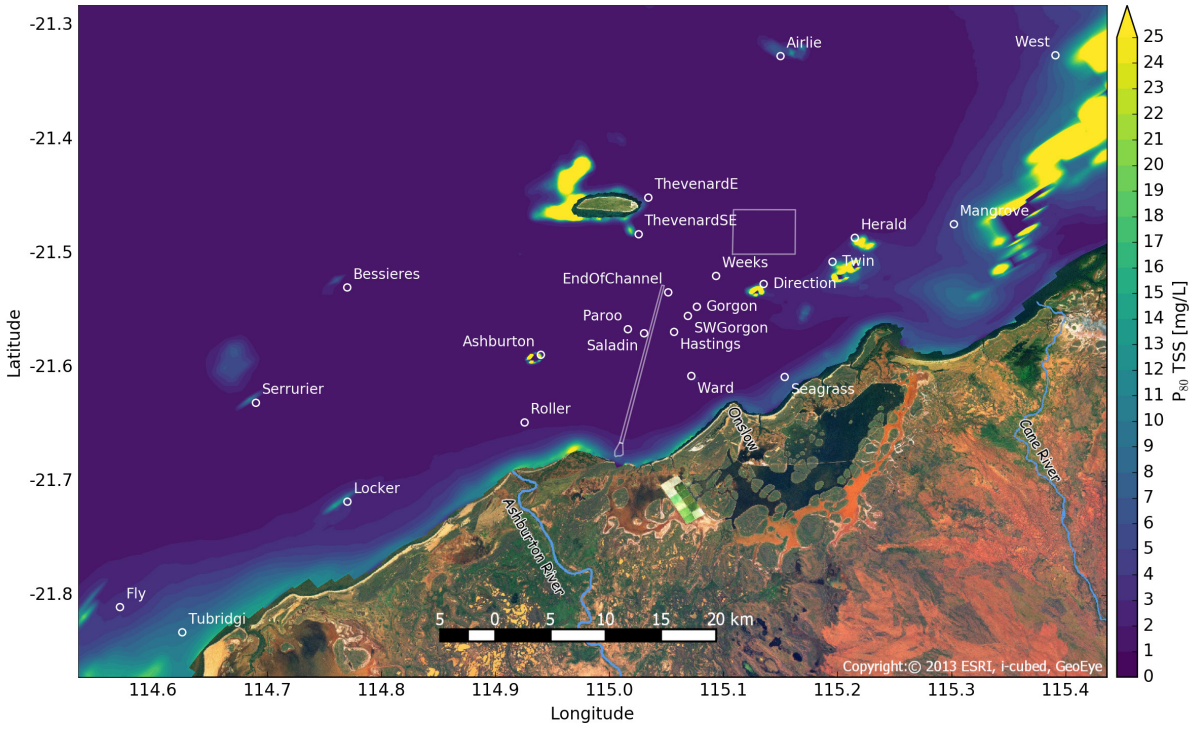

Figure 44. Spatial plot of the modelled 80th percentile near bed TSS (excluding dredging) for the period 1 April 2013 through 31 December 2013.

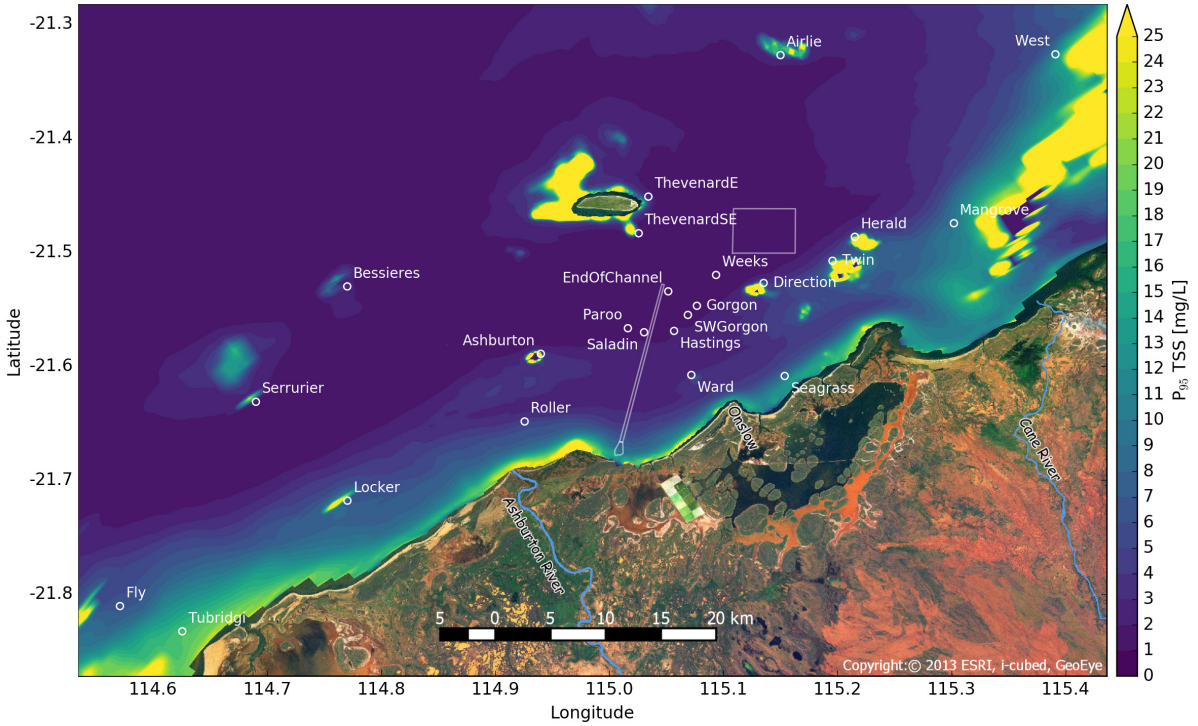

Figure 45. Spatial plot of the modelled 95th percentile near bed TSS (excluding dredging) for the period 1 April 2013 through 31 December 2013.

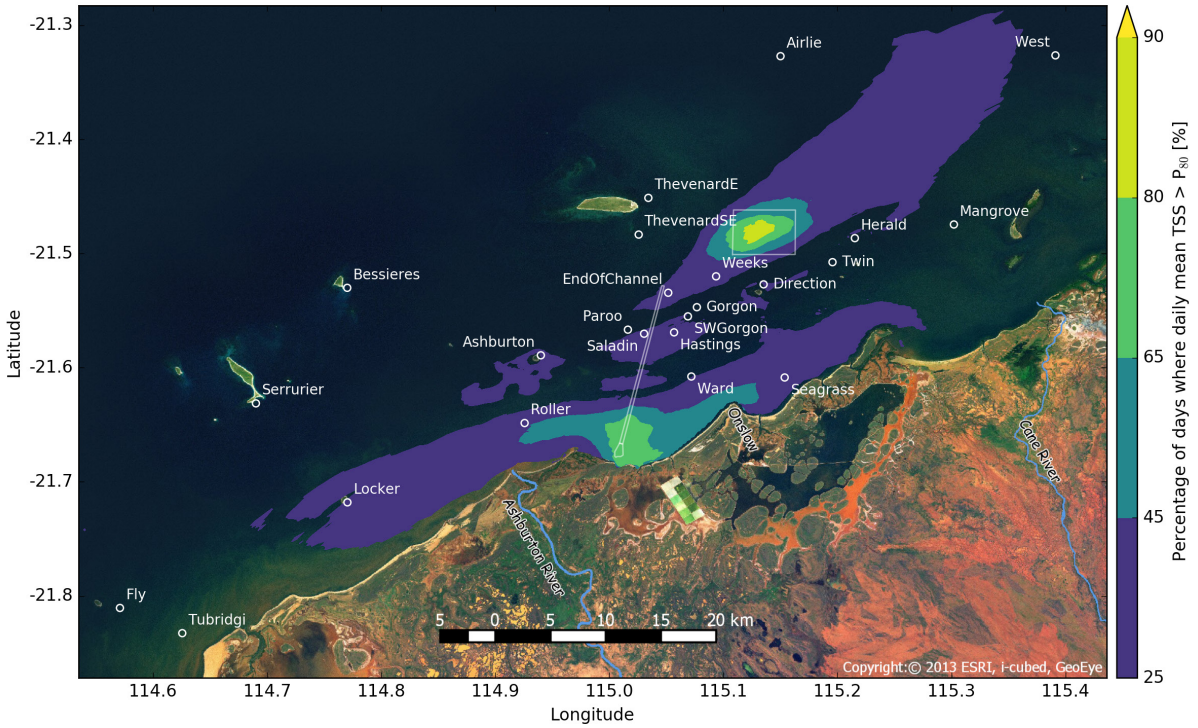

Figure 46. Spatial plot of the percentage of days where the modelled daily mean near bed TSS exceeded the 80th percentile of the modelled natural daily mean TSS for the period 1 April 2013 and 31 December 2013.

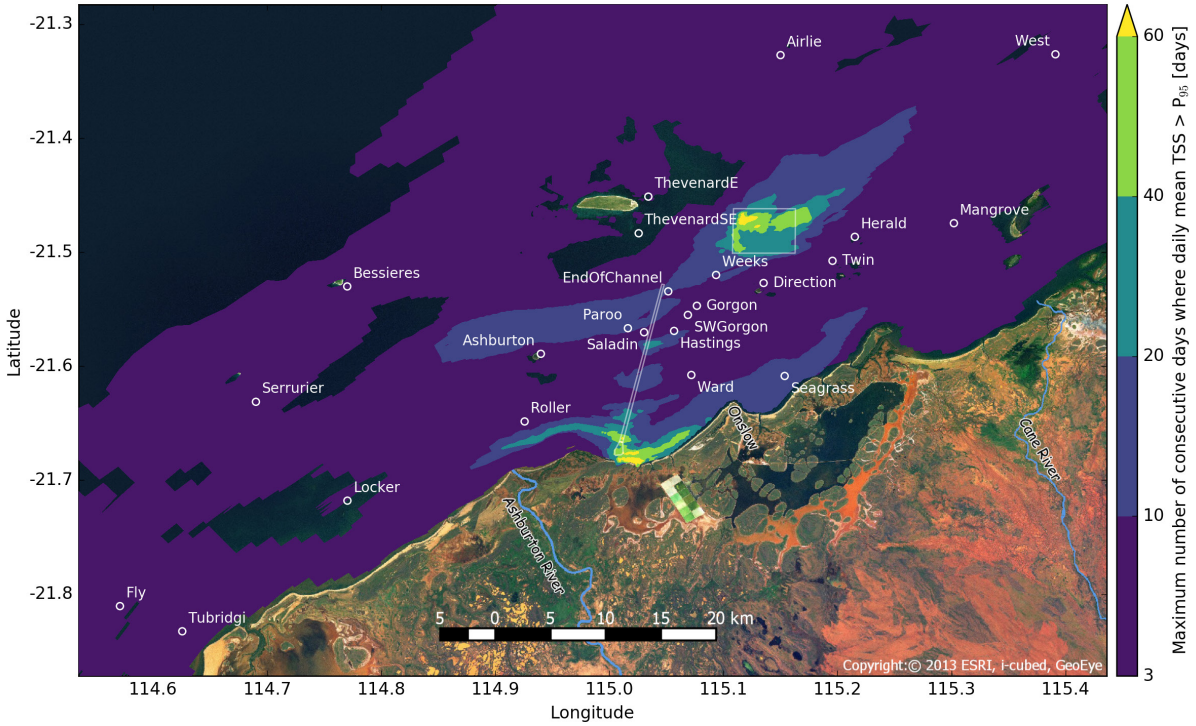

Figure 47. Spatial plot of the maximum number of consecutive days where the modelled daily mean near bed TSS exceeded the 95th percentile of the modelled natural daily mean TSS for the period 1 April 2013 and 31 December 2013

6.3.3 Daily light integral

The daily light integral (DLI) is an additional indicator that can be utilised to assess pressure for phototrophic organism. The hyperspectral light attenuation model developed in Fearns et al (2017a) was implemented to calculate the near bed photosynthetically active radiation (PAR) based on the modelled vertical profile of TSS at each point. Due to the sediment transport model underestimating the low concentration background TSS and the light model of Fearns et al (2017a) only being developed based on water samples with a TSS > 2.7 mg/L the light attenuation at 3 mg/L was applied for modelled TSS < 3 mg/L. An example time series comparison of the measured and modelled near bed TSS and DLI is provided in Figure 48, demonstrating good agreement between the measured and modelled near bed PAR. It is interesting to note that the agreement between the modelled and measured near bed PAR is quite good during the periods of elevated near bed TSS despite the model significantly underestimating the near bed TSS. A similar trend is exhibited at other nearshore sites suggesting that whilst the near bed TSS may be underestimated during these events, the TSS integrated over the water column may be reproduced well, but with an error in the vertical structure. This is of note given the shallowness of these sites and the common assumption that the water column is well mixed at these depths (< 8 m).

Table 15 presents an assessment of the ecological pressure associated with dredging due to changes in the DLI. Similar to the assessment applied to TSS, having modelled the natural TSS and near bed light dynamics allows for the calculation of spatially variable thresholds based on the 80th and 95th percentile DLI that account for local TSS forcing and site depth. For demonstration of the technique of assessing ecological impact due to changes in the light field, the fixed thresholds identified by Fisher et al (2017) for coral at Barrow Island are also applied to compare with the effect of spatially variable thresholds. The five sites with the greatest estimated pressure are indicated with a bold font. Deeper sites on the Inner Shelf are modelled to have lower DLI thresholds due to their depth (eg. EndOfChannel), similarly nearshore sites with frequent natural resuspension (eg. Tubridgi) have lower DLI thresholds, whilst nearshore sites with lower natural TSS have higher thresholds (eg. Seagrass).

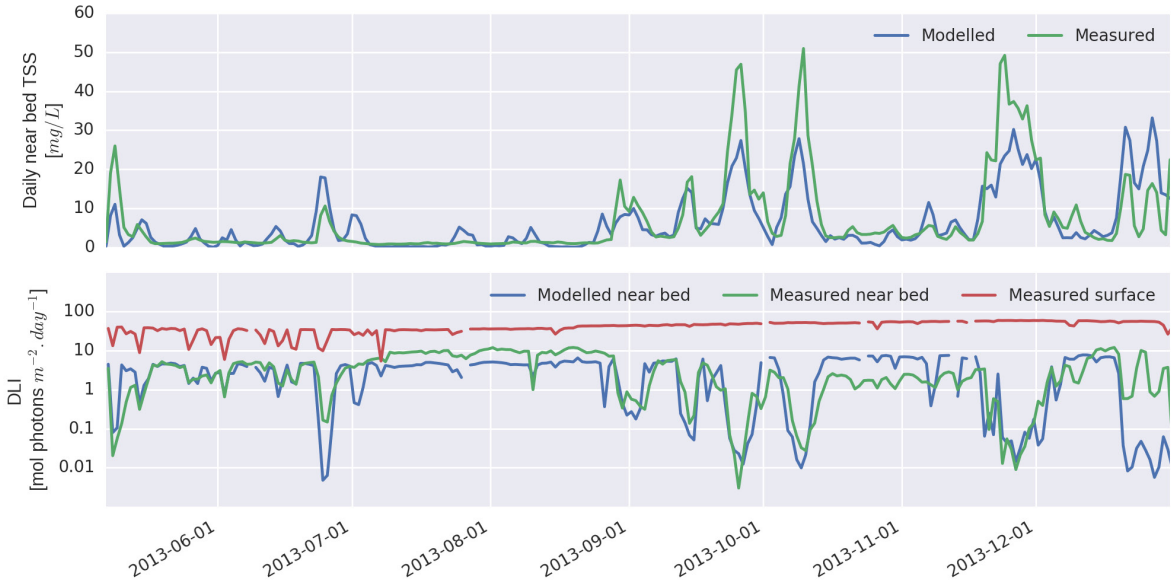

Figure 48. Example time series comparison of the modelled and measured near bed daily TSS (top) and PAR daily light integral (bottom) at the Seagrass location. Measured surface DLI was obtained from a nearby station on land.

Table 15. Thresholds and exceedances for daily light integral (DLI - mol quanta m^{-2} day^{-1}) for the fixed monitoring stations. Fixed threshold of 2.2 DLI based on Fisher et al (2017). P20 = modelled 20th percentile DLI excluding dredging fines. P5 = modelled 5th percentile DLI excluding dredging fines. Frequency, duration and intensity pressure indicated by the percentage of days, cumulative days and 14-day running mean respectively. The five sites with the greatest modelled increase in pressure due to dredging are in bold.

	Threshold (DLI)			Percentage of days below threshold (%)			Cumulative days below threshold (days)			Minimum 14-day running mean (DLI)	
Site	**Fixed**	**P20**	**P5**	**2.2 DLI**	**P20**	**P5**	**2.2 DLI**	**P20**	**P5**	**Excluding dredging**	**Including dredging**
Airlie	2.2	2.2	1.0	22.3	23.2	5.6	10	10	3	1.4	1.4
Ashburton	2.2	3.8	1.6	10.3	21.5	7.7	4	11	4	2.6	2.1
Bessieres	2.2	2.4	1.0	14.6	20.2	5.2	6	10	4	1.5	1.5
Direction	2.2	3.7	1.5	11.6	24.0	7.3	4	10	3	**2.4**	**1.7**
EndOfChannel	2.2	0.5	0.2	100.0	**30.9**	**16.7**	233	**12**	**5**	0.4	0.2
Fly	2.2	1.1	0.1	46.8	20.6	5.2	13	6	3	1.1	1.0
Gorgon	2.2	0.9	0.4	100.0	24.9	9.4	233	**12**	**5**	0.6	0.3
Hastings	2.2	1.9	0.9	42.9	**29.6**	8.2	27	**12**	4	**1.3**	**0.7**
Herald	2.2	5.9	2.4	6.9	26.6	7.7	4	10	4	3.9	3.7
Locker	2.2	4.6	1.0	12.4	26.6	7.3	4	6	3	**3.3**	**2.6**
Mangrove	2.2	1.3	0.1	29.6	21	6.4	6	5	4	1.3	1.1
Paroo	2.2	0.9	0.5	100.0	24.5	**12.4**	233	**12**	**5**	0.6	0.4
Roller	2.2	2.9	1.1	24.5	**29.6**	**14.2**	15	**15**	**9**	**1.9**	**0.6**
Saladin	2.2	1.2	0.6	92.3	24	9.4	183	**12**	**5**	0.8	0.5
Seagrass	2.2	2.6	0.3	36.5	**37.8**	**21.9**	12	**15**	**12**	**2.2**	**0.0**
Serrurier	2.2	2	0.8	28.8	20.2	5.6	13	10	4	1.2	1.2
SWGorgon	2.2	0.9	0.4	100.0	24.0	8.6	233	**12**	**5**	0.6	0.3
ThevenardE	2.2	2.6	1.1	12.0	20.2	5.2	5	10	3	1.8	1.8
ThevenardSE	2.2	1.6	0.8	51.5	20.2	5.2	103	10	3	1.1	1.1
Tubridgi	2.2	0.2	0.0	48.5	20.6	5.6	19	9	4	0.2	0.2
Twin	2.2	5.7	1.9	8.6	23.2	7.3	4	9	4	3.3	2.9
Ward	2.2	2.2	1.0	21.9	23.2	6.9	10	10	4	**1.5**	**0.9**
Weeks	2.2	0.6	0.3	100	**28.8**	**16.7**	233	**12**	**5**	0.4	0.2
West	2.2	0.3	0.0	69.5	20.2	6.0	71	6	4	0.4	0.4

7 Discussion

7.1 Source term estimation

Detailed analysis of dredging logs was conducted in order to establish the location and timing for over 22,000 separate dredging plumes across eight different operational modes utilised during the dredging campaign. The empirical source term model of Becker et al. (2015) (B2015**)** was utilised to estimate the fine sediment flux introduced into the water column for each of the plumes. The spatially and temporally varying source terms were validated to ensure mass closure of the fine sediment budget available in the excavation, consistent with the assumed parameterisation of source terms utilised in the application of B2015. The crucial calibration parameter in this respect was correctly establishing the duration of the dredging and placement phases of the dredging cycle.

The numerical model was able to reasonably reproduce the observed dispersion, settling and resuspension of the passive plumes. The Becker et al. (2015) model was applied in this case study and the estimated source terms appeared to be reasonable for the placement of dredge material at the spoil ground (based on comparison with MODIS and *in situ* data). However, the sources terms in the nearshore dredging area based on B2015 may have been underestimated, a region where dredging was primarily undertaken by a CSD. Whilst the upper limit of the suggested reasonable range for cutter head stir up was utilised in the case study, due to the shallow depth an additional source term due to ancillary vessel operation and propeller wash should have been included. B2015 suggest that this could be accounted for in the overflow source term, however in the Wheatstone project overflow was restricted in certain areas as a management measure, making the overflow term not appropriate to account for propeller wash in this study. B2015 notes the challenges associated with estimating a propeller wash term, and it is highlighted again here that B2015 applies an approach that accounts for the fines available in the excavated mass, however a source term due to ancillary operations/propeller wash does not form part of this mass balance and should be considered separately.

It is noted that dredged materials from excavating the trunklines was not considered in this modelling study due to lack of information. The total volume of materials dredged from the trunkline operations was about 3.4 Mm^3 which is not trivial, but the majority of dredged materials came from the main dredging operations of the channel and turning basin which was studied here.

The estimation of source terms based on empirical models is appropriate at the EIA stage, such as B2015, with the caveat outlined above. As mentioned, the B2015 is based on a methodology that distributes the fines available in the excavated mass across the dredging process, which in turn relies on a number of empirical parameters. Whilst some of these parameters can be estimated from more detailed models, many parameters remain empirical and need to be estimated using professional judgement and experience. For this reason it is strongly recommended that the parameters utilised during EIA are reported, validated with a plume characterisation exercise and recorded in a database for future use.

7.2 Dredge plume model

In the nearshore it appears that the vertical structure in the dredging plume was not fully reproduced in the model, in particular for the sites closest to the dredging. The inaccuracy in the vertical structure of TSS could be due to a number of reasons. Firstly, the use of a single fine sediment fraction (without a flocculation model) will not reproduce the vertical gradient that is established due to flocculation effects associated with high TSS concentration close to the dredging activity. Secondly, whilst the analysis of a range of measured data was utilised to inform model parameter estimates, a number of cohesive sediment transport model parameters are not able to be estimated from measured data (for example the erosion parameters for the fluff and buffer layers). Informed by the outcomes of the model parameter sensitivity analysis, numerous additional combinations of model parameters were tested in order to obtain a parameter set that best represented the overall TSS system across the broad range of bed shear stress climatology. It is possible that the underestimation of the vertical

structure in the nearshore could have been improved through an alternative combination of model parameters. Thirdly, the specification of the source term flux as uniform through the water column may have underestimated the three-dimensional structure of the source term. This study utilised the results of de Wit (2014) to estimate the vertical structure of the passive plumes associated with the overflow, which for shallow depths predicts a nominally uniform vertical distribution. However, a significant contribution to the passive plume in the nearshore would have been due to CSD operation, which typically generates a source closer to the seabed. As such a source term for the CSD that was concentrated in the lower water column may have improved the vertical profile in TSS in the nearshore. The modelling of the near bed light climate reproduced the reduction in near bed light intensity during elevated TSS reasonably well which suggests that the vertically integrated TSS was reproduced reasonably well.

The vertical plume structure that is present, even in shallow water (< 8 m depth), highlights the need for 3D modelling, in particular where both remote sensing and *in situ* near bed measurements are used for model calibration and validation.

7.3 Modelling of ambient suspended solids and resuspension

In this study two separate fine sediment fractions were utilised for dredging and ambient fine material. The use of two sediment fractions allowed clear separation of the influence of dredging relative to natural TSS dynamics, however using a single fraction for ambient fine sediment, the model was not able to reproduce low concentration background TSS (less than approximately 2 mg/L) that was observed across the shelf in the Wheatstone Project location. We therefore suggest that at a minimum, five sediment fractions are likely to be sufficient in many systems to model the combined effects of dredging and ambient fine sediment. One is the sand in the buffer layer, with four sediment fractions for fine material: two fractions for natural fine sediments, two for dredged fine sediment.

Due to difficulty in accounting for flocculation and uncertainty around suspended sediment particle densities (as opposed to bulk density in the seabed), the appropriate parameter to use to describe each fraction is the settling velocity, not particle size, although the class of particles are useful references. A detailed study of the flocculation behaviour of three different sediment types subjected to processing techniques applied in sand mining demonstrated that flocculation occurred with all samples, including for TSS concentrations as low as 10 mg/L (HR Wallingford, 2014). That study concluded that, *"…flocculation significantly changed the settling properties of the material and… it is not really possible to ascribe a particle size diameter to different settling behaviours."* A similar conclusion was obtained in this study through analysis of the LISST data. For the modelling of the fine sediment fractions in the passive plume the order of magnitude for settling velocity is typically between 0.01 to 2 mm/s. A pragmatic approach to modelling the passive plume dynamics is to apply one fraction with a low settling velocity (on the order of 0.01 mm/s) to reproduce the background TSS concentration and a higher settling velocity (nominally in the range 0.1 to 1 mm/s) to reproduce the TSS dynamics of resuspension events. Higher settling velocities (> 2 mm/s) are typically only relevant very close to dredging sources where large particles and flocculation is present due to the higher sediment concentration. In this region (the near- and mid- field) the influence of density effects in the plume are greater and are not adequately modelled by a far-field model.

In the future data assimilation may be a viable approach to improve the reproduction of the cumulative probability distribution of natural TSS, in particular as the prevalence of geostationary satellites to estimate TSS becomes more widespread (reducing tidal aliasing).

The accuracy of the ambient TSS model is strongly influenced by the availability of fine sediment at the seabed. A reasonable approach commonly applied to estimate the sediment distribution at the bed is to undertake a so-called 'warm up' simulation of sufficient duration so that the modelled availability of fines at the seabed reaches some dynamic equilibrium with the modelled bed shear stress forcing. Depending on the system this can take a significant period of model time (up to several model years) which requires that natural sediment fluxes into the model domain be adequately resolved. Alternatively, baseline data collection could be expanded to include additional spatial sampling of sea bed particle size distributions within the active transport layer (notionally the

top 5 – 10 cm) in order to better capture the natural variability. This data collection would assist in establishing the spatial map of initial conditions for fine sediment availability and could be informed by the numerical modelling to target the range in bed shear stress climatology and natural sediment supply likely present in the system.

It was not possible to reproduce the resuspension of easily erodible freshly deposited dredging material on the inner shelf without the use of a fluff layer model such as the van Kessel et al. (2010) model applied here (see discussion in Section 5.2). Due to the depth of the inner shelf and protection from swell energy by the broad shelf and numerous offshore islands, the inner shelf is a comparatively low shear stress environment, which requires a lower critical shear stress threshold for resuspension. The inclusion of the fluff layer model introduces several additional interdependent parameters (i.e. zero and first order erosion coefficients, burial parameter and fluff layer shear stress threshold) to the formulations for cohesive sediment transport which presents an additional challenge for model calibration. Further research into efficient techniques in parameter estimation for sediment transport models is needed. Whilst this presents a challenge it is necessary in order to incorporate resuspension of both ambient and dredging fine sediment in the assessment of absolute thresholds.

The model applied here did not account for the presence of seabed canopies and the spatial variability that this introduces to bed shear stress as it was established that measurements of the spatial distribution of the required canopy properties were not available to appropriately schematise these processes in the far field model. In addition, the models in Project 3.3 have been developed for carbonate sands in rigid coral reef environments and require further development and field scale testing for the fine cohesive sediments that comprise passive dredging plumes. It is noted that our model likely over-predicts resuspension for the shallow reefs around the offshore islands (i.e. Thevenard Island), however there was limited data measured within the canopies in order to validate this. The effects of macroscopic roughness on sediment transport has been examined in detail in Project 3.3 and implementation and validation of the models developed in that project into coastal scale numerical models is a logical extension of this work. In the interim it may be possible to utilise the passive plume model results as a boundary condition in simple 1D modelling of sedimentation and erosion for specific receptors that the far field model indicate may be impacted.

7.4 Pressure field prediction

The application of thresholds from other regions or locations is problematic due to the significant variability in TSS dynamics that may be present between the sites. Indeed, where a significant amount of dredging is required across a broad range of depth and bed shear stress climatology in a single project, the application of a single threshold for ecological pressure field prediction is also problematic. Whilst this is commonly addressed through alternative thresholds for different benthic species and assemblages which are reflective of the ecological niches established in the different environments, this depends on detailed and often species-specific pressure-response models. In this study, we demonstrated several methods of translating model output to ecological pressure fields by applying statistical measures and hypothetical thresholds, which were suggested by Fisher et al (2015).

The numerical modelling of ambient sediment dynamics provides the opportunity to utilise the model to assess absolute thresholds that combine the potential stress from both natural and dredging disturbance. Examining the spatial distribution of the TSS and light probability distributions can assist in identifying the regions where the greatest dredging pressure relative to natural pressure is experienced and this can assist in the selection of impact and reference monitoring sites. If further research could demonstrate that thresholds based on the frequency and duration of exceedance of a given percentile of the natural TSS is a robust approach to predict ecological pressure, then the modelling of ambient TSS can assist in defining the spatial distribution of these thresholds.

The modelling of both dredging and ambient sediments has significant benefits as model output can be utilised for direct comparison against measurements, as an operational tool and to identify where the impacts of dredging are likely to be, in particular in naturally turbid environments.

8 Conclusions

A hindcast model of the Wheatstone Project's dredging campaign has been developed, applying a broad range of data and analysis to define the sediment transport model parameters and processes, including the modelling of both ambient and dredging fine sediment fractions.

A detailed sensitivity analysis of the sediment transport model parameters highlighted the complexity in modelling cohesive sediment transport which grows from numerous sensitive and interdependent parameters. The final model parameter set, and configuration was identified through an extensive set of model simulations compared qualitatively and quantitatively against near-surface remote sensing data and near-bed instrument estimates of TSS. The approach of using a single sediment fraction enhanced the effectiveness of the investigation of model parameter sensitivity, advanced the understanding of the role the shear stress thresholds played in supplying sediments into water column from the fluff layer and buffer layer, and produced good results compared to observed TSS (MODIS and *in situ* monitoring data). Use of a single sediment fraction, which reproduced the initial plume settling and resuspension processes well, was not able to maintain a low background TSS concentration of ~2 mg/L that was observed to be present across the shelf. This highlights the need for fine fractions (i.e., two settling velocities) in both dredged and ambient sediments with a lower settling velocity to reproduce the background TSS concentration and a higher settling velocity to reproduce the magnitude of resuspension events.

The use of a two-layer schematisation of the seabed (fluff and buffer layer) was crucial in order to be able to adequately reproduce the resuspension of recently deposited dredging fines on the Inner Shelf region (between 7 m and 15 m depth) which is typically only exposed to low shear stress forcing due to sheltering from wave activity. In addition, reproduction of the spatial distribution of ambient TSS is particularly challenging due to the broad range in bed shear stress climatology, limited information on the spatial availability of fine sediment in the bed and the inability to represent the influence of sea-bed canopies on the bed shear stress. Despite these challenges, the model was able to reproduce well the TSS dynamics across the majority of the system influenced by passive dredging plumes, making it an appropriate and valuable tool in assessing the combined impact of both dredging and natural sediments. Based on comparison with the measured data, in particular at sites close to the dredging, the Becker et al. (2015) model is a reasonable approach to the estimation of source terms, however further research is required for definition of the numerous parameters required by the model (for example the fraction of fines released during placement) and to account for additional TSS sources due to propeller wash and ancillary vessel operations Several of the Becker et al. (2015) model parameters can be estimated by detailed models of each specific stage of the dredging process, and the parametric overflow model developed in de Wit (2014) was utilised to inform the overflow source term flux and vertical distribution.

To illustrate potential methods of translating dredge plume model output into ecologically relevant pressure fields such as deposition, total suspended solids and near bed light, the calibrated model output was applied to hypothetical thresholds which were recently estimated for corals in clear water environment near Barrow Island (Fisher et al., 2017). The study demonstrated the difficulty in applying thresholds developed for different regions and where there is significant variability in the ambient TSS climatology. The modelling of ambient sediments provides the opportunity to utilise the model to examine the spatially variability of percentiles of ambient TSS which may be used to inform threshold comparison and representative monitoring site selection. This depends on the model adequately reproducing the ambient probability distribution of total suspended solids across the system to be impacted by dredging. In addition, it requires that thresholds based on the frequency and duration of exceedance of a given percentile of the ambient TSS is a robust indicator of ecological pressure. The use of model derived spatially variable thresholds presents a significant modelling challenge. However, there are significant benefits in doing so as model output can be utilised for direct comparison against measurements of the combined influence of dredging and natural TSS during monitoring as an operational tool and to identify where the impacts of dredging are likely to be measurable against the background TSS climatology, in particular in naturally turbid environments.

Implications for management and recommendations

Establishment of a database and parameter library for dredge plume modelling

There is an urgent need to build a database and a parameter library for dredge plume modelling. The parameter library will serve as a crucial starting point for EIA modelling by providing assistance with the setup of the model and guidance on valid ranges of model parameters. The database will provide valuable validation data for hindcast, and data to validate basic assumptions for source term estimation (see Theme 2 report). EIA submissions should include all relevant information on modelling, including model parameters, model input data and subsequent validation data. These submissions will become part of the contribution to the plume modelling database and parameter library. This will provide a key evidence base for modelling practitioners to estimate source term fractions using datasets gathered in similar circumstances and to choose from a reasonable range of parameter values from the parameter library.

Improved reporting of model parameters and assumptions

An extensive review of previous EIA modelling studies highlighted significant inconsistency in the reporting of model parameters and assumptions (Sun et al 2016). It is **recommended that key model parameters and formulations be a basic reporting requirement for all EIA dredge plume modelling studies**. Examples of the level of detail recommended in reporting numerical modelling parameters and formulations from this Wheatstone case study are provided in Table 16 and Table 17.

It is also **recommended that a brief justification for the selected model formulation or value is provided** to build knowledge of reasonable parameter values and identify those that have undergone significant sensitivity analysis and calibration. Often model default values have been subjected to extensive testing and may be appropriate in many contexts and this could be noted.

Table 16. Example overview of key wave and hydrodynamic model processes and parameters from this numerical modelling study.

Description	Value/model applied	Justification
White capping model	Westhuysen (2007)	Improved modelled wave height of locally generated seas on the shelf
Wave bottom friction model	Collins (1972)	Commonly applied bed friction model
Wave bottom friction coefficient	0.015	Model default value for mixed sand seabed, confirmed through model sensitivity analysis
Hydrodynamic bottom roughness formulation	White-Colebrook (z_0)	Standard roughness formulation for 3D models
Bottom roughness coefficient	0.001 m	Based on model sensitivity analysis and calibration
Horizontal eddy viscosity coefficient	5 m^2/s	Based on model sensitivity analysis
Vertical turbulence closure model	k-ε	Commonly applied turbulence closure model applied in shallow coastal seas
Model for bottom shear stress due to waves and currents	van Rijn (2007)	Successfully applied in previous studies

Table 17. Example overview of key sediment transport model parameters from this numerical modelling study

Description	Value applied	Justification
Horizontal eddy diffusivity	0.5 m^2/s	Based on model sensitivity analysis
Background vertical eddy diffusivity	1.00E-6 m^2/s	Model default value, modelled eddy diffusivity (from k-ε mode) typically one to two orders of magnitude larger
Fluff layer 0th-order erosion parameter (M_2)	2.00E-5 m^2/s	Manually calibrated based on sensitivity analysis and numerous model calibration simulations
Fluff layer 1st-order erosion parameter (M_1)	1.00E-4 m^2/s	Manually calibrated based on sensitivity analysis and numerous model calibration simulations
Fluff layer critical shear stress threshold for erosion ($\tau_{cr,f}$)	0.15 N/m^2	Manually calibrated based on sensitivity analysis and numerous model calibration simulations
Burial fraction on deposition (α)	0.15	Manually calibrated based on sensitivity analysis and numerous model calibration simulations
Settling velocity (w_s) – dredging fines	0.2 mm/s	Established based on analysis of measured data (sediment traps and LISST data) and model sensitivity analysis
Settling velocity (w_s) – natural fines	0.5 mm/s	Established based on analysis of measured data (sediment traps and LISST data) and model sensitivity analysis
Buffer layer critical shear stress threshold for erosion ($\tau_{cr,e}$)	1.0 N/m^2	Manually calibrated based on sensitivity analysis and numerous model calibration simulations
Buffer layer erosion parameter (M_0)	2.00E-5 m^2/s	Manually calibrated based on sensitivity analysis and numerous model calibration simulations
Buffer layer thickness (d_0)	0.05 m	Manually calibrated based on sensitivity analysis and numerous model calibration simulations. Consistent with typical scale of active transport layer for mixed sand beds

Calibration/validation of the model

It is recommended that model calibration and validation is performed on relevant variables, such as residual currents and TSS, instead of water levels. It is often more important (from an ecological perspective) to reproduce the cumulative probability distribution of a parameter rather than capture individual events. As such a quantile-quantile plot can be more informative than a typical scatter plot, in particular where small errors in the phase of an event (i.e. dredging plume release or resuspension) can significantly affect a scatter plot or model skill calculation.

Metocean forcing

The local wind effects are important (i.e., land and sea breezes) in locations close to shore. Further improvement in the spatial resolution of meteorological models which resolve local wind effects will help improve model prediction.

Benefits of modelling ambient sediment

Whilst the modelling of the ambient TSS dynamics presents a significant challenge for modelling practitioners, there are significant benefits to all stakeholders involved and is considered essential for assessing ecological impact using absolute thresholds:

- Dredging proponents can better establish the magnitude of dredging impacts relative to natural processes, which is particularly relevant in naturally high TSS environments
- The combined impact of dredging and natural TSS on benthic ecology can be assessed using absolute thresholds
- The model can be utilised more effectively in an operational context for proactively managing ecological pressure during the dredge campaign
- Model output can be directly compared to monitoring data
- The near-bed light climate and associated ecological pressure of light reduction can be readily modelled
- The scientific understanding of the TSS dynamics of the systems being modelled and their relative exposure to waves, tides, cyclones and runoff are improved

Initialising ambient sediments at the seabed

The accuracy of the ambient TSS model is strongly influenced by the availability of fine sediment at the seabed. A reasonable approach to estimate the sediment distribution at the bed is to undertake a so-called 'warm up' simulation of sufficient duration so that the modelled availability of fines at the seabed reaches some dynamic equilibrium with the modelled bed shear stress forcing. Depending on the system this can take a significant period of model time (up to several model years) which requires that natural sediment fluxes into the model domain be adequately resolved. Alternatively baseline data collection could be expanded to include additional spatial sampling in surficial sediment particle size distributions. This data collection would assist in establishing the initial conditions for sediment cover and could be informed by the numerical modelling to span the range in bed shear stress climatology and natural sediment supply.

The fluff layer

It was not possible to reproduce the resuspension of easily erodible freshly deposited dredging material on the inner shelf without the use of a fluff layer model such as the one in van Kessel et al. (2010). Due to the depth of the inner shelf and protection from swell energy by the broad shelf and numerous offshore islands, the inner shelf is a comparatively low shear stress environment. Without the use of the more easily erodible fluff layer it was not possible to reproduce the observed resuspension dynamics of freshly deposited dredging fines on the inner shelf (lower bed shear stress) at the same time as resuspension in the nearshore (higher bed shear stress). The inclusion of the fluff layer model introduces several additional interdependent parameters to the formulations for cohesive sediment transport which presents an additional challenge for model calibration and is an area for future research. An alternative approach would be to utilise a spatially variable bed shear stress threshold based on the seabed particle size distribution as was applied in Dufois (2018, submitted).

Bed shear stress in vegetated canopies

The presence of seabed canopies can significantly alter the shear stress imparted on the bed within the canopy. Work undertaken as part of the DSN Theme 3 research program has developed a new model to predict the reduction in bed shear stress caused by the presence of the canopy which significantly alters the in-canopy sediment fluxes compared to bare sediment beds (Pomeroy et al. 2017). However, measurements of the spatial distribution of canopy density was insufficient to appropriately schematise these processes in the far field model. In addition, Project 3.3 have been developed for carbonate sands in rigid coral reef environments and require further development and field scale testing for the fine cohesive sediments that comprise passive dredging plumes. The effects of macroscopic roughness on sediment transport has been examined in detail in Project 3.3 and implementation and validation of the models developed in that project into coastal scale numerical models is a logical extension of this work. In the interim it may be possible to utilise the passive plume model results as a boundary condition in simple 1D modelling of sedimentation and erosion in canopies.

Number of sediment fractions and settling velocities

At a minimum, five sediment fractions are likely to be sufficient in many systems to model the combined effects of dredging and ambient fine sediment. One is the sand in the buffer layer, with four sediment fractions for fine material: two fractions for natural sediments, two for dredged material. Due to difficulty in accounting for flocculation and uncertainty around suspended sediment particle densities, the appropriate parameter to use to describe each fraction is the settling velocity, not particle size, although the class of particles are useful references. For the modelling of the fine sediment fractions in the passive plume the order of magnitude for settling velocity is typically between 0.01 to 2 mm/s, with a lower settling velocity (in the order of 0.01 mm/s) to reproduce the background TSS concentration and a higher settling velocity (nominally in the range 0.1 to 1 mm/s) used to reproduce the magnitude of resuspension events. Higher settling velocities (> 2 mm/s) are typically only relevant very close to dredging sources where large particle and strong flocculation is present due to the high sediment concentration. In this region the influence of density effects in the dynamic plume are greater and are not adequately modelled in a far-field model.

Dynamic Plume

Where high protection value ecological systems are present in close proximity (< ~2 km) to the dredging sources, it is necessary to consider the impacts of the dynamic plume. Whilst not addressed in detail in this study further research is required to advance dynamic plume modelling in order to better predict the extent and thickness of dynamic plumes at the seabed in a computationally efficient manner that can be applied during an EIA study. It is noted that significant advancements in the modelling of the dynamic plume associated with hopper overflow have been achieved in de Wit (2014), and the parametric model developed in that work is appropriate for informing the estimation of overflow source terms.

Source term estimation

The Becker et al. (2015) model was applied in this case study and the modelled source terms appeared to be reasonable for the placement of dredge material at the spoil ground. However, the sources terms in the nearshore dredging area based on the Becker model appeared to be underestimated, a region which was predominantly dredged with a CSD. Whilst the upper limit of the suggested reasonable range for cutter head stir up was utilised in the case study, due to the shallow depth an additional source term due to ancillary vessel operation and propeller wash should have been included. The Becker model accounts for the fines available in the excavated mass, however a source term due to ancillary operations/propeller wash does not form part of this mass balance and should be considered separately.

The estimation of source terms based on empirical models is appropriate at the EIA stage, such as the Becker model, with the caveat outlined above. The Becker model is based on accounting for the fines available in the excavated mass and relies on a number of empirical parameters to distribute the available fines throughout the dredging process. Whilst some of these parameters can be estimated from more detailed models, many parameters remain empirical and need to be estimated using professional judgement and experience. For this reason, it is **strongly recommended that the parameters utilised during EIA are reported, validated with a plume characterisation exercise and recorded in a database for future use.**

3D modelling

Three-dimensional (3D) modelling is important as this study has demonstrated, with subsurface plumes observed in waters as shallow as 8 metres and significant vertical structure in the residual currents due to wind forcing. Even with a 3D model, this case study under predicted the vertical gradients in TSS in the nearshore region (see Figure 3). This is likely due to utilising a vertically homogenous source term where the Cutter Suction Dredge (CSD) cutter head source was concentrated near the bed.

Data assimilation.

Data assimilation may be a viable approach to improve the representation of the cumulative probability distribution of natural TSS, in particular as the prevalence of geostationary satellites to estimate TSS becomes more widespread which reduces the problem of tidal aliasing.

Ecological pressure field prediction.

The application of thresholds from other regions or locations is problematic due to the significant variability in TSS dynamics that may be present between the sites. In addition, significant spatial variability in TSS can be present within a site due to variations in depth, exposure (to winds and waves) and sediment availability. The modelling of ambient sediment dynamics in the dredging plume model significantly improves the utility of the model predictions and the comparison against baseline data. If the ambient sediment dynamics are validated and model error well characterised it provides a significant opportunity to utilise the model to assist in application of thresholds through examining shifts in the cumulative probability distribution of TSS at each point.

9 References

Aarninkhof S, Luijendijk A (2010) Safe disposal of dredged material in an environmentally sensitive environment. Port Technology International 47: 39-45

Booij, N, Ris, R, Holthuijsen, L, (1999) A third-generation wave model for coastal regions, Part I, Model description and validation. Journal of Geophysical Research 104 (C4): 7649–7666. 1, 5

Becker J, van Eekelen E, van Wiechen J, de Lange W, Damsma T, Smolders T, van Koningsveld M. (2015) Estimating source terms for far field dredge plume modelling. Journal of environmental management. 149:282-93.

Bettington SH, Miles KE (2009) Modelling of dredge plumes. Coasts and Ports 2009: In a Dynamic Environment 2009:251

Branson PM, Sun C (2017) WAMSI Dredging Science Node: Plume Modelling Uncertainty – Hydrodynamics. Australasian Coasts & Ports 2017: Working with Nature 2017:159

Campbell Scientific (2017) OBS-3+ and OBS300 Suspended Solids and Turbidity Monitors, Instruction Manual, Revision 4/17.

Chevron (2010) Draft Environmental Impact Statement/Environmental Review and Management Programme for the Proposed Wheatstone Project: Technical Appendicied N1 and N2.

Chevron Australia (2010a) Wheatstone Project Final Interpretive Report Nearshore Geotechnical Investigation – Downstream. Rev 1 (WS1-0000-GEO-RPT-COF-000-00030-000.pdf)

Chevron (2013) Wheatstone Project Marine Facilities – Dredging Daily Progress Report, 31 December 2013 (WS1-0000-CNS-RPD-BEC-CMD-00450-000.pdf)

Chevron Australia (2014) Wheatstone Project Dredge Plume Model Validation Rev 0 (WS0-0000-HES-RPT-DHI-000-00015-000.pdf)

Chevron Australia (2014a) Wheatstone Project Marine Facilities – Dredging Daily Progress Report, 20 December 2014 (WS1-0000-CNS-RPD-BEC-CMD-00804-000.pdf)

Condie S, Andrewartha J, Mansbridge J, Waring J (2006) Modelling circulation and connectivity on Australia's North West Shelf. Technical Rep., 62 pp, CSIRO

Cushman-Roisin B, Deleersnijder E (2017) Subtleties in Reducing 3D Rotating Dynamics to a 2D Model, 4th International Symposium on Shallow Flows, Eindhoven, 26-28 June 2017

Deltares (2014a) Delft3D-FLOW User Manual Version 3.15.34158, Delft, Netherlands.

Deltares (2014b) Delft3D-WAVE User Manual Version 3.05.34160, Delft, Netherlands.

Department of Transport (2017) Beadon Creek Submergence Curve, Government of Western Australia

de Wit L, Talmon AM, van Rhee C (2014) 3D CFD simulations of trailing suction hopper dredger plume mixing: A parameter study of near-field conditions influencing the suspended sediment source flux. Marine Pollution Bulletin, 88(1):47-61

Dorji P, Fearns P, Broomhall M (2016), A semi-analytic model for estimating total suspended sediment concentration in turbid coastal waters of northern Western Australia using MODIS-Aqua 250 m data. Remote Sensing 8(7): 556

Dufois F, Lowe RJ, Branson P, Fearns P (2017) Tropical Cyclone‐Driven Sediment Dynamics Over the Australian North West Shelf. Journal of Geophysical Research: Oceans.Dufois F, Lowe RJ, Rayson M, Branson P (2018, submitted) A numerical study of tropical cyclone-induced sediment dynamics on the Australian North West Shelf. Journal of Geophysical Research: Oceans.

Durrant T, Greenslade D, Hemer M, Trenham C (2014) A Global Wave Hindcast focussed on the Central and South Pacific. CAWCR Technical Report 070

Egbert GD, Erofeeva SY (2002) Efficient Inverse Modeling of Barotropic Ocean Tides. J. Atmos. Oceanic Technol. 19:183-204

Fearns P, Dorji P, Broomhall M, Chedzey H Symonds G, Shimizu K, Contardo S, Mortimer N, Branson P, Sun C (2017a) Plume Characterisation. Final Report of Theme 2.3 Project 3.2 of the Western Australian Marine Science Institution (WAMSI) Dredging Science Node. Perth, Western Australia

Fearns P, Dorji P, Broomhall M, Branson P, Mortimer N, (2017b) Plume characterisation – Laboratory studies Final Report of Project 3.2.2 of the Western Australian Marine Science Institution (WAMSI) Dredging Science Node. Perth, Western Australia.

Fisher R, Stark C, Ridd P, Jones R. (2015) Spatial patterns in water quality changes during dredging in tropical environments. PloS one. 10(12):e0143309.

Fisher R, Walshe T, Bessell-Browne P, Jones R. (2017) Accounting for environmental uncertainty in the management of dredging impacts using probabilistic dose‐response relationships and thresholds. Journal of Applied Ecology.

Jones R, Fisher R, Stark C, Ridd P (2015) Temporal Patterns in Seawater Quality from Dredging in Tropical Environments. PLoS ONE 10(10)

Gill AE. (1982) International Geophysics, 30: Atmosphere-ocean Dynamics. Elsevier.

Grasso F, Le Hir P, Bassoullet P (2015) Numerical modelling of mixed-sediment consolidation. Ocean Dynamics, 65(4):607-616

HR Wallingford (2014) Support to Trans-Tasman Resources - Laboratory testing of sediments. Prepared for Trans-Tasman Resources, Report No. RT002, 27 October 2014.

Lane A (1989) The heat balance of the North Sea. Tech. Rep. 8, Proudman Oceanographic Laboratory. 46 pp

Lesser GR, Roelvink JA, Van Kester JATM, Stelling GS (2004) Development and validation of a three-dimensional morphological model. Coastal Eng. 51: 883–915

Margvelashvili NY, Andrewartha JR, Condie SA, Herzfeld MG, Parslow JS, Sakov PV, Waring JR (2006) Modelling suspended sediment transport on Australia's North West Shelf. Technical Rep., 43 pp, CSIRO

Mortimer N, Symonds G, Contardo S, Sun C, Shimizu K (2015) Project 3.2: Plume Characterization - Data report from CSIRO instrumentations during two fieldtrips at Onslow in OCT 2013 and JUN 2014

Ministerial Statement 873, Government of Western Australia, Minister for the Environment; Water, Hon. Bill Marmion MLA, 30 August 2011

Murphy AH (1992) Climatology, persistence, and their linear combination as standards of reference in skill scores, Weather Forecast., 7, 692 –698.

Nash JE, Sutcliffe JV (1970) River flow forecasting through conceptual models part I – A discussion of principles. Journal of Hydrology 10(3): 282 – 290.

Oke PR, Sakov P, Cahill ML, Dunn JR, Fiedler R, Griffin DA, Mansbridge JV, Ridgway KR, Schiller A (2013) Towards a dynamically balanced eddy-resolving ocean reanalysis: BRAN3. Ocean Modelling 67:52-70

Partheniades E (1965) Erosion and Deposition of Cohesive Soils. Journal of the Hydraulics Division ASCE 91 (HY 1): 105–139

Pomeroy AW, Lowe RJ, Ghisalberti M, Storlazzi C, Symonds G, Roelvink D (2017). Sediment transport in the presence of large reef bottom roughness. Journal of Geophysical Research: Oceans, 122(2), 1347-1368.

Provis DG, Aijaz S (2009) Prediction of plume generation and movement from dredging operations in Port Phillip Bay, Melbourne. Coasts and Ports 2009: In a Dynamic Environment 2009:245

Spearman, J.R., De Heer, A., Aarninkhof, S.G.J., Van Koningsveld, M., (2011). Validation of the TASS system for predicting the environmental effects of Trailing Suction Hopper Dredgers. Terra Aqua 125 (3).

Stelling GS, Leendertse JJ (1992) Approximation of Convective Processes by Cyclic AOI methods. In: M. L. Spaulding, K. Bedford and A. Blumberg, eds., Estuarine and coastal modeling. Proceedings 2nd Conference on Estuarine and Coastal Modelling ASCE, p 771–782.

Storlazzi CD, Field ME, Bothner MH. (2011). The use (and misuse) of sediment traps in coral reef environments: theory, observations, and suggested protocols. Coral Reefs, 30(1), 23-38.

Tuinhof T (2014) Modelling far-field dredge plume dispersion. Masters Thesis, TU Delft, Netherlands.

Toorman E, Berlamont J (1991) A hindered settling model for the prediction of settling and consolidation of cohesive sediment. Geo-Marine Letters, 11(3):179-183

van Kessel T, Winterwerp H, van Prooijen B, van Ledden M, Borst W (2011). Modelling the seasonal dynamics of SPM with a simple algorithm for the buffering of fines in a sandy seabed. Continental Shelf Research, 31(10), S124-S134.

van Maren DS, van Kessel T, Cronin K, Sittoni L (2015) The impact of channel deepening and dredging on estuarine sediment concentration. Cont Shelf Res 95:1–14

van Maren, DS, Cronin, K (2016) Uncertainty in complex three-dimensional sediment transport models: equifinality in a model application of the Ems Estuary, the Netherlands. Ocean Dynamics 66:1665–1679

van Prooijen, B., T. van Kessel, M. van Ledden (2007). Modelling of fine sediment in a sandy environment – the coastal zone of the Netherlands, submitted to: IAHR 2007 Conference.

van Rhee C (2002) On the Sedimentation Process in a Trailing Suction Hopper Dredger. Delft University of Technology. Ph.D. thesis

van Rijn, LC (2007). Unified View of Sediment Transport by Currents and Waves. I: Initiation of Motion, Bed Roughness, and Bed-Load Transport. Journal of Hydraulic Engineering 133 (6): 649–667.

Wahab MAA, Fromont J, Gomez O, Fisher R (2017) Comparisons of benthic filter feeder communities before and after a large-scale capital dredging program. Marine Pollution Bulletin 122(1–2): 176-193

Webster I (1985a) Wind-driven circulation on the North West Shelf of Australia. Journal of Physical Oceanography 15(11): 1357–1368

Webster I (1985b) Frictional continental shelf waves and the circulation response of a continental shelf to wind forcing. Journal of Physical Oceanography 15(7): 855–864

Westhuysen A van der, Zijlema M, Battjes J (2007) Nonlinear saturation-based white-capping dissipation in SWAN for deep and shallow water. Ph.D. thesis, Delft University of Technology.

Willmott CJ. (1981) On the validation of models. Physical Geography2: 184 – 194.

Willmott CJ, Robeson SM, Matsuura K (2012) A refined index of model performance. International Journal of Climatology. 32(13):2088-9